December 17, 2021

BP-CORR-00531-02326

Mr. M. Leblanc   Dr. A. Viktorov
Commission Secretary   Director General
Canadian Nuclear Safety Commission   Canadian Nuclear Safety Commission
P.O. Box 1046   P.O. Box 1046
280 Slater Street   280 Slater Street
Ottawa, Ontario   Ottawa, Ontario
K1P 5S9   K1P 5S9

Dear Mr. Leblanc and Dr. Viktorov:

Bruce A Unit 3:
Designated Officer Order Issued to Bruce Power:
Elevated Hydrogen Equivalent Concentrations and Delayed Hydride Cracking Initiation

The purpose of this letter is to:

1. provide the additional information described in the Commission Record of Decision (Reference 1) to confirm the accuracy of the models for elevated levels of hydrogen equivalent concentrations ($[H]_{eq}$) to support continued operation of pressures tubes with scrape marks in locations of elevated $[H]_{eq}$, and

2. based upon the information provided, request closure of the Designated Officer Order (Reference 2).

In the Record of Decision (Reference 1), the Commission concluded:

• Bruce Power demonstrated, with a high degree of confidence, that no service-induced flaws are present in the Region of Interest, thereby satisfying option (b) of the Designated Officer Order, and

• Bruce Power demonstrated, to the Commission's satisfaction, that pressure tube fracture toughness is sufficient for safe operation beyond 120 ppm, thereby satisfying Licence Condition 15.3 of the Bruce A Power Reactor Operating Licence, 18.01/2028, for the purposes of operation and the conclusion of the Unit 3 planned maintenance outage in 2021.

The Commission decision was limited to the return-to-service from the Unit 3 planned maintenance outage in 2021, pending further information with respect to the validation of crack initiation models to confirm scrape marks in locations of elevated hydrogen equivalent concentrations will not lead to crack initiation.

Bruce Power   Maury Burton, Chief Regulatory Officer
P.O. Box 1540 B10 2nd Floor E, Tiverton ON N0G 2T0
Telephone 519-361-5291
maury.burton@brucepower.com

The scrape marks in the Region of Interest are from inspection activities to assess hydrogen concentrations in Unit 3 pressure tubes; they are not susceptible to crack initiation due to their geometry which is specifically designed to be benign.

Bruce Power is providing the following items to address comments regarding Delayed Hydride Cracking (DHC) initiation from scrape marks in the Region of Interest as requested in Reference 3, and committed in Reference 4:

1. sensitivity analysis of key parameters related to DHC initiation for scrape marks to evaluate the risk of crack initiation with elevated hydrogen equivalent concentrations; and,

2. preliminary results of more recent DHC initiation tests, completed at elevated hydrogen equivalent concentrations to confirm previous conclusions.

<u>Sensitivity Analysis</u>
Enclosure 1 provides a report on sensitivity analysis of key parameters to DHC initiation for scrape marks. The results indicate that the risk of DHC initiation from scrape marks in the Region of Interest does not challenge pressure tube fitness for service.

The sensitivity analysis utilizes a 3-D finite element model of a Circumferential Wet Scrape Tool (CWEST) scrape mark with the maximum design depth of 0.384 mm and a representative root radius of 1.7 mm. It evaluates the change of key parameters for DHC initiation from scrape mark, such as the threshold stress intensity factor, K_{IH}, and threshold stress for DHC initiation at a planar surface, p_c, against the peak stress from a CWEST scrape mark. The results indicate that even with a reduction of 50% on the lower-bound values of K_{IH} (4.5 MPa√m) and p_c (450 MPa), DHC initiation is predicted to still not occur. As a result, the risk of DHC initiation from scrape marks in the Region of Interest does not challenge pressure tube fitness for service.

<u>Preliminary Results</u>
The preliminary results of DHC initiation tests, completed at elevated hydrogen equivalent concentrations, are provided in Attachment A. The results in Table A1 of Attachment A, suggest there may be a slight reduction in threshold effective stress intensity factor (K_{TH}) with high $[H]_{eq}$. However, as mentioned above, the sensitivity analysis of scrape marks has demonstrated that the risk of DHC initiation in the Region of Interest is low even with a postulated significant reduction in the key parameters of DHC initiation.

<u>Summary</u>
Bruce Power maintains that the crack initiation models remain valid at hydrogen equivalent concentrations above 120 ppm and the on-going operation of Unit 3 with scrape marks present in the Region of Interest does not challenge pressure tube fitness for service. This includes returning to service following any outage requiring cool-down of the unit.

Bruce Power respectfully requests Unit 3 be released from the Designated Officer Order based on the following:

BP-CORR-00531-02326

1. Criteria for option (b) under the Order has been satisfied;

2. Given there have never been dispositionable flaws detected within the Region of Interest in any Bruce Power unit, the satisfaction of the Designated Officer Order's option (b) is not subject to change as a result of the on-going operation of Unit 3;

3. CNSC staff acknowledgement that the Unit 3 pressure tube fracture protection is sufficient for operation with limited portions of pressure tubes having hydrogen equivalent concentrations in excess of 120 ppm; and

4. The additional information submitted herein confirms scrape marks in locations of elevated hydrogen equivalent concentrations will not lead to crack initiation.

If you require further information or have any questions regarding this submission, please contact Mr. Maury Burton, Chief Regulatory Officer, at (519) 361-2673 extension 15291, or maury.burton@brucepower.com.

Yours truly,

Maury Burton
Chief Regulatory Officer,
Bruce Power
2021.12.17 11:15:29 -05'00'

Maury Burton
Chief Regulatory Officer
Bruce Power

cc: CNSC Bruce Site Office

Attach.

Enclosure:

1.   B-REP-31100-00033, Revision 000, "Assessment of Margins Against Crack Initiation at CWEST Scrape Flaws in Regions of Interest with High Levels of Hydrogen Equivalent Concentration in Outlet Rolled Joints in Bruce Units 3 and 7".

References:

1.   Letter, Secretariat to M. Burton, "Record of Decision DEC 21-H110 Request for Authorization to Restart Bruce Nuclear Generating Station A Unit 3 following its current planned outage", November 10, 2021, e-Doc 6672394, BP-CORR-00531-02250.

2.   Letter, R. Jammal to M. Burton, "Designated Officer Order issued to Bruce Power", July 26, 2021, e-Doc 6612485, BP-CORR-00531-01904.

3.   Letter, L. Sigouin to M. Burton, "Bruce A and B: CNSC Request for Additional Information to Address the Long-Term Actions regarding Elevated Hydrogen Equivalent Concentration Measurements in Pressure Tubes – New Action Item 2021-07-23988", October 4, 2021, e-Doc 6643726, BP-CORR-00531-02112.

4.   Letter, M. Burton to L. Sigouin, "Bruce A and B: Additional Information to Address Long Term Actions regarding Elevated Hydrogen Equivalent Concentration Measurements in Pressure Tubes, Action Item 2021-07-23988", November 15, 2021, BP-CORR-00531-02192.

CANADIAN NUCLEAR SAFETY COMMISSION
REQUEST TO PROTECT CONFIDENTIAL INFORMATION

ACCOMPANYING SUBMISSION

CANADA
PROVINCE OF **Ontario**
IN THE MATTER OF

The following Bruce Power correspondence and reports provided to the CNSC:

1. **Bruce Power Letter, M. Burton to M. Leblanc and A. Viktorov, "Bruce A Unit 3: Designated Officer Order Issued to Bruce Power: Elevated Hydrogen Equivalent Concentrations and Delayed Hydride Cracking Initiation", December 17, 2021, BP-CORR-00531-02326.**

I, **James Scongack, at Post Office Box 1540, 177 Tie Road, RR#2, Tiverton, Ontario N0G 2T0**, an authorized senior officer of **Bruce Power Inc.**

DO SUBMIT THAT, WITH RESPECT OF THE **Bruce Power correspondence and reports identified above which were provided to CNSC** BY **Bruce Power Inc.** REGARDING **issues relating to measurement of hydrogen equivalent concentration in pressure tubes** FOR **Bruce A Nuclear Generation Station and Bruce B Nuclear Generating Station**, AND TO THE BEST OF MY KNOWLEDGE AND BELIEF:

1. **Bruce Power Inc.** wishes to have protected / restricted / prohibited from public disclosure the following documents (attached): **None.**

2. I understand that the Commission may deem all documents as releasable to the public, unless the document is accompanied by an accompanying submission signed by a senior officer seeking to protect / restrict / prohibit the document from public disclosure.

3. The information contained in the above-referred documents should be protected / restricted / prohibited pursuant to the CNSC Rules of Procedure, Section (1) (b) for the following reasons:

In accordance with Commission Rules of Procedure: Confidentiality, Section 12 (1)(b) Bruce Power requests that the above listed portions of the correspondence packages be protected from public disclosure. The information above contains commercially sensitive information, personal confidential information, and the data contained in the submissions is of confidential commercial, scientific, and technical nature that is treated consistently as confidential.

Please note that the portions of the correspondence that Bruce Power has agreed to release may also contain information that is consistently treated as confidential. Notwithstanding the foregoing, Bruce Power has authorized the release of that information for the express purpose of this Commission proceeding only, and such release shall be considered without prejudiced for any past or future release requests related to Commission proceedings, the Access to Information Act, or otherwise.

4. The information sought to be protected / restricted / prohibited is being provided to the CNSC in confidence and is to be received in confidence by the CNSC.

5. The information sought to be protected / restricted / prohibited is not available in public sources, to the best of my knowledge and belief.

For all the reasons discussed above, Bruce Power Inc. requests that the identified confidential information be protected / restricted / prohibited from public disclosure.

_____
James Scongack
Chief Development Officer and EVP, Operational Services
Bruce Power

<u>17DEC2021</u>
Date

Signed in the Town of Kincardine in the County of Bruce in the Province of Ontario on the 17th day of December in the year 2021.

Attachment A

Results of Delayed Hydride Cracking Initiation Tests

Attachment A:
Results of Delayed Hydride Cracking Initiation Tests

The initial tests were performed to determine the effect of elevated hydrogen equivalent concentrations on the threshold effective stress intensity factor, KTH, as proposed in Reference 4. These tests were designed to facilitate a general understanding as to the impact of elevated hydrogen concentrations within the Region of Interest.

The results in Table A1 of Attachment A, suggest there may be a slight reduction in KTH with high [H]eq. As described in Reference 4, Bruce Power will pursue additional tests on KIH and pc as these are the two key parameters for DHC initiation from scrape flaws. Results in Table A2 suggest no change in KIH at high [H]eq based on limited tests completed as of December 17, 2021. Table A3 provides the planned pc tests.

The process-zone model for DHC initiation in CSA N285.8 was developed based on a larger set of unirradiated data and validated using a smaller set of irradiated data. The formulation of the process-zone model that was developed using unirradiated data does not change with the irradiated data. The effect of irradiation is taken into account by using values of KIH and pc for irradiated material. It is currently uncertain whether the observed slight reduction in KTH from the high [H]eq crack initiation tests on unirradiated materials is similar with irradiated materials. However, as mentioned above, the sensitivity analysis of scrape marks has demonstrated that the risk of DHC initiation from scrape flaws in the Region of Interest is low even with a significant reduction in the key parameters of DHC initiation.

Additional tests on KIH and pc will be performed to further understand impacts related to elevated levels of hydrogen equivalent concentration. Another update on the test results will be provided to CNSC staff in March 2022.

Table A1: Initial Delayed Hydride Cracking (DHC) Initiation Tests at Notches
Unirradiated material: BB049, 240 ppm

Specimen Group	Applied K_{EFF}	Number of Specimens in Group	Specimen Failures	Measured K_{TH}	Status
	(MPa√m)			(MPa√m)	
ST-EH-1	8.0	6	4/6		Completed
ST-EH-2	7.0	6	4/6		Completed
ST-EH-3	7.5	6	1/6	6.5~7.0	Completed
ST-EH-4	6.5	6	0/6		Completed
ST-EH-5	6.0	6	0/6		Completed

Table A2: K_{IH} Test Matrix and Test Results Update
Unirradiated material: BB049, 60 ppm and 240 ppm

Material	$[H]_{eq}$ (ppm)	Specimen#	K_{IH} (MPa√m)	Temperature (°C)	Status/ Target Completion Date (TCD)
BB049	60	1st specimen	7.6	200	Completed
		2nd specimen	8.4	200	Completed
		3rd specimen	To be determined	200	In progress, TCD: December 2021
BB049	240	1st specimen	8.5	200	Completed
		2nd specimen	To be determined	200	In progress, TCD: December 2021
		3rd specimen	To be determined	200	In progress, TCD: January 2022

Table A3: p_c Test Matrix
Unirradiated material: G1770, 50 ppm and 220 ppm

Material	$[H]_{eq}$ (ppm)	Specimen Groups	Number of Specimens in Each Group	p_c (MPa)	Status/ Target Completion Date (TCD)
G1770	50	3	5~6	500~525	Historical data available
G1770	220 (nominal)	3 to 4	6	To be determined	In progress TCD January 2022

Enclosure

KINECTRICS NSS INC.

ASSESSMENT OF MARGINS AGAINST CRACK INITIATION AT CWEST SCRAPE FLAWS IN REGIONS OF INTEREST WITH HIGH

B-REP-31100-00033

REV. 0

☒ Accepted   ☐ Accepted As Noted – Revision Required

☐ Rejected   ☐ Accepted As Noted – No Revision Required

FOR USE AT BRUCE POWER

ACCEPTED: **DAVID CHO**   _(Signature)_
              (Print Name)

TITLE: **TECHNICAL ADVISOR**
              (Print Title)

DATE: **13DEC2021**
              (DDMMMYYYY)

ACCEPTANCE OF THIS DOCUMENT DOES NOT RELIEVE THE
CONTRACTOR OF RESPONSIBILITY FOR ANY ERRORS OR OMISSIONS.

*Associated with BP-PROC-00881, Supplier Document Acceptance Request Process

BRUCE B UNIT 7 2021 (B2171) FUEL CHANNEL OUTAGE SUPPORT AND DISPOSITION OUTAGE SUPPORT

ASSESSMENT OF MARGINS AGAINST CRACK INITIATION AT CWEST SCRAPE FLAWS IN REGIONS OF INTEREST WITH HIGH LEVELS OF HYDROGEN EQUIVALENT CONCENTRATION IN OUTLET ROLLED JOINTS IN BRUCE UNITS 3 AND 7

Kinectrics Report No. B2083/RP/0001 R00

Bruce Power Document No. B-REP-31100-00033

Prepared for
Bruce Power

Issue Date

2021-Dec-14

ASSESSMENT OF MARGINS AGAINST CRACK INITIATION AT CWEST SCRAPE FLAWS IN REGIONS OF INTEREST WITH HIGH LEVELS OF HYDROGEN EQUIVALENT CONCENTRATION IN OUTLET ROLLED JOINTS IN BRUCE UNITS 3 AND 7

Kinectrics Report No. B2083/RP/0001 R00

Prepared by	Verified by	Reviewed by	Approved by
D.A. Scarth Technical Director – Fracture Programs MMC P. Doddihal Senior Scientist, MMC Date prepared December 14, 2021	C. Liu Senior Scientist MMC Date verified December 14, 2021	A.C. Wallace Technical Director MMC Date reviewed December 14, 2021	T. Hunt Service Line Director (Acting) MMC Date approved December 14, 2021

ASSESSMENT OF MARGINS AGAINST CRACK INITIATION AT CWEST SCRAPE FLAWS IN REGIONS OF INTEREST WITH HIGH LEVELS OF HYDROGEN EQUIVALENT CONCENTRATION IN OUTLET ROLLED JOINTS IN BRUCE UNITS 3 AND 7

Kinectrics Report No. B2083/RP/0001 R00

Revision History

Rev 00	Description				
	Revision 0 issued to Bruce Power.				
	Issue Date 2021-December-14	Prepared by D.A. Scarth P. Doddihal	Verified by C. Liu	Reviewed by A.C. Wallace	Approved by T. Hunt

ASSESSMENT OF MARGINS AGAINST CRACK INITIATION AT CWEST SCRAPE FLAWS IN REGIONS OF INTEREST WITH HIGH LEVELS OF HYDROGEN EQUIVALENT CONCENTRATION IN OUTLET ROLLED JOINTS IN BRUCE UNITS 3 AND 7

Kinectrics Report No. B2083/RP/0001 R00

Executive Summary

High levels of hydrogen equivalent concentration (H_{eq}) have been detected in the outlet rolled joints of Bruce Unit 3, as well as in the outlet rolled joint of the surveillance pressure tube B6S13. The axial and radial extents of the high levels of H_{eq} inboard of the outlet rolled joint burnish mark have been found to be confined to a localized region with a central tendency about the top of the pressure tube. This localized region inboard of the outlet rolled joint burnish mark with a central tendency about the top of the pressure tube that has high levels of H_{eq} is referred to as the region of interest. Scrape sampling has been performed using the CWEST tool to determine levels of H_{eq} inboard of the outlet rolled joint burnish mark in Bruce Unit 3 during the A2131 outage, and in Bruce Unit 7 during the B2171 outage, including in the region of interest. There is currently uncertainty regarding the potential effect of high levels of H_{eq} in the region of interest on the crack initiation properties of pressure tube material. Due to the current uncertainty, a margin assessment for demonstration of protection against crack initiation from the CWEST scrape flaws inboard of the outlet rolled joint burnish mark in Bruce Unit 3 taken during the A2131 outage, and in Bruce Unit 7 taken during the B2171 outage, has been performed.

The margin assessment consisted of two approaches. The first approach was to evaluate the scrape flaws using the flaw assessment computer code PTFAP with a conservative characterization of the entry and exit corner root radii of the axial component of the scrape flaws. The objective was to determine the margins against crack initiation using the Delayed Hydride Cracking (DHC) initiation material properties and crack initiation models in the CSA Standard N285.8. The predicted margins against crack initiation from the PTFAP evaluations are substantial in terms of addressing uncertainty in crack initiation material properties at high levels of H_{eq} in the region of interest.

The second approach was a sensitivity evaluation of DHC initiation of the axial component of the scrape flaws using a representative characterization of the entry and exit corner root radii based on measurements from replicas of scrape flaws. The sensitivity of the results of the DHC initiation evaluation of the scrape flaws to the threshold stress intensity factor for DHC initiation from a crack, K_{IH}, and the threshold stress for DHC initiation at a planar surface, p_c, which are used in the evaluation, was determined. The sensitivity of the results of the DHC initiation evaluation to the scrape flaw depth, and entry and exit corner root radii, was also determined. The objective was to demonstrate that DHC initiation will not occur at the scrape flaws for a range of postulated levels of K_{IH} and p_c including very low values that are considered to be unlikely even at high levels of H_{eq}. The sensitivity evaluation was based on three-dimensional elastic finite element stress analyses of the scrape flaws and a process-zone model for DHC initiation that was developed in this report.

For all cases of the sensitivity evaluation of DHC initiation, the DHC initiation material properties K_{IH} and p_c can be simultaneously reduced from their lower-bound values by 50% and DHC initiation is predicted to still not occur. A 50% reduction in K_{IH} and p_c at high levels of H_{eq}

Proprietary and Confidential

ASSESSMENT OF MARGINS AGAINST CRACK INITIATION AT CWEST SCRAPE FLAWS IN REGIONS OF INTEREST WITH HIGH LEVELS OF HYDROGEN EQUIVALENT CONCENTRATION IN OUTLET ROLLED JOINTS IN BRUCE UNITS 3 AND 7

Kinectrics Report No. B2083/RP/0001 R00

is unlikely. There is therefore a low risk of DHC initiation at CWEST scrape flaws in the region of interest in the outlet rolled joints with potentially high levels of H_{eq} in Bruce Units 3 and 7 due to the large predicted margins against DHC initiation. The major contributor to the DHC initiation resistance at the scrape flaws is the threshold stress for DHC initiation at a planar surface, p_c. At the time of writing this report, DHC initiation tests on unirradiated pressure tube material with a high level of H_{eq} are in progress to confirm that the lower levels of p_c that were postulated in the sensitivity evaluation are unlikely.

ASSESSMENT OF MARGINS AGAINST CRACK INITIATION AT
CWEST SCRAPE FLAWS IN REGIONS OF INTEREST WITH
HIGH LEVELS OF HYDROGEN EQUIVALENT
CONCENTRATION IN OUTLET ROLLED JOINTS IN BRUCE
UNITS 3 AND 7

Kinectrics Report No.
B2083/RP/0001 R00

Table of Contents

Page No.

ASSESSMENT OF MARGINS AGAINST CRACK INITIATION AT CWEST SCRAPE FLAWS IN REGIONS OF INTEREST WITH HIGH LEVELS OF HYDROGEN EQUIVALENT CONCENTRATION IN OUTLET ROLLED JOINTS IN BRUCE UNITS 3 AND 7

Kinectrics Report No. B2083/RP/0001 R00

ASSESSMENT OF MARGINS AGAINST CRACK INITIATION AT CWEST SCRAPE FLAWS IN REGIONS OF INTEREST WITH HIGH LEVELS OF HYDROGEN EQUIVALENT CONCENTRATION IN OUTLET ROLLED JOINTS IN BRUCE UNITS 3 AND 7

Kinectrics Report No. B2083/RP/0001 R00

List of Tables

ASSESSMENT OF MARGINS AGAINST CRACK INITIATION AT CWEST SCRAPE FLAWS IN REGIONS OF INTEREST WITH HIGH LEVELS OF HYDROGEN EQUIVALENT CONCENTRATION IN OUTLET ROLLED JOINTS IN BRUCE UNITS 3 AND 7

Kinectrics Report No. B2083/RP/0001 R00

List of Figures

Page No.

Proprietary and Confidential

ASSESSMENT OF MARGINS AGAINST CRACK INITIATION AT CWEST SCRAPE FLAWS IN REGIONS OF INTEREST WITH HIGH LEVELS OF HYDROGEN EQUIVALENT CONCENTRATION IN OUTLET ROLLED JOINTS IN BRUCE UNITS 3 AND 7

Kinectrics Report No.
B2083/RP/0001 R00

ASSESSMENT OF MARGINS AGAINST CRACK INITIATION AT CWEST SCRAPE FLAWS IN REGIONS OF INTEREST WITH HIGH LEVELS OF HYDROGEN EQUIVALENT CONCENTRATION IN OUTLET ROLLED JOINTS IN BRUCE UNITS 3 AND 7

Kinectrics Report No. B2083/RP/0001 R00

List of Acronyms and Symbols

Acronyms

CSA	=	Canadian Standards Association
CWEST	=	Circumferential Wet Scrape Tool
DHC	=	Delayed Hydride Cracking
EFPH	=	Equivalent Full Power Hours
MCR	=	Major Component Replacement
ROH	=	Reactor Outlet Header

Symbols

a	=	depth of the scrape flaw
A_0	=	stress coefficient for the uniform term of the stress distribution
A_1	=	stress coefficient for the linear gradient term of the stress distribution
A_j	=	stress coefficient for the jth power term of the stress distribution
d	=	remaining wall thickness of the pressure tube at the scrape flaw
d_{FL}	=	distance between the axial location of the scrape flaw in the outlet rolled joint and the inlet end of the pressure tube
E	=	Young's modulus of the Zr-Nb pressure tube material
$F_b(s/d)$	=	geometry correction factor for the stress intensity factor for the bending stress, σ_b
$F_m(s/d)$	=	geometry correction factor for the stress intensity factor for the membrane stress, σ_m
$G_0(s/d)$	=	geometry correction factor for the stress intensity factor for the uniform term, A_0, of the linear stress distribution
$G_1(s/d)$	=	geometry correction for the stress intensity factor for the linear gradient term, A_1, of the linear stress distribution
$G_j(s/d)$	=	geometry correction factor for the stress intensity factor for the jth power term of the stress distribution
H_{eq}	=	hydrogen equivalent concentration
K_I	=	stress intensity factor
$K_I(s,p_c)$	=	stress intensity factor for the process-zone length, s, and the process-zone restraining stress, p_c
$K_I(s,\sigma(x))$	=	stress intensity factor for the process-zone length, s, and the stress distribution, $\sigma(x)$
$K_I(s,\sigma_b)$	=	stress intensity factor for the process-zone length, s, and the bending stress, σ_b
$K_I(s,\sigma_m)$	=	stress intensity factor for the process-zone length, s, and the membrane stress, σ_m
K_{IH}	=	isothermal threshold stress intensity factor for DHC initiation from a crack

ASSESSMENT OF MARGINS AGAINST CRACK INITIATION AT CWEST SCRAPE FLAWS IN REGIONS OF INTEREST WITH HIGH LEVELS OF HYDROGEN EQUIVALENT CONCENTRATION IN OUTLET ROLLED JOINTS IN BRUCE UNITS 3 AND 7

Kinectrics Report No. B2083/RP/0001 R00

k_t	=	elastic stress concentration factor with internal pressure on the flaw face
L_{PT}	=	length of the pressure tube
p_c	=	threshold stress for DHC initiation at a planar surface, or process-zone restraining stress
p_{eq}	=	equivalent internal pressure that is applied in the finite element stress analysis to account for the rolled joint residual hoop stress
p_H	=	process-zone restraining stress
p_{op}	=	operating internal pressure
Δp_{ROH}	=	pressure differential between the axial location of the scrape flaw in the outlet rolled joint and the ROH
$\Delta p_{ROH}{}^{in}$	=	pressure differential between the thermalhydraulic inlet of the fuel channel and the ROH
$\Delta p_{ROH}{}^{out}$	=	pressure differential between the thermalhydraulic outlet of the fuel channel and the ROH
R_i	=	pressure tube inside radius
s	=	process-zone length
T	=	temperature
$TSSD$	=	Terminal Solid Solubility for Hydride Dissolution
$TSSP$	=	Terminal Solid Solubility for Hydride Precipitation
$V_0(s/d)$	=	geometry factor for the crack-mouth opening displacement for the uniform term, A_0, of the linear stress distribution
$V_1(s/d)$	=	geometry factor for the crack-mouth opening displacement for the linear gradient term, A_1, of the linear stress distribution
$V_j(s/d)$	=	geometry factor for the crack-mouth opening displacement for the jth power term of the stress distribution
$V_b(s/d)$	=	geometry factor for the crack-mouth opening displacement for the bending stress, σ_b
$V_m(s/d)$	=	geometry factor for the crack-mouth opening displacement for the membrane stress, σ_m
v_c	=	critical process-zone displacement for DHC initiation
v_T	=	applied process-zone displacement
$v_T(s,p_c)$	=	crack-mouth opening displacement for the process-zone length, s, and the process-zone restraining stress, p_c
$v_T(s,\sigma(x))$	=	crack-mouth opening displacement for the process-zone length, s, and the stress distribution, $\sigma(x)$
$v_T(s,\sigma_b)$	=	crack-mouth opening displacement for the process-zone length, s, and the bending stress, σ_b
$v_T(s,\sigma_m)$	=	crack-mouth opening displacement for the process-zone length, s, and the membrane stress, σ_m
w	=	pressure tube wall thickness
x	=	local coordinate with origin at the surface
$\alpha_1(s)$	=	normalized linear stress coefficient that depends on the process-zone length, s

ASSESSMENT OF MARGINS AGAINST CRACK INITIATION AT CWEST SCRAPE FLAWS IN REGIONS OF INTEREST WITH HIGH LEVELS OF HYDROGEN EQUIVALENT CONCENTRATION IN OUTLET ROLLED JOINTS IN BRUCE UNITS 3 AND 7

Kinectrics Report No.
B2083/RP/0001 R00

β_j	=	normalized stress coefficient for the jth power term of the fitted fourth-order polynomial normalized stress distribution
ρ_s	=	corner root radius of the entry and exit of the CWEST scrape flaw
υ	=	Poisson's ratio of the Zr-Nb pressure tube material
$\sigma(x)$	=	elastic stress distribution through the wall thickness
σ_{1p}	=	peak flaw-tip principal stress
σ_a	=	nominal axial stress due to internal pressure
σ_b	=	bending stress across the remaining wall thickness, d
$\sigma_F(x)$	=	elastic stress distribution through the wall thickness from the fitted fourth-order polynomial stress distribution
σ_h	=	total nominal hoop stress due to internal pressure and rolled joint residual hoop stress
σ_{hres}	=	rolled joint residual hoop stress
σ_m	=	membrane stress across the remaining wall thickness, d
σ_{th}	=	threshold peak stress for DHC initiation

ASSESSMENT OF MARGINS AGAINST CRACK INITIATION AT
CWEST SCRAPE FLAWS IN REGIONS OF INTEREST WITH
HIGH LEVELS OF HYDROGEN EQUIVALENT
CONCENTRATION IN OUTLET ROLLED JOINTS IN BRUCE
UNITS 3 AND 7

Kinectrics Report No.
B2083/RP/0001 R00

1.   INTRODUCTION

High levels of hydrogen equivalent concentration (H_{eq}) have been detected in the outlet rolled joints of Bruce Unit 3 [1], as well as in the outlet rolled joint of the surveillance pressure tube B6S13 [2]. The axial and radial extents of the high levels of H_{eq} inboard of the outlet rolled joint burnish mark have been found to be confined to a localized region with a central tendency about the top of the pressure tube. This localized region inboard of the outlet rolled joint burnish mark with a central tendency about the top of the pressure tube that has high levels of H_{eq} is referred to as the region of interest. Scrape sampling has been performed using the Circumferential Wet Scrape Tool (CWEST) to determine levels of H_{eq} inboard of the outlet rolled joint burnish mark in Bruce Unit 3 during the A2131 outage, and in Bruce Unit 7 during the B2171 outage, including in the region of interest.

The CWEST scrape flaw is an engineered "flaw". A margin assessment for demonstration of protection against crack initiation from the scrape flaws located 20 mm inboard of the burnish mark in the outlet rolled joints in Bruce Unit 3 was provided in Reference [3]. There is currently uncertainty regarding the potential effect of high levels of H_{eq} in the region of interest on the crack initiation properties of pressure tube material. Due to the current uncertainty, a more extensive margin assessment for demonstration of protection against crack initiation from the CWEST scrape flaws located 20 mm inboard of the outlet rolled joint burnish mark in Bruce Unit 3 taken during the A2131 outage, and in Bruce Unit 7 taken during the B2171 outage, has been performed.

The margin assessment consisted of two approaches. The first approach was to evaluate the scrape flaws using the flaw assessment computer code PTFAP with a conservative characterization of the entry and exit corner root radii of the axial component of the scrape flaws. The objective was to determine the margins against crack initiation using the Delayed Hydride Cracking (DHC) initiation material properties and crack initiation models in the CSA Standard N285.8.

The second approach was a sensitivity evaluation of DHC initiation of the axial component of the scrape flaws using a representative characterization of the entry and exit corner root radii based on measurements from replicas of scrape flaws. The sensitivity of the results of the DHC initiation evaluation of the scrape flaws to the threshold stress intensity factor for DHC initiation from a crack, K_{IH}, and the threshold stress for DHC initiation at a planar surface, p_c, was determined. The sensitivity of the results of the DHC initiation evaluation to the scrape flaw depth, and entry and exit corner root radii, was also determined. The objective was to demonstrate that DHC initiation will not occur at the scrape flaws for a range of postulated levels of K_{IH} and p_c including very low values that are considered to be unlikely even at high levels of H_{eq} in the region of interest. The sensitivity evaluation was based on three-dimensional elastic finite element stress analyses of the scrape flaws and a process-zone model for DHC initiation that was developed in this report.

This work was performed for Bruce Power.

ASSESSMENT OF MARGINS AGAINST CRACK INITIATION AT
CWEST SCRAPE FLAWS IN REGIONS OF INTEREST WITH
HIGH LEVELS OF HYDROGEN EQUIVALENT
CONCENTRATION IN OUTLET ROLLED JOINTS IN BRUCE
UNITS 3 AND 7

Kinectrics Report No.
B2083/RP/0001 R00

2. OVERVIEW OF MARGIN ASSESSMENT

As described above, the axial and radial extents of the high levels of H_{eq} inboard of the outlet rolled joint burnish mark have been found to be confined to a localized region with a central tendency about the top of the pressure tube and is referred to as the region of interest. The key elements of the margin assessment for demonstration of protection against crack initiation from scrape flaws located 20 mm inboard of the burnish mark in the region of interest in the outlet rolled joints in Bruce Units 3 and 7 are summarized below.

(a) The geometry of the CWEST scrape flaws was established in Section 3 of this report. A representative value for the root radius of the entry and exit corners of the scrape flaw that is based on measurements from replicas of scrape flaws was reviewed and used in the evaluation based on three-dimensional elastic finite element stress analyses and a process-zone model for DHC initiation.

(b) An evaluation of the CWEST scrape flaws inboard of the outlet rolled joint burnish mark in Bruce Unit 3 pressure tubes taken during the A2131 outage was performed using the computer code PTFAP [4]. The margins for demonstration of protection against crack initiation due to DHC, hydrided region overloads and fatigue are quantified in Section 4.

(c) An evaluation of the CWEST scrape flaws inboard of the outlet rolled joint burnish mark in Bruce Unit 7 pressure tubes taken during the B2171 outage was performed using the computer code PTFAP. The margins for demonstration of protection against crack initiation due to DHC, hydrided region overloads and fatigue are quantified in Section 5.

(d) Three-dimensional, elastic finite element stress analyses of representative and conservative scrape flaw entry and exit corner root radii were performed as described in Section 6. The results of the stress analyses were used in the sensitivity evaluation of DHC initiation at the axial component of the scrape flaws in region of interest in outlet rolled joints in Bruce Units 3 and 7 as described in Section 8.

(e) A process-zone model that is applicable to the evaluation of DHC initiation at the axial component of a CWEST scrape flaw was developed as described in Appendix A of this report. The calculation procedure based on the process-zone model is described in Section 7.

(f) The sensitivity of the DHC initiation evaluation of the scrape flaws to the threshold stress intensity factor for DHC initiation from a crack, K_{IH}, and the threshold stress for DHC initiation at a planar surface, p_c, was determined for the representative scrape flaw entry and exit corner root radii using three-dimensional elastic finite element stress analysis and the process-zone model. The sensitivity of the evaluation results to a variation in the scrape flaw depth, and the scrape flaw entry and exit corner root radii, was also determined. The sensitivity evaluation is described in Section 8.

(g) A summary of the results of the margin assessment is described in Section 9.

ASSESSMENT OF MARGINS AGAINST CRACK INITIATION AT
CWEST SCRAPE FLAWS IN REGIONS OF INTEREST WITH
HIGH LEVELS OF HYDROGEN EQUIVALENT
CONCENTRATION IN OUTLET ROLLED JOINTS IN BRUCE
UNITS 3 AND 7

Kinectrics Report No.
B2083/RP/0001 R00

3.   GEOMETRY OF CWEST SCRAPE FLAWS

The CWEST scrape flaw is an engineered "flaw". The flaw resulting from the scraping operation using the CWEST tool is shown schematically in Figure 3-1. The cutter enters and exits in the circumferential direction. Two cuts are made during the material removal process. The first cut is a wide, shallower cut to remove surface oxide, followed by a second cut that is a narrower, deeper cut taken within the footprint of the first cut to collect sample material. The top view of a scrape flaw is shown in Figure 3-2.

The cross-section of a scrape flaw in the radial-circumferential plane of the pressure tube, corresponding to Section A-A in Figure 3-2, is shown in Figure 3-3. The scrape tool is designed to remove material up to a total depth of 0.384 mm [5,6]. Accordingly, the maximum scrape flaw depth used in the evaluations in this report is 0.384 mm. The actual total cut depths by the tool are expected to be less than the maximum depth of 0.384 mm. Before deploying the CWEST tool on channel, 60 cuts are performed as part of Tool Demonstration Testing [6] and the measured total depths were found to be not deeper than 0.323 mm. A scrape flaw depth of 0.323 mm was also used in the sensitivity evaluation of DHC initiation using the process-zone model in Sections 6 and 8 of this report to determine the sensitivity of the evaluation results to the scrape flaw depth. A circumferential arc length of 15° has been specified in [6] and has been used as the length of the circumferential component of the scrape flaw in the evaluations in this report.

The corner root radius for the total scrape flaw depth is from the sample cut, and the sample cut root radius was used in the evaluation. A review was performed in Reference [7] of root radii of sample cuts from available replica images from test cut coupons generated using different tool heads deployed in the 2021 Bruce Unit 3 A2131 and Bruce Unit 7 B2171 outages, and in outages from another utility, including an in-situ replica of a CWEST scrape flaw. The entry and exit corner root radii of the sample cuts were measured. An example of a replica with the measured root radius is shown in Figure 3-4. Based on the review in Reference [7], which included 23 measurements, a value of 1.7 mm was the lowest measured value and was recommended as the representative root radius for evaluations. As described in Section 2 of this report, the CWEST scrape flaws have been evaluated using the flaw evaluation computer code PTFAP [4], as well as a process-zone model for DHC initiation. The PTFAP evaluations were performed for a conservative entry and exit root radius equal to the flaw depth of 0.384 mm to be within the validity limits of the stress concentration factor equations and the crack initiation models in PTFAP.

The cross-section of a scrape flaw in the radial-axial plane of the pressure tube, corresponding to Section B-B in Figure 3-2, is shown in Figure 3-5. The root radii of the corners of the sample cut are equal to 0.330 mm, corresponding to the minimum nominal value provided in [6]. The width of the cut (axial length of the scrape flaw) is primarily determined by the width of the cutter tips and is 6.17 mm for the oxide cut and 5.03 mm for the sample cut [6]. A bounding width of 6.2 mm was used as the length of the axial component of the scrape flaw in the evaluations.

ASSESSMENT OF MARGINS AGAINST CRACK INITIATION AT CWEST SCRAPE FLAWS IN REGIONS OF INTEREST WITH HIGH LEVELS OF HYDROGEN EQUIVALENT CONCENTRATION IN OUTLET ROLLED JOINTS IN BRUCE UNITS 3 AND 7

Kinectrics Report No. B2083/RP/0001 R00
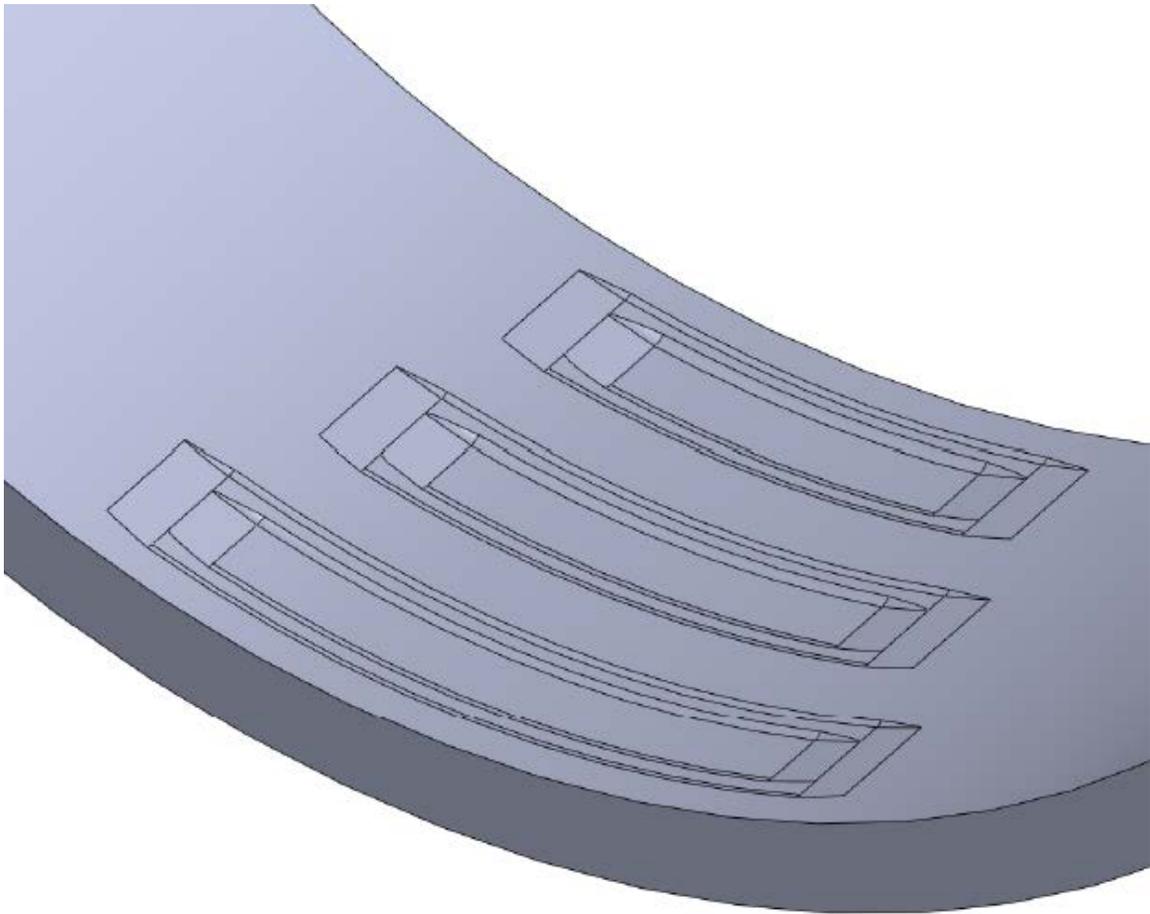
Figure 3-1: Illustration of CWEST Scrape Flaws

ASSESSMENT OF MARGINS AGAINST CRACK INITIATION AT CWEST SCRAPE FLAWS IN REGIONS OF INTEREST WITH HIGH LEVELS OF HYDROGEN EQUIVALENT CONCENTRATION IN OUTLET ROLLED JOINTS IN BRUCE UNITS 3 AND 7

Kinectrics Report No. B2083/RP/0001 R00
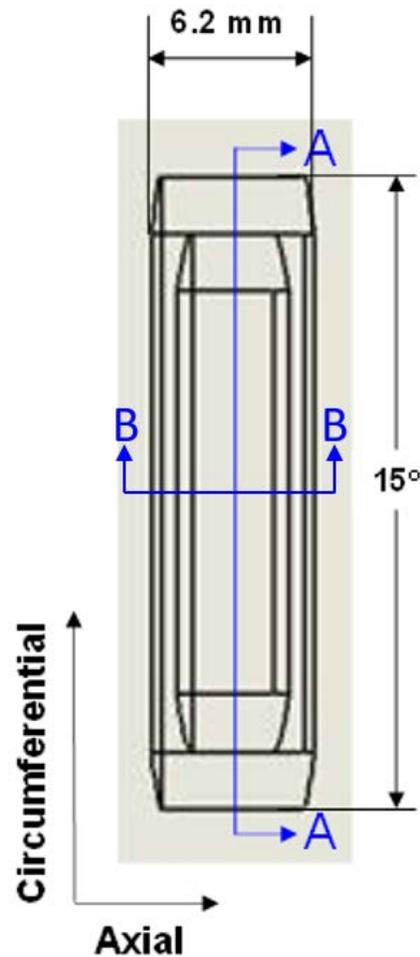
Figure 3-2: Top View of CWEST Scrape Flaw

ASSESSMENT OF MARGINS AGAINST CRACK INITIATION AT CWEST SCRAPE FLAWS IN REGIONS OF INTEREST WITH HIGH LEVELS OF HYDROGEN EQUIVALENT CONCENTRATION IN OUTLET ROLLED JOINTS IN BRUCE UNITS 3 AND 7

Kinectrics Report No. B2083/RP/0001 R00
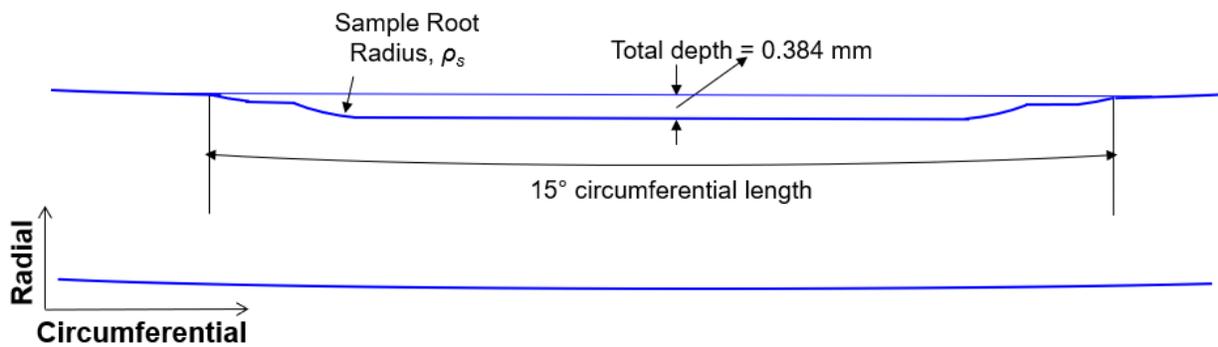
Figure 3-3: CWEST Scrape Flaw Geometry in the Radial-Circumferential Plane of the Pressure Tube (Section A-A of Figure 3-2)

ASSESSMENT OF MARGINS AGAINST CRACK INITIATION AT CWEST SCRAPE FLAWS IN REGIONS OF INTEREST WITH HIGH LEVELS OF HYDROGEN EQUIVALENT CONCENTRATION IN OUTLET ROLLED JOINTS IN BRUCE UNITS 3 AND 7

Kinectrics Report No. B2083/RP/0001 R00
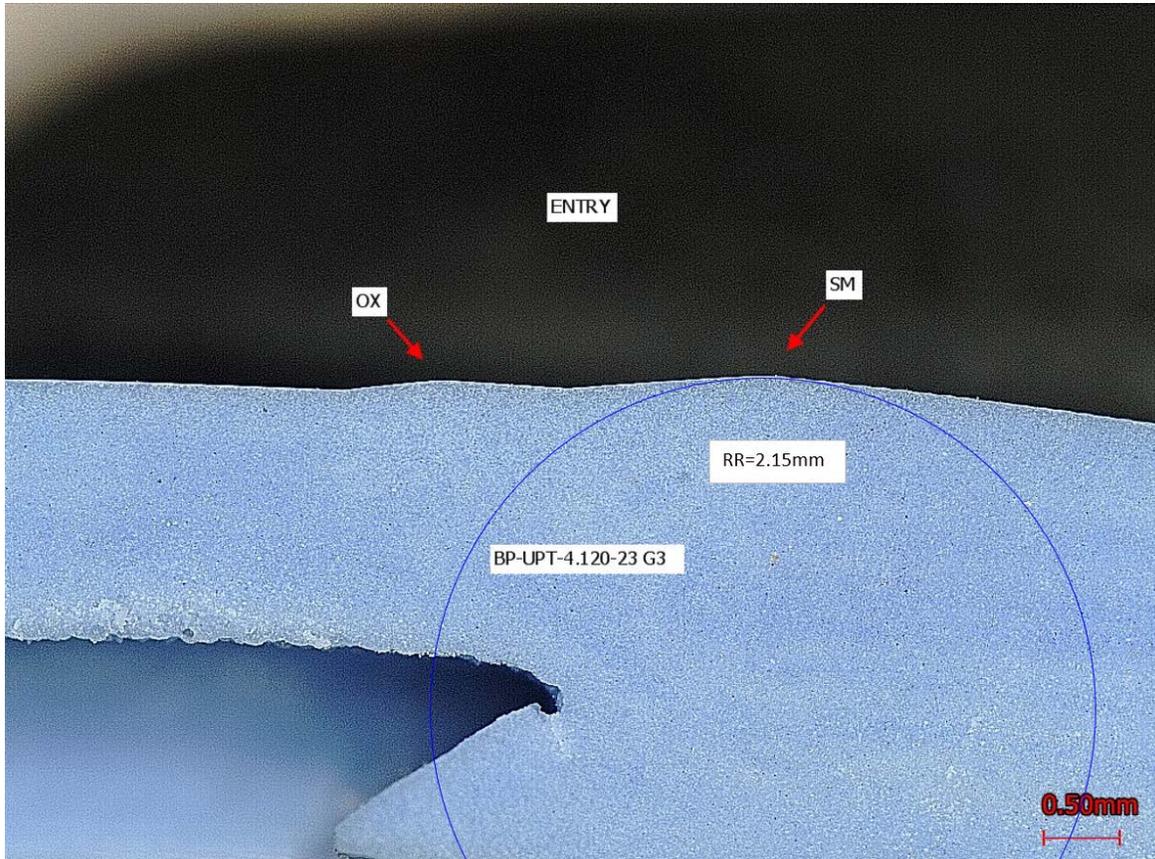
OX: Oxide cut
SM: Sample cut
RR: Root radius
The image shows the measured entry root radius of the sample cut.

Figure 3-4: Replica of CWEST Scrape Flaw with Fitted Corner Root Radius of the Sample Cut
(Figure 13 of Reference [7])

ASSESSMENT OF MARGINS AGAINST CRACK INITIATION AT CWEST SCRAPE FLAWS IN REGIONS OF INTEREST WITH HIGH LEVELS OF HYDROGEN EQUIVALENT CONCENTRATION IN OUTLET ROLLED JOINTS IN BRUCE UNITS 3 AND 7

Kinectrics Report No. B2083/RP/0001 R00
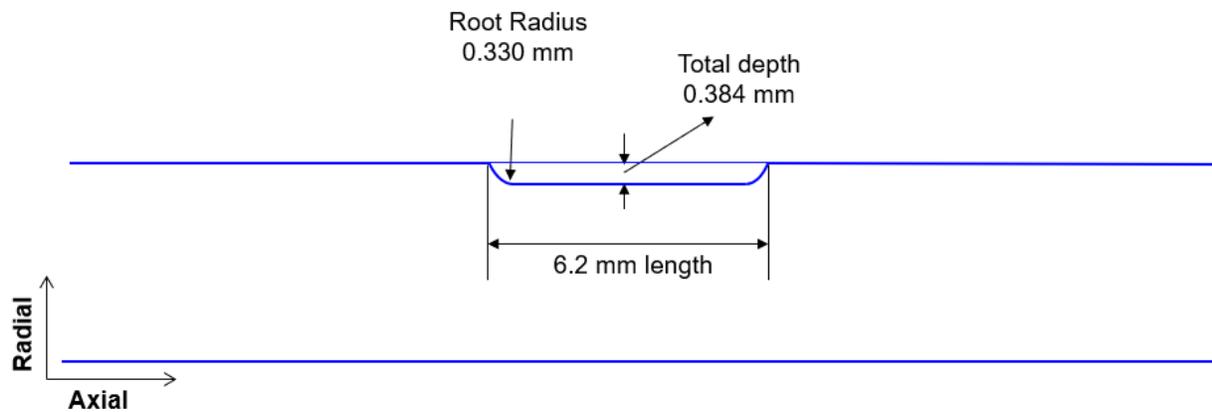
Figure 3-5: CWEST Scrape Flaw Geometry in the Radial-Axial Plane of the Pressure Tube (Section B-B of Figure 3-2)

ASSESSMENT OF MARGINS AGAINST CRACK INITIATION AT CWEST SCRAPE FLAWS IN REGIONS OF INTEREST WITH HIGH LEVELS OF HYDROGEN EQUIVALENT CONCENTRATION IN OUTLET ROLLED JOINTS IN BRUCE UNITS 3 AND 7

Kinectrics Report No. B2083/RP/0001 R00

4. MARGIN ASSESSMENT BASED ON PTFAP FOR CWEST SCRAPE FLAWS IN THE REGION OF INTEREST WITH HIGH HYDROGEN EQUIVALENT CONCENTRATIONS IN OUTLET ROLLED JOINTS IN BRUCE UNIT 3

An evaluation of the acceptability of the CWEST scrape flaws inboard of the outlet rolled joint burnish mark in Bruce Unit 3 pressure tubes taken during the A2131 outage has been performed as described in Reference [8]. The evaluation was performed using PTFAP V5-1 [4,9], which implements the requirements of Clause 5 of the CSA Standard N285.8-15 [10]. The evaluation was performed to an end of evaluation period of 246,000 EFPH.

The margins against crack initiation due to DHC, hydrided region overloads, and fatigue for the scrape flaws in the high levels of H_{eq} regions of interest inboard of the burnish mark in outlet rolled joints in Bruce Unit 3 are provided in this section.

4.1 Overview of PTFAP Evaluation of CWEST Scrape Flaws Inboard of the Outlet Rolled Joint Burnish Mark in Bruce Unit 3

4.1.1 Methodology

Each CWEST scrape flaw was resolved into axial and circumferential components. The axial component of each scrape flaw was treated as volumetric and assessed for crack initiation due to DHC under sustained loading conditions, hydrided region overloads, fatigue, and for minimum safety factors against plastic collapse. The circumferential component of each CWEST scrape flaw was treated as planar and assessed for flaw growth due to fatigue and DHC, as well as for minimum safety factors against plastic collapse and fracture initiation.

Scrape sampling in the outlet rolled joint region was performed at the three locations given below [11] to better characterize the H_{eq} profiles.

- 20 mm inboard of the outlet burnish mark
- 43 mm inboard of the outlet burnish mark
- nominally 303 mm inboard of the outlet burnish mark

The scrape flaws at 20 mm inboard of the outlet rolled joint burnish mark are subjected to rolled joint residual stresses. For Bruce Unit 3, the rolled joint type is normal clearance, non-overextended and stress relieved. The rolled joint residual stress relaxes with time due to thermal creep. The residual stress relaxation is dependent on the channel-specific operating temperature, and varies slightly for each pressure tube. Since the scrape flaw at 20 mm inboard of the outlet rolled joint burnish mark is subjected to residual stresses, with a higher total stress compared to the other two scrape locations, the scrape flaw at the 20 mm location is bounding in terms of margins against crack initiation due to DHC and hydrided region overloads. A bounding evaluation was performed in Reference [8] for scrape flaws at the 20 mm location inboard of the outlet rolled joint burnish mark. The bounding evaluation was performed for all

ASSESSMENT OF MARGINS AGAINST CRACK INITIATION AT CWEST SCRAPE FLAWS IN REGIONS OF INTEREST WITH HIGH LEVELS OF HYDROGEN EQUIVALENT CONCENTRATION IN OUTLET ROLLED JOINTS IN BRUCE UNITS 3 AND 7

Kinectrics Report No. B2083/RP/0001 R00

channels scraped during the A2131 outage in the outlet rolled joint region and operated in the fuelled condition.

Since there are no scrape flaws that are located at a distance less than 20 mm inboard of the burnish mark in the outlet rolled joints in Bruce Unit 3, the evaluation was performed only for scrape flaws at a location 20 mm inboard of the burnish mark. The results of the evaluation would be applicable to scrape flaws that are located at a distance less than 20 mm inboard of the burnish mark based on the rationale given below.

(a) Any variation in the pressure tube dimensions and internal pressure over a distance within 20 mm inboard of the burnish mark is insignificant. From Clause A.4.4.4 of Annex A of the CSA Standard N285.8 [10], for a normal clearance, non-overextended and stress relieved rolled joint, there is no credit for end fitting support at a distance of 20 mm inboard of the burnish mark. If a scrape flaw was located within 10 mm inboard of the burnish mark, end fitting support could be credited to reduce the hoop stress due to internal pressure by 5%. For a scrape flaw located within 10 mm inboard of the burnish mark, the use of the evaluation results for a scrape flaw located 20 mm inboard of the burnish mark would be conservative.

(b) The rolled joint residual stresses that are used in the evaluation are the maximum in the rolled joint region, and are applicable to any location within a distance of 20 mm inboard of the burnish mark.

Three channels are being operated in a defuelled state in Bruce Unit 3. These three channels have been scraped, and the recommended bounding H_{eq} at a distance of 20 mm inboard of the outlet rolled joint burnish mark at the end of the evaluation period is 100 ppm [1]. The margin assessment for Bruce Unit 3 was therefore performed for scrape flaws in fuelled channels only.

4.1.2 Inputs for Crack Initiation Evaluation

Pressure Tube Dimensions: Conservative pressure tube dimensions calculated at 250,000 EFPH, which bounds the end of the evaluation period of 246,000 EFPH, [12] were used.

Flaw Location: The evaluation in Reference [8] was performed for scrape flaws at the 20 mm location inboard of the outlet rolled joint burnish mark. The flaw rotary start is 350° with respect to the inspection end and measured clockwise from the top of the pressure tube.

Flaw Geometry: The CWEST scrape is circumferentially oriented, with an axial length of 6.2 mm, a circumferential length of 15 degrees, and a maximum depth of 0.384 mm. The flaw geometry of the axial component was evaluated as a bearing pad fretting flaw with an axial length of 6.2 mm and a depth of 0.384 mm. From Section 3 of this report, the lowest measured corner root radius of the sample scrapes of 1.7 mm is recommended as a representative value for evaluations [7]. The more conservative root radius of the entry and exit corners of the scrape flaw of 0.384 mm that is equal to the flaw depth was used to remain within the root radius

Proprietary and Confidential

ASSESSMENT OF MARGINS AGAINST CRACK INITIATION AT CWEST SCRAPE FLAWS IN REGIONS OF INTEREST WITH HIGH LEVELS OF HYDROGEN EQUIVALENT CONCENTRATION IN OUTLET ROLLED JOINTS IN BRUCE UNITS 3 AND 7

Kinectrics Report No. B2083/RP/0001 R00

validity limits of the equations for the stress concentration factor and the crack initiation models. The circumferential component of the scrape flaw was evaluated as a planar flaw.

Flaw Formation Time: The flaw formation time and inspection time were 231,964 EFPH that is the operating time to the A2131 outage.

Operating and Loading Conditions: The operating pressures and temperatures specific to the flaw location were calculated in PTFAP. As stated above, for Bruce Unit 3, the rolled joint type is normal clearance, non-overextended and stress relieved. The rolled joint residual stress relaxes with time due to thermal creep. The rolled joint residual hoop stresses at the scrape flaws were calculated in PTFAP at the current time of 231,964 EFPH, and these residual hoop stresses were used in the flaw evaluations.

Hydrogen Equivalent Concentration: An H_{eq} of 220 ppm at the end of evaluation period of 246,000 EFPH was used in the evaluation of the scrape flaws at the 20 mm location inboard of the outlet rolled joint burnish mark as recommended in [1]. This level of H_{eq} is significantly higher than the H_{eq} at the onset of hydride ratcheting at fuel channel outlet operating temperatures of nominally 65 ppm or lower [10]. Under hydride ratcheting conditions, the predictions from the crack initiation models are not dependent on the level of H_{eq} [10]. The onset of hydride precipitation is predicted to occur at the temperature at which the Terminal Solid Solubility for Hydride Precipitation (*TSSP*) is equal to the hydrogen equivalent concentration in solution [10]. The hydrogen equivalent concentration in solution is equal to the product of the Terminal Solid Solidity for Hydride Dissolution (*TSSD*) at the peak temperature times an amplification factor that depends on the peak flaw-tip stress. For levels of bulk H_{eq} that are greater than *TSSD* at the peak temperature, as in the case of scrape flaws in the region of interest in outlet rolled joints in Bruce Unit 3, the hydrogen equivalent concentration in solution at the peak temperature does not increase with higher levels of the bulk H_{eq}. The temperature at the onset of hydride precipitation therefore also does not increase with an increase in the level of bulk H_{eq} beyond *TSSD* at the peak temperature.

4.1.3   Results

The DHC, hydrided region overload and fatigue crack initiation evaluation results for the axial component of the scrape flaws are summarized in Table 4-1. From Table 4-1, crack initiation due to DHC, hydrided region overloads and fatigue is predicted to not occur up to the end of the evaluation period of 246,000 EFPH. The detailed evaluation results, including the results for the plastic collapse evaluation, are provided in Reference [8]. The axial component of the scrape flaws satisfies the requirements of the CSA Standard N285.8-15 [10] until the end of the evaluation period as given in Reference [8].

The DHC and fatigue crack growth evaluation results for the circumferential component of the scrape flaws are summarized in Table 4-2. Crack growth due to DHC is predicted to not occur up to the end of the evaluation period for the flaw dimensions that include postulated fatigue crack growth. The detailed evaluation results, including the results for the fracture initiation and

Proprietary and Confidential

ASSESSMENT OF MARGINS AGAINST CRACK INITIATION AT CWEST SCRAPE FLAWS IN REGIONS OF INTEREST WITH HIGH LEVELS OF HYDROGEN EQUIVALENT CONCENTRATION IN OUTLET ROLLED JOINTS IN BRUCE UNITS 3 AND 7

Kinectrics Report No. B2083/RP/0001 R00

plastic collapse evaluation, are provided in Reference [8]. The circumferential component of the scrape flaws satisfies the requirements of the CSA Standard N285.8-15 until the end of the evaluation period as given in Reference [8].

4.2 Margins Against Crack Initiation due to DHC, Hydrided Region Overloads and Fatigue for Axial Component of CWEST Scrape Flaws Inboard of the Outlet Rolled Joint Burnish Mark in Bruce Unit 3

4.2.1 Margins Against Crack Initiation due to DHC

The onset of hydride precipitation was predicted to occur during reactor Cooldown over the temperature range below 250°C and at a reduced pressure [8]. For the DHC initiation evaluation, the peak flaw-tip stress that is relevant is the peak stress at the pressure and temperature during reactor Cooldown at the onset of flaw-tip hydride precipitation [10]. The factor on the DHC initiation threshold stress, which is the ratio of the predicted threshold peak flaw-tip stress for DHC initiation divided by the applied peak flaw-tip stress at hydride precipitation during Cooldown, is provided in Table 4-1. The factor on the DHC initiation threshold stress ranges from 1.67 to 1.78, with the minimum being 1.67 for the scrape flaw in pressure tube B3N04. The highest H_{eq} at the 20 mm location inboard of the outlet rolled joint burnish mark during the A2131 scrape campaign was measured in pressure tube B3F16. The factor on the DHC initiation threshold stress for pressure tube B3F16 is 1.72. Based on these results, the threshold peak stress for DHC initiation at the high levels of H_{eq} could be reduced by as much as 40% relative to the predicted threshold peak stress in the PTFAP evaluation and DHC initiation would still be predicted to not occur.

4.2.2 Margins Against Crack Initiation due to a Hydrided Region Overload

The factor on the critical stress for crack initiation due to a hydrided region overload, which is the ratio of the critical stress for crack initiation due to a hydrided region overload divided by the maximum applied stress during the overload event, is provided in Table 4-1. The factor on the critical stress for crack initiation due to a hydrided region overload ranges from 2.34 to 2.47, with the minimum being 2.34 for pressure tube B3N04. The factor for pressure tube B3F16 is 2.40. Based on these results, the critical stress for crack initiation due to a hydrided region overload at the high levels of H_{eq} could be reduced by as much as 57% relative to the predicted critical stress for crack initiation due to a hydrided region overload in the PTFAP evaluation and crack initiation due to a hydrided region overload would still be predicted to not occur.

4.2.3 Margins Against Crack Initiation due to Fatigue

From Table 4-1, the cumulative fatigue usage factor for the scrape flaws in the outlet rolled joints of all of the pressure tubes is only 0.002. This very low cumulative fatigue usage factor is considered to address any uncertainty in the effect of high levels of H_{eq} on the resistance to fatigue crack initiation.

ASSESSMENT OF MARGINS AGAINST CRACK INITIATION AT CWEST SCRAPE FLAWS IN REGIONS OF INTEREST WITH HIGH LEVELS OF HYDROGEN EQUIVALENT CONCENTRATION IN OUTLET ROLLED JOINTS IN BRUCE UNITS 3 AND 7

Kinectrics Report No.
B2083/RP/0001 R00

4.2.4 Unquantified Margins Against Crack Initiation for Axial Component of CWEST Scrape Flaws

The results in Table 4-1 show that there are substantial margins against crack initiation due to DHC, hydrided region overloads and fatigue. This is expected considering the shallow flaw depth of 0.384 mm and the blunt root radius of 0.384 mm used in the evaluations. In addition, as described in Section 3 of this report, the CWEST scrape flaw is an engineered "flaw". The geometry is designed to ensure that the scrape flaw does not pose a structural integrity issue for the pressure tube. From Section 3 of this report, the lowest measured corner root radius of the sample scrape of 1.7 mm is recommended as a representative value for evaluations [7]. The more conservative root radius of the entry and exit corners of the scrape flaw of 0.384 mm that is equal to the flaw depth was used to remain within the root radius validity limits of the equations for the stress concentration factor and the crack initiation models.

4.3 Margins Against Onset of DHC Growth for Circumferential Component of CWEST Scrape Flaws Inboard of the Outlet Rolled Joint Burnish Mark in Bruce Unit 3

The factor on the lower-bound threshold stress intensity factor for the onset of DHC growth from a circumferential crack, K_{IH}, of 15 MPa$\sqrt{}$m, which is the ratio of the threshold K_{IH} divided by the applied stress intensity factor, is provided in Table 4-2. The minimum factor on the lower-bound K_{IH} is 1.91. This large factor is expected considering the shallow depth of the scrape flaw. Based on these results, the threshold K_{IH} at the high levels of H_{eq} could be reduced by as much as 48% relative to the threshold K_{IH} used in the PTFAP evaluation and the onset of DHC growth would still be predicted to not occur.

ASSESSMENT OF MARGINS AGAINST CRACK INITIATION AT CWEST SCRAPE FLAWS IN REGIONS OF INTEREST WITH HIGH LEVELS OF HYDROGEN EQUIVALENT CONCENTRATION IN OUTLET ROLLED JOINTS IN BRUCE UNITS 3 AND 7

Kinectrics Report No. B2083/RP/0001 R00

TABLE 4-1: SUMMARY OF DHC, HYDRIDED REGION OVERLOAD AND FATIGUE CRACK INITIATION RESULTS FOR AXIAL COMPONENT OF SCRAPE FLAWS AT THE 20 mm LOCATION FROM OUTLET ROLLED JOINT BURNISH MARK IN ALL CHANNELS IN BRUCE UNIT 3 SCRAPED DURING THE A2131 OUTAGE AND OPERATED IN THE FUELLED CONDITION

Channel Identification	H_{eq} at Flaw Location at End of Evaluation Period of 246,000 EFPH (ppm)	Stress Concentration Factor, k_t	Normal Operating Temperature (°C)	Applied Peak Flaw-Tip Stress for DHC Initiation Evaluation (MPa)	Threshold Peak Stress for DHC Initiation (MPa)	Ratio of Threshold Peak Stress for DHC Initiation / Applied Peak Flaw-Tip Stress	Ratio of Critical Overload Stress / Applied Overload Stress	Fatigue Cumulative Usage Factor
B3F16	220	2.45	295.8	359.9	618.2	1.72	2.40	0.002
B3C11	220	2.45	300.1	348.2	618.2	1.78	2.47	0.002
B3L11	220	2.45	296.1	359.0	618.2	1.72	2.40	0.002
B3D16	220	2.45	293.3	367.0	618.2	1.68	2.35	0.002
B3D07	220	2.45	299.9	348.9	618.2	1.77	2.47	0.002
B3E20	220	2.45	299.5	350.1	618.2	1.77	2.46	0.002
B3G10	220	2.45	296.2	359.1	618.2	1.72	2.40	0.002
B3G14	220	2.45	296.0	359.8	618.2	1.72	2.40	0.002
B3K15	220	2.45	295.6	360.8	618.2	1.71	2.39	0.002
B3M13	220	2.45	295.2	361.9	618.2	1.71	2.38	0.002
B3Q23	220	2.45	297.1	356.7	618.2	1.73	2.42	0.002
B3V18	220	2.45	298.6	352.6	618.2	1.75	2.44	0.002
B3B12	220	2.45	299.1	351.0	618.2	1.76	2.45	0.002
B3C15	220	2.45	299.6	349.6	618.2	1.77	2.46	0.002
B3E05	220	2.45	299.5	349.9	618.2	1.77	2.46	0.002
B3F04	220	2.45	298.8	351.7	618.2	1.76	2.45	0.002
B3G15	220	2.45	296.0	359.3	618.2	1.72	2.40	0.002
B3K16	220	2.45	294.9	362.4	618.2	1.71	2.38	0.002

ASSESSMENT OF MARGINS AGAINST CRACK INITIATION AT CWEST SCRAPE FLAWS IN REGIONS OF INTEREST WITH HIGH LEVELS OF HYDROGEN EQUIVALENT CONCENTRATION IN OUTLET ROLLED JOINTS IN BRUCE UNITS 3 AND 7

Kinectrics Report No. B2083/RP/0001 R00

Channel Identification	H_{eq} at Flaw Location at End of Evaluation Period of 246,000 EFPH (ppm)	Stress Concentration Factor, k_t	Normal Operating Temperature (°C)	Applied Peak Flaw-Tip Stress for DHC Initiation Evaluation (MPa)	Threshold Peak Stress for DHC Initiation (MPa)	Ratio of Threshold Peak Stress for DHC Initiation / Applied Peak Flaw-Tip Stress	Ratio of Critical Overload Stress / Applied Overload Stress	Fatigue Cumulative Usage Factor
B3M02	220	2.45	298.0	354.0	618.2	1.75	2.43	0.002
B3Q16	220	2.45	294.6	363.2	618.2	1.70	2.38	0.002
B3T03	220	2.45	294.7	363.0	618.2	1.70	2.38	0.002
B3U20	220	2.45	298.5	352.5	618.2	1.75	2.44	0.002
B3V17	220	2.45	298.4	352.9	618.2	1.75	2.44	0.002
B3H06	220	2.45	293.3	366.9	618.2	1.68	2.35	0.002
B3O20	220	2.45	294.7	363.0	618.2	1.70	2.38	0.002
B3Q12	220	2.45	294.7	363.0	618.2	1.70	2.38	0.002
B3X09	220	2.45	296.0	359.5	618.2	1.72	2.40	0.002
B3F05	220	2.45	299.9	348.9	618.2	1.77	2.47	0.002
B3L12	220	2.45	295.0	362.4	618.2	1.71	2.38	0.002
B3L22	220	2.45	299.5	350.2	618.2	1.77	2.46	0.002
B3N04	220	2.45	292.5	369.5	618.2	1.67	2.34	0.002
B3O13	220	2.45	295.2	361.8	618.2	1.71	2.39	0.002
B3O15	220	2.45	296.1	359.3	618.2	1.72	2.40	0.002
B3O17	220	2.45	295.9	359.9	618.2	1.72	2.40	0.002
B3P14	220	2.45	295.7	360.4	618.2	1.72	2.39	0.002
B3Q13	220	2.45	294.9	362.7	618.2	1.70	2.38	0.002
B3S13	220	2.45	293.9	365.5	618.2	1.69	2.36	0.002
B3R10	220	2.45	294.3	364.4	618.2	1.70	2.37	0.002

ASSESSMENT OF MARGINS AGAINST CRACK INITIATION AT CWEST SCRAPE FLAWS IN REGIONS OF INTEREST WITH HIGH LEVELS OF HYDROGEN EQUIVALENT CONCENTRATION IN OUTLET ROLLED JOINTS IN BRUCE UNITS 3 AND 7

Kinectrics Report No.
B2083/RP/0001 R00

TABLE 4-2: SUMMARY OF DHC AND FATIGUE CRACK GROWTH EVALUATION RESULTS FOR CIRCUMFERENTIAL COMPONENT OF SCRAPE FLAWS AT THE 20 mm LOCATION FROM OUTLET ROLLED JOINT BURNISH MARK IN ALL CHANNELS IN BRUCE UNIT 3 SCRAPED DURING THE A2131 OUTAGE AND OPERATED IN THE FUELLED CONDITION

Channel Identification	H_{eq} at Flaw Location at End of Evaluation Period of 246,000 EFPH (ppm)	Flaw Depth (mm)	Flaw Length (mm)	Post-Fatigue Growth Flaw Depth (mm)	Post-Fatigue Growth Flaw Length (mm)	Applied Stress Intensity Factor, K_I (MPa√m)	Lower-Bound Threshold Stress Intensity Factor, K_{IH} (MPa√m)	Ratio of Lower-Bound K_{IH} / Applied K_I	Allowable Heatup/Cooldown Cycles
B3F16	220	0.384	13.700	0.412	13.748	7.68	15	1.95	51
B3C11	220	0.384	13.700	0.412	13.748	7.48	15	2.01	51
B3L11	220	0.384	13.700	0.412	13.748	7.66	15	1.96	51
B3D16	220	0.384	13.700	0.412	13.748	7.80	15	1.92	51
B3D07	220	0.384	13.700	0.412	13.748	7.49	15	2.00	51
B3E20	220	0.384	13.700	0.412	13.748	7.51	15	2.00	51
B3G10	220	0.384	13.700	0.412	13.748	7.66	15	1.96	51
B3G14	220	0.384	13.700	0.412	13.748	7.67	15	1.96	51
B3K15	220	0.384	13.700	0.412	13.748	7.69	15	1.95	51
B3M13	220	0.384	13.700	0.412	13.748	7.71	15	1.95	51
B3Q23	220	0.384	13.700	0.412	13.748	7.62	15	1.97	51
B3V18	220	0.384	13.700	0.412	13.748	7.55	15	1.99	51
B3B12	220	0.384	13.700	0.412	13.748	7.52	15	1.99	51
B3C15	220	0.384	13.700	0.412	13.748	7.50	15	2.00	51
B3E05	220	0.384	13.700	0.412	13.748	7.50	15	2.00	51
B3F04	220	0.384	13.700	0.412	13.748	7.54	15	1.99	51
B3G15	220	0.384	13.700	0.412	13.748	7.67	15	1.96	51
B3K16	220	0.384	13.700	0.412	13.748	7.72	15	1.94	51

ASSESSMENT OF MARGINS AGAINST CRACK INITIATION AT CWEST SCRAPE FLAWS IN REGIONS OF INTEREST WITH HIGH LEVELS OF HYDROGEN EQUIVALENT CONCENTRATION IN OUTLET ROLLED JOINTS IN BRUCE UNITS 3 AND 7

Kinectrics Report No. B2083/RP/0001 R00

Channel Identification	H_{eq} at Flaw Location at End of Evaluation Period of 246,000 EFPH (ppm)	Flaw Depth (mm)	Flaw Length (mm)	Post-Fatigue Growth Flaw Depth (mm)	Post-Fatigue Growth Flaw Length (mm)	Applied Stress Intensity Factor, K_I (MPa√m)	Lower-Bound Threshold Stress Intensity Factor, K_{IH} (MPa√m)	Ratio of Lower-Bound K_{IH} / Applied K_I	Allowable Heatup/Cooldown Cycles
B3M02	220	0.384	13.700	0.412	13.748	7.57	15	1.98	51
B3Q16	220	0.384	13.700	0.412	13.748	7.73	15	1.94	51
B3T03	220	0.384	13.700	0.412	13.748	7.73	15	1.94	51
B3U20	220	0.384	13.700	0.412	13.748	7.55	15	1.99	51
B3V17	220	0.384	13.700	0.412	13.748	7.56	15	1.98	51
B3H06	220	0.384	13.700	0.412	13.748	7.80	15	1.92	51
B3O20	220	0.384	13.700	0.412	13.748	7.73	15	1.94	51
B3Q12	220	0.384	13.700	0.412	13.748	7.73	15	1.94	51
B3X09	220	0.384	13.700	0.412	13.748	7.67	15	1.96	51
B3F05	220	0.384	13.700	0.412	13.748	7.49	15	2.00	51
B3L12	220	0.384	13.700	0.412	13.748	7.72	15	1.94	51
B3L22	220	0.384	13.700	0.412	13.748	7.51	15	2.00	51
B3N04	220	0.384	13.700	0.412	13.748	7.84	15	1.91	51
B3O13	220	0.384	13.700	0.412	13.748	7.71	15	1.95	51
B3O15	220	0.384	13.700	0.412	13.748	7.66	15	1.96	51
B3O17	220	0.384	13.700	0.412	13.748	7.67	15	1.96	51
B3P14	220	0.384	13.700	0.412	13.748	7.68	15	1.95	51
B3Q13	220	0.384	13.700	0.412	13.748	7.72	15	1.94	51
B3S13	220	0.384	13.700	0.412	13.748	7.77	15	1.93	51
B3R10	220	0.384	13.700	0.412	13.748	7.75	15	1.94	51

Proprietary and Confidential

ASSESSMENT OF MARGINS AGAINST CRACK INITIATION AT CWEST SCRAPE FLAWS IN REGIONS OF INTEREST WITH HIGH LEVELS OF HYDROGEN EQUIVALENT CONCENTRATION IN OUTLET ROLLED JOINTS IN BRUCE UNITS 3 AND 7

Kinectrics Report No. B2083/RP/0001 R00

5. MARGIN ASSESSMENT BASED ON PTFAP FOR CWEST SCRAPE FLAWS IN THE REGION OF INTEREST WITH HIGH HYDROGEN EQUIVALENT CONCENTRATIONS IN OUTLET ROLLED JOINTS IN BRUCE UNIT 7

An evaluation of the acceptability of the CWEST scrape flaws inboard of the outlet rolled joint burnish mark in Bruce Unit 7 pressure tubes that were planned to be taken during the B2171 outage has been performed as described in Reference [13]. The evaluation was performed using PTFAP V5-1 [4,9], which implements the requirements of Clause 5 of the CSA Standard N285.8-15 [10]. The evaluation was performed to an end of evaluation period of 300,000 EFPH.

The margins to crack initiation due to DHC, hydrided region overloads, and fatigue for these scrape flaws in the high levels of H_{eq} regions of interest inboard of the burnish marks in outlet rolled joints in Bruce Unit 7 are provided in this section.

5.1 Overview of PTFAP Evaluation of CWEST Scrape Flaws Inboard of the Outlet Rolled Joint Burnish Mark in Bruce Unit 7

5.1.1 Methodology

The methodology was essentially the same as described for Bruce Unit 3 in Section 4.1.1 of this report. Each CWEST scrape flaw was resolved into axial and circumferential components. The axial component of each scrape flaw was treated as volumetric and assessed for crack initiation due to DHC under sustained loading conditions, hydrided region overloads, fatigue, and for minimum safety factors against plastic collapse. The circumferential component of each CWEST scrape flaw was treated as planar and assessed for flaw growth due to fatigue and DHC, as well as for minimum safety factors against plastic collapse and fracture initiation.

Scrape sampling in the outlet rolled joint region is planned to be performed at the three locations given below [14] to better characterize the H_{eq} profiles.

- 20 mm inboard of the outlet burnish mark
- 43 mm inboard of the outlet burnish mark
- 60 mm inboard of the outlet burnish mark

The scrape flaws at 20 mm inboard of the outlet rolled joint burnish mark are subjected to rolled joint residual stresses. For Bruce Unit 7, the rolled joint type is zero clearance. Since the scrape flaw at 20 mm inboard of the outlet rolled joint burnish mark is subjected to residual stresses, with a higher total stress compared to the two other scrape locations, the scrape flaw at the 20 mm location is bounding in terms of margins against crack initiation due to DHC and hydrided region overloads. A bounding evaluation was performed in Reference [13] for scrape flaws residing at the 20 mm location inboard of the outlet rolled joint burnish mark. The bounding evaluation was performed for all channels scraped during the B2171 outage in the outlet rolled joint region.

ASSESSMENT OF MARGINS AGAINST CRACK INITIATION AT CWEST SCRAPE FLAWS IN REGIONS OF INTEREST WITH HIGH LEVELS OF HYDROGEN EQUIVALENT CONCENTRATION IN OUTLET ROLLED JOINTS IN BRUCE UNITS 3 AND 7

Kinectrics Report No. B2083/RP/0001 R00

Since there are no scrape flaws that are located at a distance less than 20 mm inboard of the burnish mark in the outlet rolled joints in Bruce Unit 7, the evaluation was performed only for scrape flaws at 20 mm inboard of the burnish mark. The results of the evaluation would be applicable to scrape flaws that are located at a distance less than 20 mm inboard of the burnish mark based on the rationale given below.

(a) Any variation in the pressure tube dimensions and internal pressure over a distance within 20 mm inboard of the burnish mark is insignificant. From Clause A.4.4.4 of Annex A of the CSA Standard N285.8 [10], for a zero clearance rolled joint, the distance inboard of the burnish mark of either 10 or 20 mm over which credit can be taken for a 5% reduction in the hoop stress due to internal pressure from end fitting support depends on the initial diametral clearance of the rolled joint. In some cases of a scrape flaw located within 10 mm inboard of the burnish mark, the use of the evaluation results for a scrape flaw located 20 mm inboard of the burnish mark would be conservative.

(b) The rolled joint residual stresses that are used in the evaluation are the maximum in the rolled joint region, and are applicable to any location within a distance of 20 mm inboard of the burnish mark.

5.1.2   Inputs for Crack Initiation Evaluation

Pressure Tube Dimensions: Conservative pressure tube dimensions calculated at the end of the evaluation period of 300,000 EFPH [12] were used.

Flaw Location: The evaluation in Reference [13] was performed for scrape flaws with the outboard edge of the scrape flaw at the 20 mm location inboard of the outlet rolled joint burnish mark. The flaw rotary start is 350° with respect to the inspection end and measured clockwise from the top of the pressure tube.

Flaw Geometry: The CWEST scrape flaw geometry is described in Section 4.1.2 of this report. The circumferential component of the scrape flaw was evaluated as a planar flaw.

Flaw Formation Time: The flaw formation time and inspection time were 252,708 EFPH that is the operating time to the B2171 outage.

Operating and Loading Conditions: The operating pressures and temperatures specific to the flaw location were calculated in PTFAP. As stated above, for Bruce Unit 7, the rolled joint type is zero clearance. The rolled joint residual stress relaxes with time due to thermal creep. The rolled joint residual hoop stresses at the scrape flaws were calculated in PTFAP at the current time of 252,708 EFPH, and these residual hoop stresses were used in the flaw evaluations.

Hydrogen Equivalent Concentration: An H_{eq} of 300 ppm at the end of evaluation period of 300,000 EFPH was used in the evaluation of the scrape flaws at the 20 mm location inboard of the outlet rolled joint burnish mark [13]. This level of H_{eq} is significantly higher than the H_{eq} at

Proprietary and Confidential

ASSESSMENT OF MARGINS AGAINST CRACK INITIATION AT CWEST SCRAPE FLAWS IN REGIONS OF INTEREST WITH HIGH LEVELS OF HYDROGEN EQUIVALENT CONCENTRATION IN OUTLET ROLLED JOINTS IN BRUCE UNITS 3 AND 7

Kinectrics Report No. B2083/RP/0001 R00

the onset of hydride ratcheting at fuel channel outlet operating temperatures of nominally 65 ppm or lower [10]. Under hydride ratcheting conditions, the predictions from the crack initiation models are not dependent on the level of H_{eq} [10]. As described in Section 4.1.2 of this report, for levels of bulk H_{eq} that are greater than *TSSD* at the peak temperature, as in the case of scrape flaws in the region of interest in outlet rolled joints in Bruce Unit 7, the hydrogen equivalent concentration in solution at the peak temperature, and therefore the temperature at the onset of hydride precipitation, do not increase with an increase in the level of bulk H_{eq} beyond *TSSD* at the peak temperature.

5.1.3   Results

The DHC, hydrided region overload and fatigue crack initiation evaluation results for the axial component of the scrape flaws are summarized in Table 5-1. From Table 5-1, crack initiation due to DHC, hydrided region overloads and fatigue is predicted to not occur up to the end of the evaluation period of 300,000 EFPH. The detailed evaluation results, including the results for the plastic collapse evaluation, are provided in Reference [13]. The axial component of the scrape flaws satisfies the requirements of the CSA Standard N285.8-15 [10] until the end of the evaluation period as given in Reference [13].

The DHC and fatigue crack growth evaluation results for the circumferential component of the scrape flaws are summarized in Table 5-2. Crack growth due to DHC is predicted to not occur up to the end of the evaluation period for the flaw dimensions that include postulated fatigue crack growth. The detailed evaluation results, including the results for the fracture initiation and plastic collapse evaluation, are provided in Reference [13]. The circumferential component of the scrape flaws satisfies the requirements of the CSA Standard N285.8-15 until the end of the evaluation period as given in Reference [13].

5.2   Margins Against Crack Initiation due to DHC, Hydrided Region Overloads and Fatigue for Axial Component of CWEST Scrape Flaws Inboard of the Outlet Rolled Joint Burnish Mark in Bruce Unit 7

5.2.1   Margins Against Crack Initiation due to DHC

The onset of hydride precipitation was predicted to occur during reactor Cooldown over the temperature range below 250°C and at a reduced pressure [13]. As described in Section 4.2.1 of this report, for the DHC initiation evaluation, the peak flaw-tip stress that is relevant is the peak stress at the pressure and temperature during reactor Cooldown at the onset of flaw-tip hydride precipitation [10]. The factor on the DHC initiation threshold stress, which is the ratio of the predicted threshold peak flaw-tip stress for DHC initiation divided by the applied peak flaw-tip stress at hydride precipitation during Cooldown, is provided in Table 5-1. The factor on the DHC initiation threshold stress ranges from 1.81 to 2.29. Based on these results, the threshold peak stress for DHC initiation at the high levels of H_{eq} could be reduced by as much as 45% relative to the predicted threshold peak stress in the PTFAP evaluation and DHC initiation would still be predicted to not occur.

Proprietary and Confidential

ASSESSMENT OF MARGINS AGAINST CRACK INITIATION AT
CWEST SCRAPE FLAWS IN REGIONS OF INTEREST WITH
HIGH LEVELS OF HYDROGEN EQUIVALENT
CONCENTRATION IN OUTLET ROLLED JOINTS IN BRUCE
UNITS 3 AND 7

Kinectrics Report No.
B2083/RP/0001 R00

5.2.2   Margins Against Crack Initiation due to a Hydrided Region Overload

The factor on the critical stress for crack initiation due to a hydrided region overload, which is the ratio of the critical stress for crack initiation due to a hydrided region overload divided by the maximum applied stress during the overload event, is provided in Table 5-1. The factor on the critical stress for crack initiation due to a hydrided region overload ranges from 2.11 to 3.13. Based on these results, the critical stress for crack initiation due to a hydrided region overload at the high levels of H_{eq} could be reduced by as much as 53% relative to the predicted critical stress for crack initiation due to a hydrided region overload in the PTFAP evaluation and crack initiation due to a hydrided region overload would still be predicted to not occur.

5.2.3   Margins Against Crack Initiation due to Fatigue

From Table 5-1, the cumulative fatigue usage factor for the scrape flaws in the outlet rolled joints of all of the pressure tubes is only 0.004. This very low cumulative fatigue usage factor is considered to address any uncertainty in the effect of high levels of H_{eq} on the resistance to fatigue crack initiation.

5.3   Margins Against Onset of DHC Growth for Circumferential Component of CWEST Scrape Flaws Inboard of the Outlet Rolled Joint Burnish Mark in Bruce Unit 7

The factor on the lower-bound threshold stress intensity factor for the onset of DHC growth from a circumferential crack, K_{IH}, of 15 MPa√m, which is the ratio of the threshold K_{IH} divided by the applied stress intensity factor, is provided in Table 5-2. The minimum factor on the lower-bound K_{IH} is 2.28. Based on these results, the threshold K_{IH} at the high levels of H_{eq} could be reduced by as much as 56% relative to the threshold K_{IH} used in the PTFAP evaluation and the onset of DHC growth would still be predicted to not occur.

ASSESSMENT OF MARGINS AGAINST CRACK INITIATION AT
CWEST SCRAPE FLAWS IN REGIONS OF INTEREST WITH
HIGH LEVELS OF HYDROGEN EQUIVALENT
CONCENTRATION IN OUTLET ROLLED JOINTS IN BRUCE
UNITS 3 AND 7

Kinectrics Report No.
B2083/RP/0001 R00

TABLE 5-1: SUMMARY OF DHC, HYDRIDED REGION OVERLOAD AND FATIGUE CRACK INITIATION RESULTS FOR AXIAL COMPONENT OF SCRAPE FLAWS AT THE 20 mm LOCATION FROM OUTLET ROLLED JOINT BURNISH MARK IN ALL CHANNELS IN BRUCE UNIT 7 SCRAPED DURING THE B2171 OUTAGE

Channel Identification	H_{eq} at Flaw Location at End of Evaluation Period of 300,000 EFPH (ppm)	Stress Concentration Factor, k_t	Normal Operating Temperature (°C)	Applied Peak Flaw-Tip Stress for DHC Initiation Evaluation (MPa)	Threshold Peak Stress for DHC Initiation (MPa)	Ratio of Threshold Peak Stress for DHC Initiation / Applied Peak Flaw-Tip Stress	Ratio of Critical Overload Stress / Applied Overload Stress	Fatigue Cumulative Usage Factor
B7G04	300	2.446	301.6	311.5	618.2	1.98	2.11	0.004
B7G09	300	2.446	299.7	304.0	618.2	2.03	2.80	0.004
B7H03	300	2.446	300.8	340.4	618.2	1.82	2.52	0.004
B7L02	300	2.446	299.0	269.5	618.2	2.29	3.13	0.004
B7M14	300	2.446	299.3	269.7	618.2	2.29	3.12	0.004
B7N16	300	2.446	300.1	340.5	618.2	1.82	2.52	0.004
B7N17	300	2.446	301.7	269.7	618.2	2.29	3.12	0.004
B7O17	300	2.446	301.2	269.5	618.2	2.29	3.13	0.004
B7O18	300	2.446	300.7	340.7	618.2	1.81	2.52	0.004
B7P23	300	2.446	297.9	269.8	618.2	2.29	3.12	0.004
B7Q14	300	2.446	299.4	269.7	618.2	2.29	3.12	0.004
B7R13	300	2.446	300.2	269.7	618.2	2.29	3.12	0.004
B7R15	300	2.446	300.4	340.7	618.2	1.81	2.52	0.004
B7W07	300	2.446	297.4	340.4	618.2	1.82	2.52	0.004
B7W08	300	2.446	300.8	269.8	618.2	2.29	3.12	0.004

ASSESSMENT OF MARGINS AGAINST CRACK INITIATION AT CWEST SCRAPE FLAWS IN REGIONS OF INTEREST WITH HIGH LEVELS OF HYDROGEN EQUIVALENT CONCENTRATION IN OUTLET ROLLED JOINTS IN BRUCE UNITS 3 AND 7

Kinectrics Report No.
B2083/RP/0001 R00

TABLE 5-2: SUMMARY OF DHC AND FATIGUE CRACK GROWTH EVALUATION RESULTS FOR CIRCUMFERENTIAL COMPONENT OF SCRAPE FLAWS AT THE 20 mm LOCATION FROM OUTLET ROLLED JOINT BURNISH MARK IN ALL CHANNELS IN BRUCE UNIT 7 SCRAPED DURING THE B2171 OUTAGE

Channel Identification	H_{eq} at Flaw Location at End of Evaluation Period of 300,000 EFPH (ppm)	Flaw Depth (mm)	Flaw Length (mm)	Post-Fatigue Growth Flaw Depth (mm)	Post-Fatigue Growth Flaw Length (mm)	Applied Stress Intensity Factor, K_I (MPa√m)	Lower-Bound Threshold Stress Intensity Factor, K_{IH} (MPa√m)	Ratio of Lower-Bound K_{IH} / Applied K_I	Allowable Heatup/Cooldown Cycles
B7G04	300	0.384	13.600	0.425	13.721	6.09	15	2.46	65
B7G09	300	0.384	13.600	0.425	13.721	5.96	15	2.52	65
B7H03	300	0.384	13.600	0.425	13.721	6.59	15	2.28	65
B7L02	300	0.384	13.600	0.425	13.721	5.36	15	2.80	65
B7M14	300	0.384	13.600	0.425	13.721	5.36	15	2.80	65
B7N16	300	0.384	13.600	0.425	13.721	6.59	15	2.28	65
B7N17	300	0.384	13.600	0.425	13.721	5.36	15	2.80	65
B7O17	300	0.384	13.600	0.425	13.721	5.36	15	2.80	65
B7O18	300	0.384	13.600	0.425	13.721	6.59	15	2.28	65
B7P23	300	0.384	13.600	0.425	13.721	5.36	15	2.80	65
B7Q14	300	0.384	13.600	0.425	13.721	5.36	15	2.80	65
B7R13	300	0.384	13.600	0.425	13.721	5.36	15	2.80	65
B7R15	300	0.384	13.600	0.425	13.721	6.59	15	2.28	65
B7W07	300	0.384	13.600	0.425	13.721	6.59	15	2.28	65
B7W08	300	0.384	13.600	0.425	13.721	5.36	15	2.80	65

Proprietary and Confidential

ASSESSMENT OF MARGINS AGAINST CRACK INITIATION AT CWEST SCRAPE FLAWS IN REGIONS OF INTEREST WITH HIGH LEVELS OF HYDROGEN EQUIVALENT CONCENTRATION IN OUTLET ROLLED JOINTS IN BRUCE UNITS 3 AND 7

Kinectrics Report No. B2083/RP/0001 R00

6. FINITE ELEMENT STRESS ANALYSES OF CWEST SCRAPE FLAWS

Three-dimensional, elastic finite element stress analyses of the CWEST scrape flaws using representative and conservative entry and exit corner root radii were performed as described below. The stress analyses included loading due to internal pressure, as well as rolled joint residual hoop stresses. The results of the stress analyses were used in the sensitivity evaluation of DHC initiation of the axial component of the scrape flaws in the region of interest in outlet rolled joints in Bruce Units 3 and 7 as described in Section 8 of this report.

6.1 Inputs for Finite Element Stress Analyses

6.1.1 Pressure Tube Dimensions

For Bruce Unit 3, pressure tube dimensions at the outlet rolled joint that were calculated for an operating time of 250,000 EFPH that bounds the estimated time to Major Component Replacement (MCR) were used. The pressure tube inner radius is 52.52 mm and the wall thickness is 3.92 mm [12].

For Bruce Unit 7, pressure tube dimensions at the outlet rolled joint that were calculated for an operating time of 300,000 EFPH were used. The pressure tube inner radius is 52.76 mm and the wall thickness is 3.96 mm [12].

6.1.2 Internal Pressure

6.1.2.1 Internal Pressure at Outlet Rolled Joints of Bruce Unit 3

A normal operating internal pressure of 9.55 MPa was used for the outlet rolled joints in Bruce Unit 3 [15].

The procedure to calculate the pressure differential between the location of the scrape flaw in the outlet rolled joint in a fuelled channel and the Reactor Outlet Header (ROH) was taken from Reference [16]. The pressure differential between the location of the scrape flaw and the ROH depends on the temperature. The pressure differential between the thermalhydraulic inlet of the fuel channel and the ROH is given by [16]

$$\Delta p_{ROH}{}^{in} \;=\; 1.68285 \;-\; 2.80919 \times 10^{-3}\,T \tag{6-1}$$

and the pressure differential between the thermalhydraulic outlet of the fuel channel and the ROH is given by [16]

$$\Delta p_{ROH}{}^{out} \;=\; 0.47729 \;-\; 6.40345 \times 10^{-4}\,T \tag{6-2}$$

where

ASSESSMENT OF MARGINS AGAINST CRACK INITIATION AT CWEST SCRAPE FLAWS IN REGIONS OF INTEREST WITH HIGH LEVELS OF HYDROGEN EQUIVALENT CONCENTRATION IN OUTLET ROLLED JOINTS IN BRUCE UNITS 3 AND 7

Kinectrics Report No. B2083/RP/0001 R00

$\Delta p_{ROH}{}^{in}$ = pressure differential between the thermalhydraulic inlet of the fuel channel and the ROH, MPa

$\Delta p_{ROH}{}^{out}$ = pressure differential between the thermalhydraulic outlet of the fuel channel and the ROH, MPa

T = temperature, °C

The pressure differential between the axial location of the scrape flaw in the outlet rolled joint, which is inboard of the thermalhydraulic outlet of the fuel channel, and the ROH was calculated by linear interpolation along the pressure tube [16].

$$\Delta p_{ROH} = \Delta p_{ROH}{}^{in} - \frac{d_{FL}}{L_{PT}}\left(\Delta p_{ROH}{}^{in} - \Delta p_{ROH}{}^{out}\right) \tag{6-3}$$

where

d_{FL} = distance between the axial location of the scrape flaw in the outlet rolled joint and the inlet end of the pressure tube, = 6.243 m

L_{PT} = length of the pressure tube, = 6.312 m

Δp_{ROH} = pressure differential between the axial location of the scrape flaw in the outlet rolled joint and the ROH, MPa

Based on the PTFAP evaluation of scrape flaws in the region of interest in outlet rolled joints in Bruce Unit 3 [8], and as described in Section 4.2.1 of this report, the onset of hydride precipitation was predicted to occur during reactor Cooldown over the temperature range below 250°C and at a reduced pressure. The representative value of Δp_{ROH} over the temperature range below 250°C corresponding to hydride precipitation was calculated to be 0.40 MPa. Based on the recently revised ROH pressure-temperature operating limits for reactor Heatup and Cooldown for Bruce Unit 3 that are provided in Reference [17], the maximum ROH pressure over the temperature range below 250°C corresponding to hydride precipitation is 7.30 MPa. The representative internal pressure at the location of the scrape flaw over the temperature range below 250°C corresponding to hydride precipitation was calculated to be 7.70 MPa.

6.1.2.2 Internal Pressure at Outlet Rolled Joints of Bruce Unit 7

A normal operating internal pressure of 9.65 MPa was used for the outlet rolled joints in Bruce Unit 7 [15].

The pressure differential between the thermalhydraulic inlet of the fuel channel and the ROH is given by [16]

$$\Delta p_{ROH}{}^{in} = 1.64909 - 1.46845 \times 10^{-3}\, T \tag{6-4}$$

Proprietary and Confidential

ASSESSMENT OF MARGINS AGAINST CRACK INITIATION AT CWEST SCRAPE FLAWS IN REGIONS OF INTEREST WITH HIGH LEVELS OF HYDROGEN EQUIVALENT CONCENTRATION IN OUTLET ROLLED JOINTS IN BRUCE UNITS 3 AND 7

Kinectrics Report No. B2083/RP/0001 R00

and the pressure differential between the thermalhydraulic outlet of the fuel channel and the ROH is given by [16]

$$\Delta p_{ROH}{}^{out} \;=\; 0.30908 \;+\; 3.28911 \times 10^{-4} T \qquad (6\text{-}5)$$

where

d_{FL}	=	distance between the axial location of the scrape flaw in the outlet rolled joint and the inlet end of the pressure tube, = 6.254 m
L_{PT}	=	length of the pressure tube, = 6.319 m

Based on the PTFAP evaluation of scrape flaws in the region of interest in outlet rolled joints in Bruce Unit 7 [13], and as described in Section 5.2.1 of this report, the onset of hydride precipitation was predicted to occur during reactor Cooldown over the temperature range below 250°C and at a reduced pressure. The maximum value of Δp_{ROH} over the temperature range below 250°C corresponding to hydride precipitation was calculated to be 0.40 MPa. Based on the ROH pressure-temperature operating limits for reactor Heatup and Cooldown for Bruce Unit 7 that are provided in Reference [16], the maximum ROH pressure over the temperature range below 250°C corresponding to hydride precipitation is 7.30 MPa. The maximum pressure at the location of the scrape flaw over the temperature range below 250°C corresponding to hydride precipitation was calculated to be 7.70 MPa.

6.1.3   Rolled Joint Residual Hoop Stresses

The rolled joint type in Bruce Unit 3 is normal clearance, non-overextended and stress relieved. The rolled joint type in Bruce Unit 7 is zero clearance. The rolled joint residual hoop stress relaxes with time due to thermal creep. The relaxed levels of rolled joint residual hoop stress were calculated as described below.

6.1.3.1 Procedure and Inputs for Calculation of Relaxation of Residual Hoop Stresses

The calculations of relaxation due to creep of rolled joint residual hoop stresses in outlet rolled joints in Bruce Units 3 and 7 were performed using the rolled joint residual hoop stress model and related parameters that are provided in Reference [18].

A normal operating internal pressure of 9.55 MPa was used for the outlet rolled joints in Bruce Unit 3, and 9.65 MPa was used for the outlet rolled joints in Bruce Unit 7 [15]. A lower normal operating temperature will result in lower creep strain rates and less relaxation of rolled joint residual hoop stresses. A conservative normal operating temperature of 290°C that is at the lower end of the range of normal operating outlet temperatures [19] was used for Bruce Units 3 and 7.

ASSESSMENT OF MARGINS AGAINST CRACK INITIATION AT CWEST SCRAPE FLAWS IN REGIONS OF INTEREST WITH HIGH LEVELS OF HYDROGEN EQUIVALENT CONCENTRATION IN OUTLET ROLLED JOINTS IN BRUCE UNITS 3 AND 7

Kinectrics Report No.
B2083/RP/0001 R00

6.1.3.2 Relaxed Levels of Residual Hoop Stress in the Outlet Rolled Joints in Bruce Unit 3

Calculations of stress relaxation were performed for the initial statistical upper-bound residual hoop stress for normal clearance, non-overextended and stress relieved rolled joints of 157 MPa that is used in flaw evaluations [20]. At 231,964 EFPH or 271,330 hot hours that was the operating time to the A2131 outage, the initial upper-bound value of 157 MPa is predicted to have relaxed to 32 MPa.

6.1.3.3 Relaxed Levels of Residual Hoop Stress in the Outlet Rolled Joints in Bruce Unit 7

The as-rolled residual hoop stresses in zero clearance rolled joints decrease with a decrease in the initial diametral clearance. The statistical upper-bound values of as-rolled residual hoop stresses in zero clearance rolled joints that are used in flaw evaluations are provided in Reference [4] for a range of initial diametral clearances. The outlet rolled joint in Bruce Unit 7 that will be scrape sampled using the CWEST tool during the B2171 outage that has the highest initial diametral clearance is in fuel channel B7G04 with an initial diametral clearance of -0.002 in. [21]. For an initial diametral clearance of -0.002 in., the as-rolled residual hoop stress is 43 MPa [4]. The as-rolled residual hoop stress of 43 MPa is predicted to relax to a very low level of 10 MPa at 252,708 EFPH or 281,760 hot hours that was the operating time to the B2171 outage. For the purpose of the evaluation, a relaxed rolled joint residual hoop stress of 15 MPa was used.

6.2   Finite Element Modelling of Scrape Flaws

Three-dimensional, elastic finite element stress analyses of the scrape flaws were performed [22]. The finite element computer code *ANSYS 2021 R1* [23] was used. The stress analyses were in accordance with Revision 1 of *Guidelines for Pressure Tube Flaw-Tip Stress Analysis* [24].

6.2.1   Finite Element Models

The geometry of the CWEST scrape flaw is described in Section 3 of this report. With reference to Section 3, for Bruce Units 3 and 7, in all cases the scrape flaw was modelled using an axial length of 6.2 mm, and a circumferential length of 15°. The root radii of the entry and exit corners of the axial component of the scrape flaw were the same, and are referred to below as the corner root radius. A root radius of the corners of the circumferential component of the scrape flaw of 0.330 mm was used.

The dimensions of the axial component of the scrape flaws that were used in the evaluation are given in Table 6-1. For the baseline cases for Bruce Units 3 and 7, the depth of the scrape flaw was 0.384 mm. The recommended representative root radius of the entry and exit corners of the axial component of the scrape flaw of 1.7 mm [7] was used in the baseline cases. In Table 6-1,

ASSESSMENT OF MARGINS AGAINST CRACK INITIATION AT CWEST SCRAPE FLAWS IN REGIONS OF INTEREST WITH HIGH LEVELS OF HYDROGEN EQUIVALENT CONCENTRATION IN OUTLET ROLLED JOINTS IN BRUCE UNITS 3 AND 7

Kinectrics Report No. B2083/RP/0001 R00

the baseline Case for Bruce Unit 3 is denoted as B3-1. Only the baseline Case was evaluated for Bruce Unit 7, and this is denoted as B7-1 in Table 6-1.

Additional scrape flaw geometries were evaluated for Bruce Unit 3 to determine the sensitivity of the DHC initiation evaluation results to the corner root radius of the axial component and the flaw depth. With reference to Table 6-1, a corner root radius of 1.5 mm was used for Case B3-2, 1.25 mm was used for Case B3-3, and 1.0 mm was used for Case B3-4. Based on the measurements of root radii from replicas of the scrape flaws in Reference [7], corner root radii as small as 1.0 mm are considered to be unlikely. A flaw depth of 0.323 mm and a corner root radius of 1.7 mm were used for Case B3-5.

A three-dimensional, one-quarter symmetry finite element model with two planes of symmetry was used for each case. The end fitting was not included in the finite element model, and there was no credit for end fitting support, which is conservative. The three-dimensional one-quarter symmetry finite element model of pressure tube with the CWEST scrape flaw in Bruce Unit 3 for the baseline Case B3-1 with a depth of 0.384 mm and a corner root radius of 1.7 mm is shown in Figure 6-1. A view of the CWEST scrape flaw in Bruce Unit 3 for the baseline Case B3-1 in the three-dimensional one-quarter symmetry finite element model is shown in Figure 6-2. Convergence was assessed by replacing the 20-node hexahedral elements with 8-node hexahedral bricks [22]. The number of elements was identical, but the number of nodes was decreased from 380,416 to 97,246. The peak flaw-tip stress was within 0.3%, and convergence was demonstrated.

6.2.2 Material Modelling

A value of Young's modulus, E, of 94,500 MPa, and Poisson's ratio, υ, of 0.4 [10], were used in the finite element stress analyses.

6.2.3 Applied Loads

The total nominal hoop stress due to internal pressure including pressure on the flaw face and rolled joint residual hoop stress is given by

$$\sigma_h \;=\; p_{op}\left(\frac{R_i}{w} + 1\right) + \sigma_{hres} \tag{6-6}$$

where

p_{op}	=	operating internal pressure
R_i	=	pressure tube inside radius
w	=	pressure tube wall thickness
σ_h	=	total nominal hoop stress due to internal pressure and rolled joint residual hoop stress

ASSESSMENT OF MARGINS AGAINST CRACK INITIATION AT CWEST SCRAPE FLAWS IN REGIONS OF INTEREST WITH HIGH LEVELS OF HYDROGEN EQUIVALENT CONCENTRATION IN OUTLET ROLLED JOINTS IN BRUCE UNITS 3 AND 7

Kinectrics Report No. B2083/RP/0001 R00

σ_{hres} =   rolled joint residual hoop stress

Internal pressure loading was applied to all wetted surfaces. The operating internal pressure at the scrape flaw locations is the internal pressure during flaw-tip hydride precipitation for Bruce Units 3 and 7 of 7.70 MPa. The total nominal hoop stress included the rolled joint residual hoop stress of 32 MPa for Bruce Unit 3 and 15 MPa for Bruce Unit 7. The total nominal hoop stress during hydride precipitation due to the operating internal pressure, as calculated with pressure on the flaw face, and the residual hoop stress, for Bruce Unit 3 was 142.9 MPa and for Bruce Unit 7 was 125.3 MPa. The total nominal hoop stresses are given in Table 6-1.

The equivalent internal pressure that is applied in the finite element analysis to account for the rolled joint residual hoop stress is given by writing

$$p_{eq}\left(\frac{R_i}{w} + 1 \right) = p_{op}\left(\frac{R_i}{w} + 1 \right) + \sigma_{hres} \tag{6-7}$$

Or,

$$p_{eq} = p_{op} + \frac{\sigma_{hres}}{\left(\dfrac{R_i}{w} + 1 \right)} \tag{6-8}$$

where

p_{eq} =   equivalent internal pressure that is applied in the finite element analysis to account for the rolled joint residual hoop stress

For example, for Bruce Unit 3, for the total nominal hoop stress of 142.9 MPa, the equivalent internal pressure is 9.92 MPa.

The end load on the pressure tube due to internal pressure was applied as an axial stress on the end of the finite element model and is given by

$$\sigma_a = p_{op} \frac{R_i}{2w} \tag{6-9}$$

where

σ_a =   nominal axial stress due to internal pressure

Proprietary and Confidential

ASSESSMENT OF MARGINS AGAINST CRACK INITIATION AT
CWEST SCRAPE FLAWS IN REGIONS OF INTEREST WITH
HIGH LEVELS OF HYDROGEN EQUIVALENT
CONCENTRATION IN OUTLET ROLLED JOINTS IN BRUCE
UNITS 3 AND 7

Kinectrics Report No.
B2083/RP/0001 R00

6.3   Finite Element Stress Analysis Results

The maximum principal stress contours at the CWEST scrape flaw in Bruce Unit 3 for the baseline Case B3-1 with a depth of 0.384 mm, a corner root radius of 1.7 mm, and a total nominal hoop stress during hydride precipitation of 142.9 MPa including pressure on the flaw face, is shown in Figure 6-3. The peak principal stress occurs at the entry and exit corners of the scrape flaws. A close-up view of maximum principal stress contours at the corner of the axial component of the CWEST scrape flaw in Bruce Unit 3 for the baseline Case B3-1 is shown in Figure 6-4. From this figure, the peak flaw-tip principal stress at the corner, midway along the axial length and on the radial-circumferential plane of symmetry (lower right-hand plane in Figure 6-2), for the baseline Case B3-1 is 225.7 MPa.

The three-dimensional elastic stress concentration factor from the elastic finite element stress analyses was calculated using Eq. (6-10), where internal pressure on the flaw face was taken into account.

$$k_t = \frac{\sigma_{1p}}{p_{eq}\left(\dfrac{R_i}{w} + 1\right)} \tag{6-10}$$

where

k_t =   elastic stress concentration factor with internal pressure on the flaw face

σ_{1p} =   peak principal flaw-tip stress calculated in the finite element analysis

The elastic stress concentration factor and peak flaw-tip principal stress at the corner, midway along the axial length and on the radial-circumferential plane of symmetry, for all cases are given in Table 6-1. As expected, the elastic stress concentration factor and peak flaw-tip principal stress increase with a decrease in the scrape flaw corner root radius.

With reference to Figure 6-3, the elastic distribution of maximum principal stress from the corner into the interior below the surface was extracted from the finite element results. A fourth-order polynomial representation of the principal stress distribution at the CWEST scrape flaw in Bruce Unit 3 for the baseline Case B3-1 with a depth of 0.384 mm, a corner root radius of 1.7 mm, and a total nominal hoop stress during hydride precipitation of 142.9 MPa including pressure on the flaw face, is shown in Figure 6-5. The elastic distribution of maximum principal stress such as shown in Figure 6-5 was then normalized by dividing by the peak flaw-tip principal stress at the corner of the scrape flaw. The normalized elastic distribution of maximum principal stress was used in the process-zone DHC initiation evaluation.

ASSESSMENT OF MARGINS AGAINST CRACK INITIATION AT
CWEST SCRAPE FLAWS IN REGIONS OF INTEREST WITH
HIGH LEVELS OF HYDROGEN EQUIVALENT
CONCENTRATION IN OUTLET ROLLED JOINTS IN BRUCE
UNITS 3 AND 7

Kinectrics Report No.
B2083/RP/0001 R00

TABLE 6-1
**DIMENSIONS OF AXIAL COMPONENT OF SCRAPE FLAWS, ELASTIC STRESS CONCENTRATION FACTOR
AND PEAK STRESS DURING HYDRIDE PRECIPITATION FROM ELASTIC FINITE ELEMENT STRESS ANALYSIS**

Reactor Unit	Case	Axial Length of Scrape Flaw (mm)	Depth of Scrape Flaw (mm)	Corner Root Radius of Scrape Flaw (mm)	Total Hoop Stress at Reduced Pressure During Hydride Precipitation, σ_h (MPa)	Elastic Stress Concentration Factor of Axial Component of Scrape Flaw, k_t	Peak Stress at Axial Component of Scrape Flaw During Hydride Precipitation σ_{1p} (MPa)
Bruce Unit 3	B3-1	6.2	0.384	1.70	142.9	1.580	225.7
Bruce Unit 3	B3-2	6.2	0.384	1.50	142.9	1.617	231.0
Bruce Unit 3	B3-3	6.2	0.384	1.25	142.9	1.676	239.4
Bruce Unit 3	B3-4	6.2	0.384	1.00	142.9	1.756	250.8
Bruce Unit 3	B3-5	6.2	0.323	1.70	142.9	1.525	217.8
Bruce Unit 7	B7-1	6.2	0.384	1.70	125.3	1.579	197.8

ASSESSMENT OF MARGINS AGAINST CRACK INITIATION AT CWEST SCRAPE FLAWS IN REGIONS OF INTEREST WITH HIGH LEVELS OF HYDROGEN EQUIVALENT CONCENTRATION IN OUTLET ROLLED JOINTS IN BRUCE UNITS 3 AND 7

Kinectrics Report No. B2083/RP/0001 R00
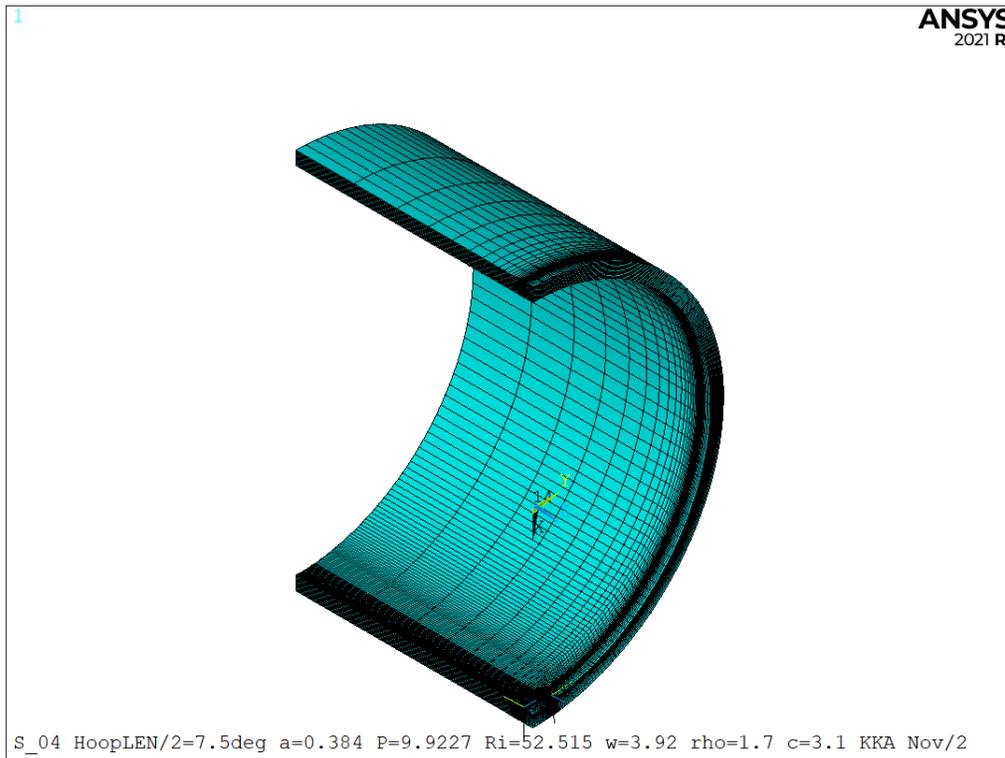
Figure 6-1: Three-Dimensional One-Quarter Symmetry Finite Element Model of Pressure Tube with the CWEST Scrape Flaw in Bruce Unit 3 for the Baseline Case B3-1 with a Flaw Depth of 0.384 mm and a Corner Root Radius of 1.7 mm

ASSESSMENT OF MARGINS AGAINST CRACK INITIATION AT
CWEST SCRAPE FLAWS IN REGIONS OF INTEREST WITH
HIGH LEVELS OF HYDROGEN EQUIVALENT
CONCENTRATION IN OUTLET ROLLED JOINTS IN BRUCE
UNITS 3 AND 7

Kinectrics Report No.
B2083/RP/0001 R00
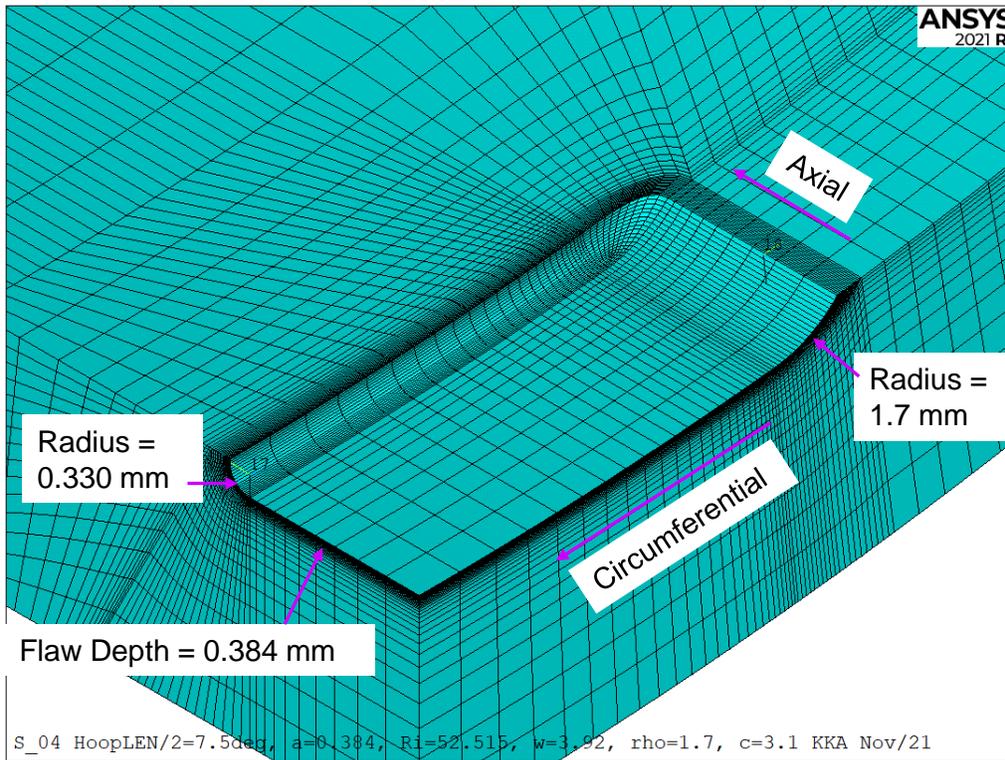
Figure 6-2: View of CWEST Scrape Flaw in Bruce Unit 3 for the Baseline Case B3-1 with a Flaw Depth of 0.384 mm and a Corner Root Radius of 1.7 mm in the Three-Dimensional One-Quarter Symmetry Finite Element Model

ASSESSMENT OF MARGINS AGAINST CRACK INITIATION AT CWEST SCRAPE FLAWS IN REGIONS OF INTEREST WITH HIGH LEVELS OF HYDROGEN EQUIVALENT CONCENTRATION IN OUTLET ROLLED JOINTS IN BRUCE UNITS 3 AND 7

Kinectrics Report No. B2083/RP/0001 R00
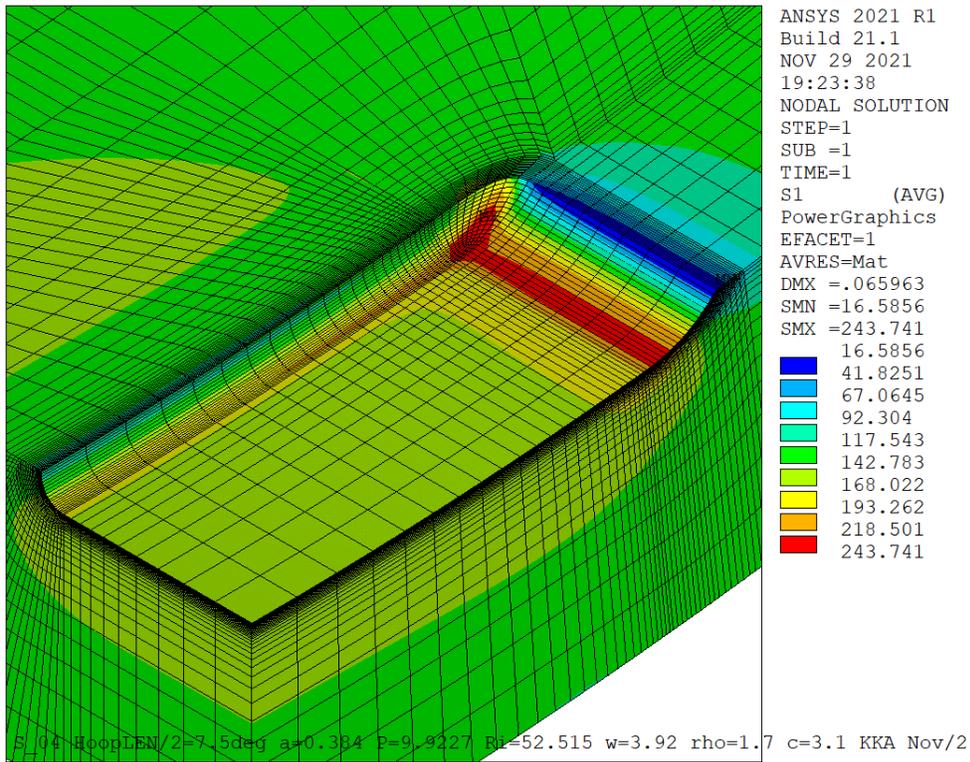
Figure 6-3: Maximum Principal Stress Contours at CWEST Scrape Flaw in Bruce Unit 3 for the Baseline Case B3-1 with a Flaw Depth of 0.384 mm, a Corner Root Radius of 1.7 mm, and a Total Nominal Hoop Stress During Hydride Precipitation of 142.9 MPa Including Pressure on the Flaw Face

ASSESSMENT OF MARGINS AGAINST CRACK INITIATION AT
CWEST SCRAPE FLAWS IN REGIONS OF INTEREST WITH
HIGH LEVELS OF HYDROGEN EQUIVALENT
CONCENTRATION IN OUTLET ROLLED JOINTS IN BRUCE
UNITS 3 AND 7

Kinectrics Report No.
B2083/RP/0001 R00
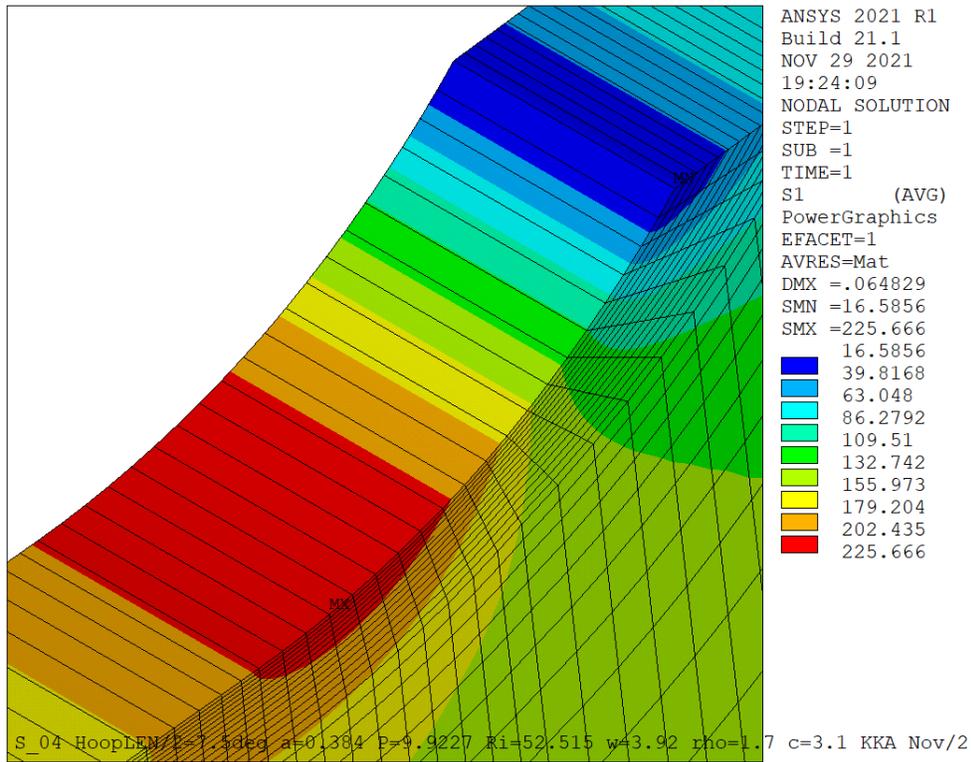
Figure 6-4: Close-Up View of Maximum Principal Stress Contours at CWEST Scrape Flaw in Bruce Unit 3 for the Baseline Case B3-1 with a Flaw Depth of 0.384 mm, a Corner Root Radius of 1.7 mm, and a Total Nominal Hoop Stress During Hydride Precipitation of 142.9 MPa Including Pressure on the Flaw Face

ASSESSMENT OF MARGINS AGAINST CRACK INITIATION AT CWEST SCRAPE FLAWS IN REGIONS OF INTEREST WITH HIGH LEVELS OF HYDROGEN EQUIVALENT CONCENTRATION IN OUTLET ROLLED JOINTS IN BRUCE UNITS 3 AND 7

Kinectrics Report No.
B2083/RP/0001 R00
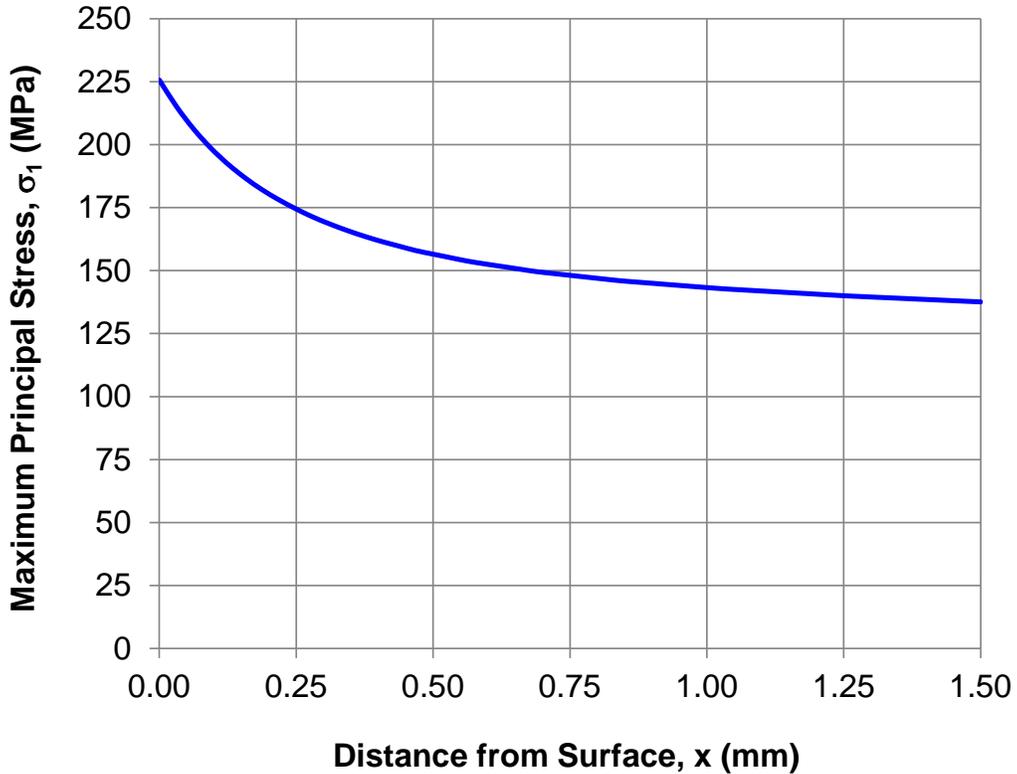
Figure 6-5: Fourth-Order Polynomial Representation of the Principal Stress Distribution at CWEST Scrape Flaw in Bruce Unit 3 for the Baseline Case B3-1 with a Flaw Depth of 0.384 mm, a Corner Root Radius of 1.7 mm, and a Total Nominal Hoop Stress During Hydride Precipitation of 142.9 MPa Including Pressure on the Flaw Face

Proprietary and Confidential

ASSESSMENT OF MARGINS AGAINST CRACK INITIATION AT
CWEST SCRAPE FLAWS IN REGIONS OF INTEREST WITH
HIGH LEVELS OF HYDROGEN EQUIVALENT
CONCENTRATION IN OUTLET ROLLED JOINTS IN BRUCE
UNITS 3 AND 7

Kinectrics Report No.
B2083/RP/0001 R00

7. PROCESS-ZONE CALCULATION PROCEDURE FOR EVALUATION OF DHC INITIATION AT THE AXIAL COMPONENT OF THE CWEST SCRAPE FLAW

As described in Section 3 of this report, the entry and exit corner root radii of the axial components of the CWEST scrape flaws are significantly larger than the flaw depth. The models for calculation of the stress concentration factor at a flaw, and the process-zone models for evaluation of DHC initiation at flaws, which are in the CSA Standard N285.8 [10] are not applicable to a flaw geometry where the flaw root radius is significantly larger than the flaw depth. For this reason, a process-zone model that is applicable to the evaluation of DHC initiation at the axial component of a CWEST scrape flaw was developed as described in Appendix A of this report.

The process-zone model that was developed in Appendix A of this report is an adaptation of previously developed process-zone models for DHC initiation that are provided in References [10,25,26]. The basic fundamentals and criteria for DHC initiation in the process-zone model for a scrape flaw are the same as in the previously developed models. The main difference is that the process-zone models in References [10,25,26] were developed primarily for a flaw with a root radius less than or equal to the flaw depth, whereas the process-zone model for a scrape flaw was developed for a flaw root radius significantly larger than the flaw depth. As described in Appendix A, a process-zone model based on a hydrided region at a planar surface is considered to be a reasonable representation for the geometry of a CWEST scrape flaw.

The procedure to calculate the threshold peak stress for DHC initiation based on the process-zone model for the scrape flaw is given below.

7.1 Stress Distribution Through the Wall Thickness Adjacent to the Scrape Flaw

A process zone emanating from a planar surface and subjected to an applied linear stress distribution is shown in Figure 7-1. The stress distribution adjacent to the scrape flaw through the wall thickness is approximated as linear as given below

$$\sigma(x) = A_0 + A_1\left(\frac{x}{s}\right) \tag{7-1}$$

where

A_0 = stress coefficient for the uniform term of the stress distribution
A_1 = stress coefficient for the linear gradient term of the stress distribution
s = process-zone length
x = local coordinate with origin at the surface
$\sigma(x)$ = elastic stress distribution through the wall thickness

Proprietary and Confidential

ASSESSMENT OF MARGINS AGAINST CRACK INITIATION AT
CWEST SCRAPE FLAWS IN REGIONS OF INTEREST WITH
HIGH LEVELS OF HYDROGEN EQUIVALENT
CONCENTRATION IN OUTLET ROLLED JOINTS IN BRUCE
UNITS 3 AND 7

Kinectrics Report No.
B2083/RP/0001 R00

Equation (7-1) is also written in terms of the peak flaw-tip principal stress.

$$\sigma(x) = \sigma_{1p} + A_1\left(\frac{x}{s}\right) \tag{7-2}$$

where

σ_{1p} =   peak flaw-tip principal stress

Equation (7-1) is written in a normalized form.

$$\frac{\sigma(x)}{A_0} = 1 + \alpha_1(s)\left(\frac{x}{s}\right) \tag{7-3}$$

where

$$\alpha_1(s) = \frac{A_1}{A_0} \tag{7-4}$$

and

$\alpha_1(s)$ =   normalized linear stress coefficient that depends on the process-zone length, s

A fourth-order polynomial representation of the normalized stress distribution adjacent to the scrape flaw was fitted to the normalized distance through the wall thickness from the elastic finite element stress analysis with the form

$$\frac{\sigma_F(x)}{A_0} = 1 + \beta_1\left(\frac{x}{d}\right) + \beta_2\left(\frac{x}{d}\right)^2 + \beta_3\left(\frac{x}{d}\right)^3 + \beta_4\left(\frac{x}{d}\right)^4 \tag{7-5}$$

where

$$d = w - a \tag{7-6}$$

and

a =   depth of the scrape flaw
β_j =   normalized stress coefficient for the jth power term of the fitted fourth-order polynomial normalized stress distribution
d =   remaining wall thickness of the pressure tube at the scrape flaw

ASSESSMENT OF MARGINS AGAINST CRACK INITIATION AT CWEST SCRAPE FLAWS IN REGIONS OF INTEREST WITH HIGH LEVELS OF HYDROGEN EQUIVALENT CONCENTRATION IN OUTLET ROLLED JOINTS IN BRUCE UNITS 3 AND 7

Kinectrics Report No. B2083/RP/0001 R00

w	=	wall thickness of the pressure tube
x	=	local coordinate with origin at the surface
$\sigma_F(x)$	=	elastic stress distribution through the wall thickness from the fitted fourth-order polynomial stress distribution

The linear approximation of the normalized stress distribution through the wall thickness was conservatively treated as a secant to the fitted fourth-order polynomial normalized stress distribution where the linear approximation intersects the fourth-order normalized polynomial stress distribution at the distance x equal to s. The normalized stress coefficient $\alpha_1(s)$ therefore depends on the length, s, of the process zone. At x equal to s, one can write

$$\alpha_1(s) = \beta_1\left(\frac{s}{d}\right) + \beta_2\left(\frac{s}{d}\right)^2 + \beta_3\left(\frac{s}{d}\right)^3 + \beta_4\left(\frac{s}{d}\right)^4 \tag{7-7}$$

The conservative linear stress distribution approximation to the normalized fourth-order polynomial representation of the principal stress distribution at the scrape flaw in Bruce Unit 3 for the baseline Case B3-1 with a corner root radius of 1.7 mm is illustrated in Figure 7-2.

7.2 Process-Zone Length

The process-zone length, s, is given by solving the equation given below, where the only unknown is s.

$$\left(\frac{K_{IH}}{p_c}\right)^2 = 5.1869\, s\alpha_1(s)\frac{\left[G_0(s/d)V_1(s/d) - G_1(s/d)V_0(s/d)\right]}{G_0(s/d) + \alpha_1 G_1(s/d)} \tag{7-8}$$

where

$G_0(s/d)$	=	geometry correction factor for the stress intensity factor for the uniform term, A_0, of the linear stress distribution
$G_1(s/d)$	=	geometry correction for the stress intensity factor for the linear gradient term, A_1, of the linear stress distribution
K_{IH}	=	isothermal threshold stress intensity factor for DHC initiation from a crack
p_c	=	threshold stress for DHC initiation at a planar surface
s	=	process-zone length
$V_0(s/d)$	=	geometry factor for the crack-mouth opening displacement for the uniform term, A_0, of the linear stress distribution
$V_1(s/d)$	=	geometry factor for the crack-mouth opening displacement for the linear gradient term, A_1, of the linear stress distribution

Proprietary and Confidential

ASSESSMENT OF MARGINS AGAINST CRACK INITIATION AT CWEST SCRAPE FLAWS IN REGIONS OF INTEREST WITH HIGH LEVELS OF HYDROGEN EQUIVALENT CONCENTRATION IN OUTLET ROLLED JOINTS IN BRUCE UNITS 3 AND 7

Kinectrics Report No. B2083/RP/0001 R00

Equations to calculate $G_0(s/d)$ and $G_1(s/d)$ are provided in A-4 of Appendix A of this report. Equations to calculate $V_0(s/d)$ and $V_1(s/d)$ are provided in A-5 of Appendix A. The only unknown in Eq. (7-9) is the process-zone length, s. Equation (7-9) is solved iteratively for s.

7.3 Threshold Peak Stress for DHC Initiation

After the process-zone length, s, has been determined, the threshold peak stress for DHC initiation, σ_{th}, is calculated using the equation given below.

$$\sigma_{th} = \frac{p_c G_0(s/d)}{G_0(s/d) + \alpha_1 G_1(s/d)} \tag{7-9}$$

From Eqs. (7-8) and (7-9), the process-zone length and threshold peak stress for DHC initiation are not dependent on Young's modulus, E.

ASSESSMENT OF MARGINS AGAINST CRACK INITIATION AT CWEST SCRAPE FLAWS IN REGIONS OF INTEREST WITH HIGH LEVELS OF HYDROGEN EQUIVALENT CONCENTRATION IN OUTLET ROLLED JOINTS IN BRUCE UNITS 3 AND 7

Kinectrics Report No.
B2083/RP/0001 R00

$$\sigma(x) = \sigma_{1p} + A_1\left(\frac{x}{s}\right)$$

Slope = A_1/s

p_c

v_T

Hydrided region modelled as a process zone

s

Flaw with large radius

x

Planar surface idealization

w
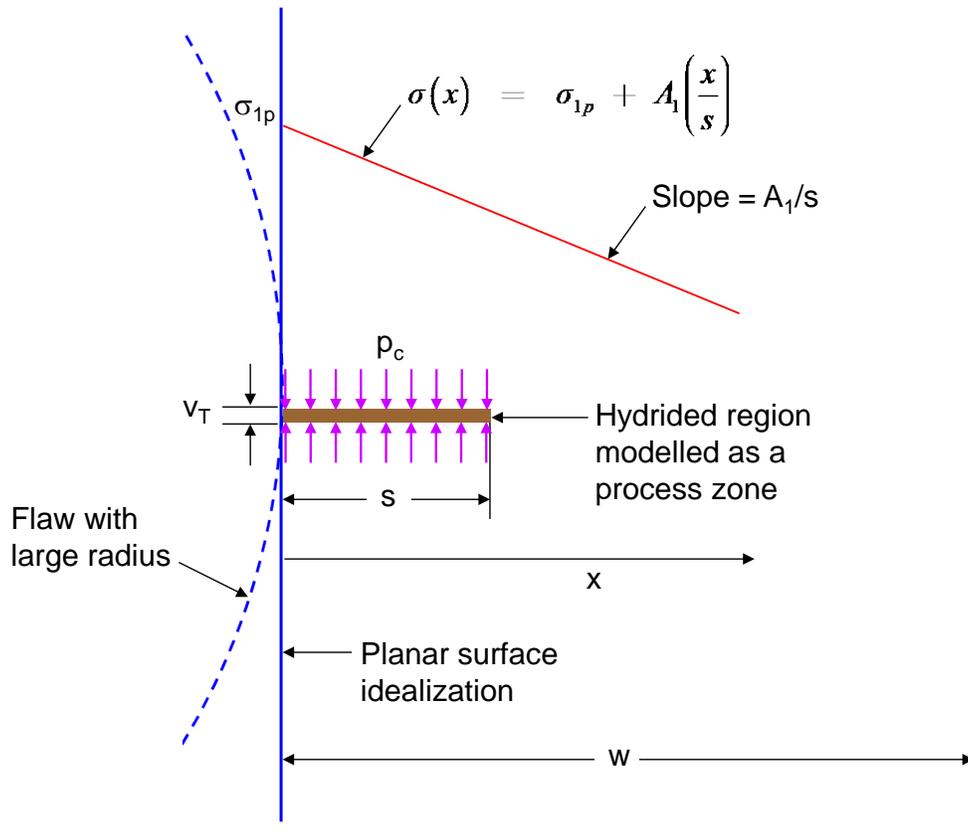
Figure 7-1: Process Zone Emanating from a Planar Surface and Subjected to an Applied Linear Stress Distribution

ASSESSMENT OF MARGINS AGAINST CRACK INITIATION AT
CWEST SCRAPE FLAWS IN REGIONS OF INTEREST WITH
HIGH LEVELS OF HYDROGEN EQUIVALENT
CONCENTRATION IN OUTLET ROLLED JOINTS IN BRUCE
UNITS 3 AND 7

Kinectrics Report No.
B2083/RP/0001 R00
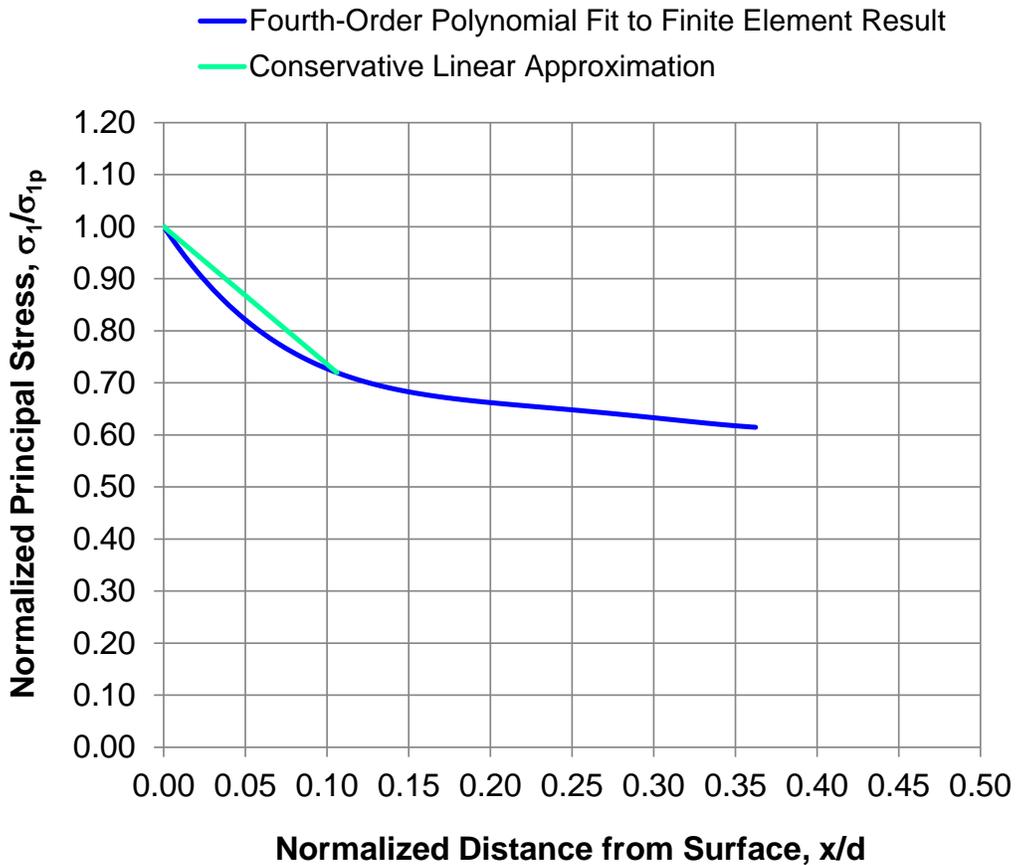
Figure 7-2: Illustration of the Conservative Linear Stress Distribution Approximation to the Normalized Fourth-Order Polynomial Representation of the Principal Stress Distribution at the Scrape Flaw in Bruce Unit 3 for Baseline Case B3-1 with a Corner Root Radius of 1.7 mm

ASSESSMENT OF MARGINS AGAINST CRACK INITIATION AT CWEST SCRAPE FLAWS IN REGIONS OF INTEREST WITH HIGH LEVELS OF HYDROGEN EQUIVALENT CONCENTRATION IN OUTLET ROLLED JOINTS IN BRUCE UNITS 3 AND 7

Kinectrics Report No. B2083/RP/0001 R00

8.   SENSITIVITY EVALUATION OF DHC INITIATION AT AXIAL COMPONENT OF CWEST SCRAPE FLAWS IN REGION OF INTEREST IN OUTLET ROLLED JOINTS IN BRUCE UNITS 3 AND 7

The sensitivity of the results of the DHC initiation evaluation of the scrape flaws to the threshold stress intensity factor for DHC initiation from a crack, K_{IH}, and the threshold stress for DHC initiation at a planar surface, p_c, was determined for the representative scrape flaw entry and exit corner root radii using three-dimensional elastic finite element stress analysis and the process-zone model that was developed in Appendix A of this report. The sensitivity of the evaluation results to a variation in the scrape flaw depth, and the scrape flaw entry and exit corner root radii, was also determined. The root radii of the entry and exit corners of the axial component of the scrape flaw were the same, and are referred to below as the corner root radius. The sensitivity evaluation was performed for CWEST scrape flaws in the region of interest with potentially high levels of H_{eq} in the outlet rolled joints of Bruce Units 3 and 7.

The results of the sensitivity evaluation are applicable to scrape flaws that are located within a distance up to and including 20 mm inboard of the burnish mark. The rationale for the applicability is the same as given in Sections 4.1.1 and 5.1.1 of this report.

8.1   Outline of Procedure for Sensitivity Evaluation

The procedure to calculate the threshold peak stress for DHC initiation at the scrape flaw, σ_{th}, is provided in Section 7 of this report and is outlined below.

(a) With reference to Figure 6-5, the elastic distribution of maximum principal stress from the scrape flaw corner into the interior below the surface was extracted from the finite element results. From Section 7.1 of this report, the elastic distribution of maximum principal stress was then normalized by dividing by the peak flaw-tip principal stress at the corner of the scrape flaw. A fourth-order polynomial representation of the principal stress distribution was fitted using the method of least squares in Excel where the goodness of fit as given by R^2 was 0.989 or higher. The resultant normalized stress coefficients, β_j, are given in Table 8-1 for each scrape flaw geometry case.

(b) The process-zone length, s, was calculated as described in Section 7.2.

(c) After the process-zone length, s, was determined, the threshold peak stress for DHC initiation, σ_{th}, was calculated as described in Section 7.3.

8.2   Baseline Sensitivity Evaluation of DHC Initiation at Scrape Flaws in Outlet Rolled Joints in Bruce Units 3 and 7

The threshold peak stress for DHC initiation, σ_{th}, was predicted using values of K_{IH} of 2.25 through 4.5 MPa√m, and values of p_c of 200 through 450 MPa. The reorientation stress to form a radial hydrided region that is a prerequisite to initiation of a radial DHC crack is nominally

Proprietary and Confidential

ASSESSMENT OF MARGINS AGAINST CRACK INITIATION AT CWEST SCRAPE FLAWS IN REGIONS OF INTEREST WITH HIGH LEVELS OF HYDROGEN EQUIVALENT CONCENTRATION IN OUTLET ROLLED JOINTS IN BRUCE UNITS 3 AND 7

Kinectrics Report No.
B2083/RP/0001 R00

200 MPa [27]. The use of K_{IH} as low as 2.25 MPa√m, and p_c as low as 200 MPa, is for the sensitivity evaluation only and does not imply that actual values could be this low.

The variation of the predicted process-zone length, s, with p_c for a range of K_{IH} for the Bruce Unit 3 baseline Case B3-1, with a scrape flaw depth of 0.384 mm and a corner root radius of 1.7 mm, is shown in Figure 8-1. The process-zone length decreases with an increase in p_c, and this is expected. From Appendix A of this report, at threshold conditions for DHC initiation, the process-zone restraining stress is equal to p_c, and a higher restraining stress will result in a shorter process-zone length. The process-zone length increases with an increase in K_{IH}. A higher K_{IH} will result in a higher threshold peak stress, as well as a higher stress distribution through the wall thickness that will increase the process-zone length. These trends are consistent with other process-zone models for DHC initiation [25,26].

For all combinations of K_{IH} and p_c, the maximum difference between the threshold peak stress for the Bruce Unit 3 baseline Case B3-1, and the Bruce Unit 7 baseline Case B7-1, with a scrape flaw depth of 0.384 mm and a corner root radius of 1.7 mm, is only 0.017%. The threshold peak stress for DHC initiation is insensitive to the differences in pressure tube dimensions. The variation of the predicted threshold peak stress for DHC initiation, σ_{th}, with p_c for a range of K_{IH} for the Bruce Unit 3 baseline Case B3-1, and Bruce Unit 7 baseline Case B7-1, is shown in Figure 8-2. Curves of the threshold peak stress are plotted for values of K_{IH} of 2.25 through 4.5 MPa√m. The threshold peak stress for DHC initiation increases with an increase in p_c, and increases with an increase in K_{IH} but to a lesser extent. The black dashed line in this figure has a slope of 1.0, and values of peak stress along this line are equal to p_c. The contribution of p_c to the threshold peak stress therefore corresponds to the value of peak stress along the dashed line. The contribution of K_{IH} to the threshold peak stress at any value of p_c corresponds to the vertical distance between the curve of threshold peak stress for a given value of K_{IH} and the dashed line. From this figure, p_c is the major contributor to the threshold peak stress for the scrape flaws. This is a result of the large corner root radius relative to the flaw depth.

The applied peak flaw-tip principal stresses during hydride precipitation, σ_{1p}, for the Bruce Unit 3 baseline Case B3-1 of 225.7 MPa, and for the Bruce Unit 7 baseline Case B7-1 of 197.8 MPa, are also plotted in Figure 8-2. The applied peak flaw-tip principal stresses, and the minimum threshold peak stress for DHC initiation based on K_{IH} equal to 2.25 MPa√m and p_c equal to 200 MPa, are given in Table 8-2. DHC initiation is predicted to not occur when the threshold peak stress is greater than the applied peak stress, and DHC initiation was predicted to not occur for all combinations of K_{IH} and p_c used in the evaluation. Both K_{IH} and p_c can be simultaneously reduced from their lower-bound values of 4.5 MPa√m and 450 MPa, respectively [10], by 50% and DHC initiation is predicted to still not occur. A 50% reduction in K_{IH} and p_c at high levels of H_{eq} is unlikely. At the time of writing this report, DHC initiation tests on unirradiated pressure tube material with a high level of H_{eq} are in progress to confirm that the lower levels of p_c that were postulated in the sensitivity evaluation are unlikely.

ASSESSMENT OF MARGINS AGAINST CRACK INITIATION AT CWEST SCRAPE FLAWS IN REGIONS OF INTEREST WITH HIGH LEVELS OF HYDROGEN EQUIVALENT CONCENTRATION IN OUTLET ROLLED JOINTS IN BRUCE UNITS 3 AND 7

Kinectrics Report No.
B2083/RP/0001 R00

8.3 Sensitivity Evaluation of DHC Initiation at Scrape Flaws in Outlet Rolled Joints in Bruce Unit 3 with Variations in Scrape Flaw Geometry

The threshold peak stress for DHC initiation, σ_{th}, was predicted using values of K_{IH} of 2.25 through 4.5 MPa√m, and values of p_c of 200 through 450 MPa. The applied peak flaw-tip principal stress, and the minimum threshold peak stress for DHC initiation based on K_{IH} equal to 2.25 MPa√m and p_c equal to 200 MPa, are given in Table 8-2 for the Bruce Unit 3 Cases B3-2, B3-3, B3-4 and B3-5. From Table 8-2, the threshold peak stress for DHC initiation increases with a decrease in the corner root radius of the scrape flaw. This is a result of the stress gradient from the surface increasing as the root radius decreases, and is consistent with the trends in other process-zone models [25,26].

(a) For the Bruce Unit 3 Case B3-2, with a scrape flaw depth of 0.384 mm and a corner root radius of 1.5 mm, DHC initiation was predicted to not occur for all combinations of K_{IH} and p_c used in the evaluation.

(b) For the Bruce Unit 3 Case B3-3, with a scrape flaw depth of 0.384 mm and a corner root radius of 1.25 mm, the only combinations of K_{IH} and p_c that do not result in a predicted threshold peak stress for DHC initiation greater than applied peak flaw-tip principal stress are:

p_c = 200 MPa and K_{IH} = 2.25 MPa√m
p_c = 200 MPa and K_{IH} = 2.50 MPa√m

(c) The variation of the predicted threshold peak stress for DHC initiation with p_c for a range of K_{IH} for the Bruce Unit 3 Case B3-4 with a scrape flaw depth of 0.384 mm and a corner root radius of 1.0 mm is shown in Figure 8-3. Curves of the threshold peak stress are plotted for values of K_{IH} of 2.25 through 4.5 MPa√m. The applied peak flaw-tip principal stress during hydride precipitation, σ_{1p}, for Case B3-4 of 250.8 MPa is also plotted in Figure 8-3. For the Bruce Unit 3 Case B3-4, the only combinations of K_{IH} and p_c that do not result in a predicted threshold peak stress for DHC initiation greater than applied peak flaw-tip principal stress are:

p_c = 200 MPa and K_{IH} = 2.25 MPa√m
p_c = 200 MPa and K_{IH} = 2.50 MPa√m
p_c = 200 MPa and K_{IH} = 3.00 MPa√m
p_c = 210 MPa and K_{IH} = 2.25 MPa√m

(d) For the Bruce Unit 3 Case B3-5, with a scrape flaw depth of 0.323 mm and a corner root radius of 1.7 mm, DHC initiation was predicted to not occur for all combinations of K_{IH} and p_c used in the evaluation. From Table 8-2, the threshold peak stress of 231.5 MPa for the Bruce Unit 3 Case B3-5 is very close to the threshold peak stress of 231.9 MPa for the Bruce Unit 3 baseline Case B3-1 with a flaw depth of 0.384 mm. The threshold peak stress is insensitive to flaw depth, and this is consistent with other process-zone models for DHC initiation [10,25,26].

ASSESSMENT OF MARGINS AGAINST CRACK INITIATION AT CWEST SCRAPE FLAWS IN REGIONS OF INTEREST WITH HIGH LEVELS OF HYDROGEN EQUIVALENT CONCENTRATION IN OUTLET ROLLED JOINTS IN BRUCE UNITS 3 AND 7

Kinectrics Report No.
B2083/RP/0001 R00

For each of the above cases, both K_{IH} and p_c can be simultaneously reduced from their lower-bound values of 4.5 MPa√m and 450 MPa, respectively [10], by 50% and DHC initiation is predicted to still not occur.

8.4 Summary of Sensitivity Evaluation of DHC Initiation at Scrape Flaws in Outlet Rolled Joints in Bruce Units 3 and 7

For all of the sensitivity cases evaluated, both K_{IH} and p_c can be simultaneously reduced from their lower-bound values of 4.5 MPa√m and 450 MPa, respectively [10], by 50% and DHC initiation is predicted to still not occur. A 50% reduction in K_{IH} and p_c at high levels of H_{eq} is unlikely. There is therefore a low risk of DHC initiation at CWEST scrape flaws in the region of interest in the outlet rolled joints with potentially high levels of H_{eq} in Bruce Units 3 and 7 due to the large predicted margins against DHC initiation. The major contributor to the threshold peak stress for DHC initiation at the scrape flaws is the threshold stress for DHC initiation at a planar surface, p_c. At the time of writing this report, DHC initiation tests on unirradiated pressure tube material with a high level of H_{eq} are in progress to confirm that the lower levels of p_c that were postulated in the sensitivity evaluation are unlikely.

Proprietary and Confidential

ASSESSMENT OF MARGINS AGAINST CRACK INITIATION AT
CWEST SCRAPE FLAWS IN REGIONS OF INTEREST WITH
HIGH LEVELS OF HYDROGEN EQUIVALENT
CONCENTRATION IN OUTLET ROLLED JOINTS IN BRUCE
UNITS 3 AND 7

Kinectrics Report No.
B2083/RP/0001 R00

TABLE 8-1
NORMALIZED STRESS COEFFICIENTS FROM ELASTIC FINITE ELEMENT STRESS ANALYSES AT AXIAL COMPONENT OF SCRAPE FLAW

Reactor Unit	Case	Depth of Scrape Flaw (mm)	Corner Root Radius of Scrape Flaw (mm)	β_1	β_2	β_3	β_4
Bruce Unit 3	B3-1	0.384	1.70	-4.698	25.547	-64.486	59.789
Bruce Unit 3	B3-2	0.384	1.50	-5.142	28.914	-74.284	69.590
Bruce Unit 3	B3-3	0.384	1.25	-5.831	34.276	-90.126	85.585
Bruce Unit 3	B3-4	0.384	1.00	-6.739	41.549	-112.010	107.940
Bruce Unit 3	B3-5	0.323	1.70	-4.729	26.754	-69.427	65.858
Bruce Unit 7	B7-1	0.384	1.70	-4.751	26.139	-66.740	62.593

TABLE 8-2
APPLIED PEAK FLAW-TIP STRESS AND CALCULATED THRESHOLD PEAK STRESS FOR DHC INITIATION BASED ON LOWEST POSTULATED DHC PROPERTIES FOR AXIAL COMPONENT OF SCRAPE FLAW

Reactor Unit	Case	Depth of Scrape Flaw (mm)	Corner Root Radius of Scrape Flaw (mm)	Peak Stress at Axial Component of Scrape Flaw During Hydride Precipitation σ_{1p} (MPa)	Threshold Peak Stress for DHC Initiation based on $K_{IH} = 2.25$ MPa√m and $p_c = 200$ MPa σ_{th} (MPa)
Bruce Unit 3	B3-1	0.384	1.70	225.7	231.9
Bruce Unit 3	B3-2	0.384	1.50	231.0	233.7
Bruce Unit 3	B3-3	0.384	1.25	239.4	236.4
Bruce Unit 3	B3-4	0.384	1.00	250.8	239.8
Bruce Unit 3	B3-5	0.323	1.70	217.8	231.5
Bruce Unit 7	B7-1	0.384	1.70	197.8	231.9

ASSESSMENT OF MARGINS AGAINST CRACK INITIATION AT CWEST SCRAPE FLAWS IN REGIONS OF INTEREST WITH HIGH LEVELS OF HYDROGEN EQUIVALENT CONCENTRATION IN OUTLET ROLLED JOINTS IN BRUCE UNITS 3 AND 7

Kinectrics Report No. B2083/RP/0001 R00
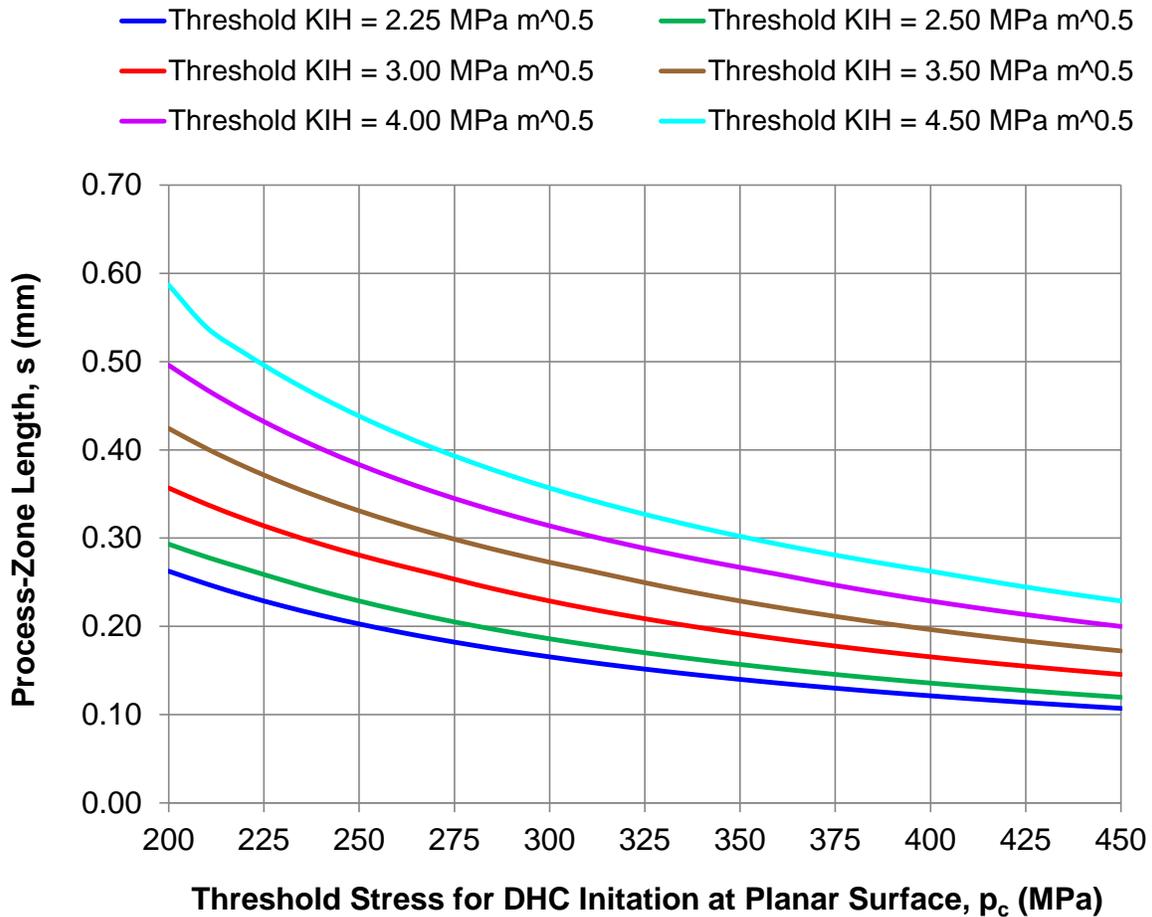
Figure 8-1: Variation of Predicted Process-Zone Length, *s*, with *p_c* for a Range of *K_{IH}* for Bruce Unit 3 Baseline Case B3-1 with a Scrape Flaw Depth of 0.384 mm and a Corner Root Radius of 1.7 mm

ASSESSMENT OF MARGINS AGAINST CRACK INITIATION AT CWEST SCRAPE FLAWS IN REGIONS OF INTEREST WITH HIGH LEVELS OF HYDROGEN EQUIVALENT CONCENTRATION IN OUTLET ROLLED JOINTS IN BRUCE UNITS 3 AND 7

Kinectrics Report No. B2083/RP/0001 R00
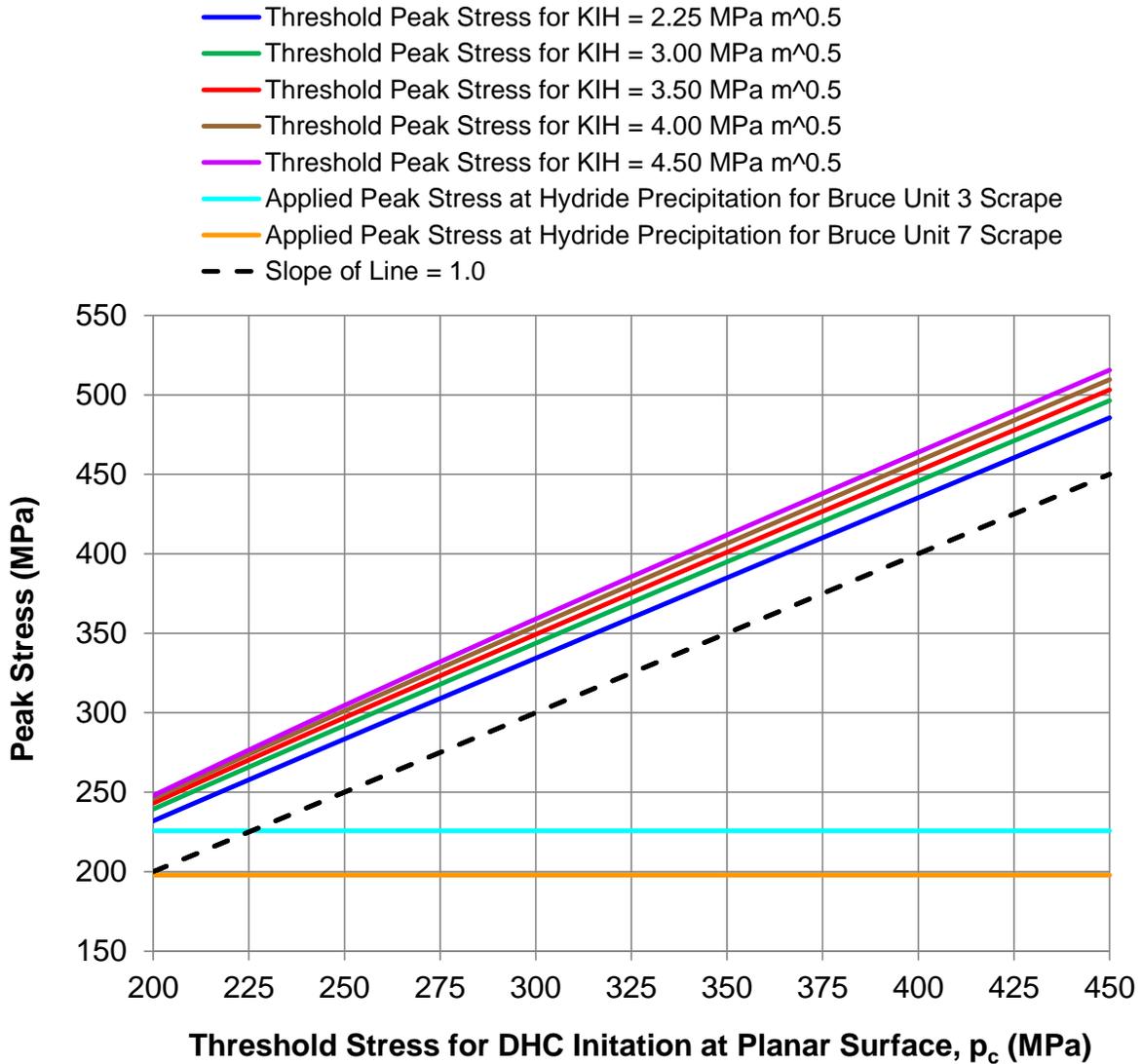
Figure 8-2: Variation of Predicted Threshold Peak Stress for DHC Initiation, σ_{th}, with p_c for a Range of K_{IH} for Bruce Unit 3 Baseline Case B3-1, and Bruce Unit 7 Baseline Case B7-1, with a Scrape Flaw Depth of 0.384 mm and a Corner Root Radius of 1.7 mm, with the Applied Peak Stresses

ASSESSMENT OF MARGINS AGAINST CRACK INITIATION AT CWEST SCRAPE FLAWS IN REGIONS OF INTEREST WITH HIGH LEVELS OF HYDROGEN EQUIVALENT CONCENTRATION IN OUTLET ROLLED JOINTS IN BRUCE UNITS 3 AND 7

Kinectrics Report No. B2083/RP/0001 R00
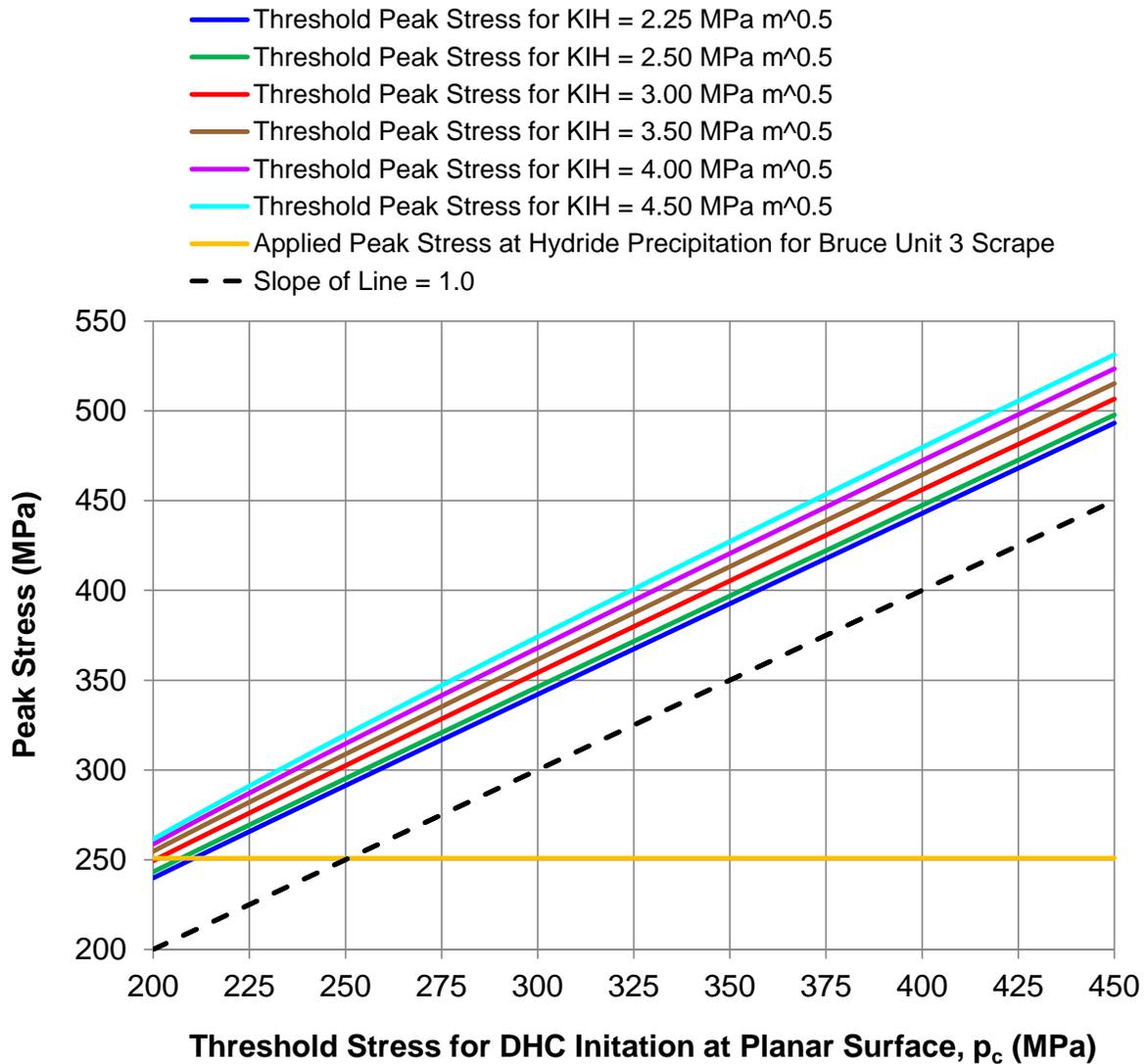
Figure 8-3: Variation of Predicted Threshold Peak Stress for DHC Initiation, σ_{th}, with p_c for a Range of K_{IH} for Bruce Unit 3 Case B3-4 with a Scrape Flaw Depth of 0.384 mm and a Corner Root Radius of 1.0 mm, with the Applied Peak Stress

ASSESSMENT OF MARGINS AGAINST CRACK INITIATION AT CWEST SCRAPE FLAWS IN REGIONS OF INTEREST WITH HIGH LEVELS OF HYDROGEN EQUIVALENT CONCENTRATION IN OUTLET ROLLED JOINTS IN BRUCE UNITS 3 AND 7

Kinectrics Report No.
B2083/RP/0001 R00

9. SUMMARY

(a) High levels of H_{eq} have been detected in the outlet rolled joints of Bruce Unit 3, as well as in the outlet rolled joint of the surveillance pressure tube B6S13. The axial and radial extents of the high levels of H_{eq} inboard of the outlet rolled joint burnish mark have been found to be confined to a localized region with a central tendency about the top of the pressure tube. This localized region inboard of the outlet rolled joint burnish mark with a central tendency about the top of the pressure tube that has high levels of H_{eq} is referred to as the region of interest. Scrape sampling has been performed using the CWEST tool to determine levels of H_{eq} inboard of the outlet rolled joint burnish mark in Bruce Unit 3 during the A2131 outage, and in Bruce Unit 7 during the B2171 outage, including in the region of interest.

(b) There is currently uncertainty regarding the potential effect of high levels of H_{eq} in the region of interest on the crack initiation properties of pressure tube material. Due to the current uncertainty, a margin assessment for demonstration of protection against crack initiation from the CWEST scrape flaws at the 20 mm location inboard of the outlet rolled joint burnish mark in Bruce Unit 3 taken during the A2131 outage, and in Bruce Unit 7 taken during the B2171 outage, has been performed.

(c) The geometry of the CWEST scrape flaws was established. A representative value for the root radius of the entry and exit corners of the scrape flaw that is based on measurements from replicas of scrape flaws was reviewed and used in the evaluation based on three-dimensional elastic finite element stress analyses and a process-zone model for DHC initiation.

(d) The margin assessment consisted of two approaches. The first approach was to evaluate the scrape flaws using the flaw assessment computer code PTFAP with a conservative characterization of the entry and exit corner root radii of the axial component of the scrape flaw that is equal to the flaw depth of 0.384 mm to remain within the root radius validity limits of the equations for the stress concentration factor and the crack initiation models. The objective was to determine the margins against crack initiation using the DHC initiation material properties and crack initiation models in the CSA Standard N285.8. The scrape flaws at the 20 mm location inboard of the outlet rolled joint burnish mark, determined to be the bounding location for the margin assessment, satisfy the requirements of CSA N285.8-15. The threshold peak stress for DHC initiation at the high levels of H_{eq} could be reduced by as much as 40% relative to the predicted threshold peak stress for Bruce Unit 3, and by as much as 45% for Bruce Unit 7, and DHC initiation would still be predicted to not occur. The critical stress for crack initiation due to a hydrided region overload at the high levels of H_{eq} could be reduced by as much as 57% relative to the predicted critical stress for crack initiation due to a hydrided region overload for Bruce Unit 3, and by as much as 53% for Bruce Unit 7, and crack initiation due to a hydrided region overload would still be predicted to not occur. The cumulative fatigue usage factor for the scrape flaws in the outlet rolled joints of all of the pressure tubes scraped is only 0.002 for Bruce Unit 3, and 0.004 for Bruce Unit 7. These margins against crack initiation are substantial in terms of addressing uncertainty in crack initiation material properties at high levels of H_{eq} in the region of interest.

ASSESSMENT OF MARGINS AGAINST CRACK INITIATION AT CWEST SCRAPE FLAWS IN REGIONS OF INTEREST WITH HIGH LEVELS OF HYDROGEN EQUIVALENT CONCENTRATION IN OUTLET ROLLED JOINTS IN BRUCE UNITS 3 AND 7

Kinectrics Report No. B2083/RP/0001 R00

(e) The second approach was a sensitivity evaluation of DHC initiation of the axial component of the scrape flaws using a representative characterization of the entry and exit corner root radii based on measurements from replicas of scrape flaws. The sensitivity of the results of the DHC initiation evaluation of the scrape flaws to the threshold stress intensity factor for DHC initiation from a crack, K_{IH}, and the threshold stress for DHC initiation at a planar surface, p_c, was determined. The sensitivity of the results of the DHC initiation evaluation to the scrape flaw depth, and the scrape flaw entry and exit corner root radii, was also determined. The objective was to demonstrate that DHC initiation will not occur at the scrape flaws for a range of postulated levels of K_{IH} and p_c including very low values that are considered to be unlikely even at high levels of H_{eq}. The sensitivity evaluation was based on three-dimensional elastic finite element stress analyses of the scrape flaws and a process-zone model for DHC initiation that was developed in this report.

(f) For all cases of the sensitivity evaluation of DHC initiation, the DHC initiation material properties K_{IH} and p_c can be simultaneously reduced from their lower-bound values by 50% and DHC initiation is predicted to still not occur. A 50% reduction in K_{IH} and p_c at high levels of H_{eq} is unlikely. There is therefore a low risk of DHC initiation at CWEST scrape flaws in the region of interest in the outlet rolled joints with potentially high levels of H_{eq} in Bruce Units 3 and 7 due to the large predicted margins against DHC initiation. The major contributor to the threshold peak stress for DHC initiation at the scrape flaws is the threshold stress for DHC initiation at a planar surface, p_c. At the time of writing this report, DHC initiation tests on unirradiated pressure tube material with a high level of H_{eq} are in progress to confirm that the lower levels of p_c that were postulated in the sensitivity evaluation are unlikely.

10.   ACKNOWLEDGMENTS

ASSESSMENT OF MARGINS AGAINST CRACK INITIATION AT CWEST SCRAPE FLAWS IN REGIONS OF INTEREST WITH HIGH LEVELS OF HYDROGEN EQUIVALENT CONCENTRATION IN OUTLET ROLLED JOINTS IN BRUCE UNITS 3 AND 7

Kinectrics Report No.
B2083/RP/0001 R00

REFERENCES

1. Letter from C. Nam and K. Harrison to D. Scarth, "Postulated Bounding [H]$_{eq}$ Levels for Bruce Unit 3 Fracture Protection Evaluation," Kinectrics File No. B2038/LET/0009 R00, August 24, 2021.

2. Letter to J. Goldberg, "Engineering Evaluation for Continued Operation of Bruce Power Units 4, 5, 7 and 8 Pressure Tubes with Higher than Expected Hydrogen Equivalent Concentration in the Back-End Outlet Rolled Joint Region," Kinectrics File No. B2210/LET/0003 R01, July 12, 2021.

3. Letter to J. Goldberg, "Justification for Application of Crack Initiation Models to High Hydrogen Equivalent Concentration Regions in Pressure Tubes," Kinectrics File No. B2038/LET/0012 R00, September 16, 2021.

4. Mok, D.H.B., "Software Theory and User Manual for Computer Code PTFAP Version 5-0," Kinectrics File No. PS275/MA/001 R00, June 08, 2018.

5. Kratt, A., "Establishment of Bounding Cases for Cut Parameters," Kinectrics Document No. K-014949-TN-0001 R01, October 2014.

6. Reichert, D., "Summary of CWEST Cut Profile Parameters," Kinectrics Document No. K-402200-TM-0011 R00, December 8, 2021.

7. Kinectrics Letter from K. Tsai to D. Scarth, "Representative CWEST Sample Cut Root Radius in the Radial-Circumferential Plane," Kinectrics File No. B2083/RE/0039 R00, December 10, 2021.

8. Klarner, L., "A2131 Assessment of Bounding CWEST Flaws," Kinectrics File No. B2038/RE/0083 R01, December 2, 2021.

9. Mok, D.H.B., Letter to R. Ahmad and A. Glover, "Release of Computer Code PTFAP Version 5-1," Kinectrics File No. PS275/025/000001 R00, August 30, 2018.

10. "Technical Requirements for In-Service Evaluation of Zirconium Alloy Pressure Tubes in CANDU Reactors," Canadian Standards Association, CSA Standard N285.8-15, with Update No. 1.

11. Letter to L. Micuda, "Re: Recommended Outage Inspection Scope for the A2131 Additional Revisit Window," Kinectrics File No. B2038/SOW/0001 R00, July 29, 2021.

12. Robertson, J., "B3-B8 EOL Pressure Tube Dimensions at BM+20mm for Application in Pressure Tube Flaw Assessments and Fracture Protection Evaluations", Kinectrics File No. B2083/RE/0040 R01, November 30, 2021.

ASSESSMENT OF MARGINS AGAINST CRACK INITIATION AT CWEST SCRAPE FLAWS IN REGIONS OF INTEREST WITH HIGH LEVELS OF HYDROGEN EQUIVALENT CONCENTRATION IN OUTLET ROLLED JOINTS IN BRUCE UNITS 3 AND 7

Kinectrics Report No.
B2083/RP/0001 R00

13. Klarner, L., "B2171 Assessment of Bounding CWEST Flaws," Kinectrics File No. B2083/RE/0034 R00, December 2, 2021.

14. Huang, K., "Recommended Fuel Channel Inspection Scope for B2171 Planned Outage – Scope of Work", Kinectrics File B2083/PL/004 R01, November 15, 2021.

15. Manu, C., "Rolled Joint As-Rolled Residual Hoop Stresses 20 mm Inboard the Burnish Mark in Ontario CANDU Nuclear Reactors," COG Other Product No. OP-JP-4583-V078, Kinectrics NSS File: KN053/RP/001 R00, 2019.

16. Doddihal, P. and Scarth, D.A., "Implicit Safety Factors on Pressure for Heatup and Cooldown in Ontario Power Generation and Bruce Power Reactors," COG Report No. COG-JP-4583-V032-R00, November 2018.

17. Choudhry, A., "Technical Review Report for Revised Operational Envelope of Primary Heat Transport System (PHT) W.R.T System Transients," Bruce Power Document No. NK21-REP-30000-00005-Rev000, Tetra Tech No. 705-70518848602.283-REP-M0001-00, Tetra Tech, September 29, 2021.

18. Scarth, D.A. and Gutkin, L., "Evaluation of Predicted Pressure Tube Rolled Joint Residual Hoop Stresses in Support of Pre-Conditioning Procedure for Hydrided Burst Test Specimens," COG Report No. COG-JP-4583-V079-R00, March 11, 2019.

19. Email from A. Sahoo, "Information on irradiation temperature is needed urgently," Kinectrics, Kinectrics File No. K-024045, May 23, 2020.

20. Camacho, F., memorandum to G.R.S. Evans, "Percentiles of Normal-Clearance Stress Relieved Rolled Joint Residual Stresses," Ontario Hydro Technologies File No. 809.717, April 5, 1994.

21. Email from T. Hunt, "RJ Residual Stresses in the Outlet Rolled Joint for B2171 CWEST channels in the ROI," Kinectrics File No. B2083/RE/0049 R00, December 7, 2021.

22. Kawa, D.M., "Bruce Scrape Elastic Stress Analysis," Kinectrics File No. B2083/RE/0050 R00, November 30, 2021.

23. "ANSYS, Version 2021 R1," ANSYS, Inc., Southpointe, 275 Technology Drive, Canonsburg, PA, January 2021.

24. Mok, D.H.B., "Guidelines for Pressure Tube Flaw-Tip Stress Analysis," Revision 1, Nuclear Safety Solutions Report No. G0055/RP/001 R01, January 19, 2007.

ASSESSMENT OF MARGINS AGAINST CRACK INITIATION AT
CWEST SCRAPE FLAWS IN REGIONS OF INTEREST WITH
HIGH LEVELS OF HYDROGEN EQUIVALENT
CONCENTRATION IN OUTLET ROLLED JOINTS IN BRUCE
UNITS 3 AND 7

Kinectrics Report No.
B2083/RP/0001 R00

25. Scarth, D.A. and Smith, E., "Developments in Flaw Evaluation for CANDU Reactor Zr-Nb Pressure Tubes," *Proceedings of the 1999 ASME Pressure Vessels and Piping Conference*, Boston, Massachusetts, August 2-5, PVP Volume 391, pp. 35-45, also published in the *ASME Journal of Pressure Vessel Technology*, Volume 123, February 2001, pp. 41-48.

26. Smith, E. and Scarth, D.A., "Extending Fracture Mechanics for Cracks to the Behaviour of Notches," *Proceedings of the 2001 ASME Pressure Vessels and Piping Conference*, Atlanta, Georgia, July 22-26.

27. Leger, M. and Donner, A., "The Effect of Stress on Orientation of Hydrides in Zirconium Alloy Pressure Tube Materials," *Canadian Metallurgical Quarterly*, 24:3, 1985, 235-243, DOI: 10.1179/cmq.1985.24.3.235.

28. Dugdale, D.S., "Yielding of Steel Sheets Containing Slits," *Journal of Mechanics and Physics of Solids*, Vol. 8, pp. 100-104, 1960.

29. Bilby, B.A., Cottrell, A.H. and Swinden, K.H., "The Spread of Plastic Yield from a Notch," *Proceedings, Royal Society of London*, Vol. A-272, pp. 304-314, 1963.

30. Tada, H., Paris, P.C. and Irwin, G.R., *The Stress Analysis of Cracks Handbook*, Third Edition, American Society of Mechanical Engineers, New York, NY, 2000.

31. Stallybrass, M.P., "A Crack Perpendicular to an Elastic Half-Plane," *International Journal of Engineering Science*, Vol. 8, pp. 351-362, 1970.

ASSESSMENT OF MARGINS AGAINST CRACK INITIATION AT
CWEST SCRAPE FLAWS IN REGIONS OF INTEREST WITH
HIGH LEVELS OF HYDROGEN EQUIVALENT
CONCENTRATION IN OUTLET ROLLED JOINTS IN BRUCE
UNITS 3 AND 7

Kinectrics Report No.
B2083/RP/0001 R00

APPENDIX A

DEVELOPMENT OF PROCESS-ZONE MODEL FOR EVALUATION OF DHC INITIATION AT THE AXIAL COMPONENT OF A CWEST SCRAPE FLAW

A-1 INTRODUCTION

As described in Section 3 of this report, the entry and exit corner root radii of the axial components of the CWEST scrape flaws are significantly larger than the flaw depth. The models for calculation of the stress concentration factor at a flaw, and the process-zone models for evaluation of DHC initiation at flaws, which are in the CSA Standard N285.8 [10] are not applicable to a flaw geometry where the flaw root radius is significantly larger than the flaw depth. For this reason, a process-zone model that is applicable to the evaluation of DHC initiation at the axial component of a CWEST scrape flaw was developed as described in this Appendix.

The process-zone model that was developed below is an adaptation of previously developed process-zone models for DHC initiation that are provided in References [10,25,26]. The basic fundamentals and criteria for DHC initiation in the process-zone model for a scrape flaw are the same as in the previously developed models. The main difference is that the process-zone models in References [10,25,26] were developed primarily for a flaw with a root radius less than or equal to the flaw depth, whereas the process-zone model for a scrape flaw was developed for a flaw root radius significantly larger than the flaw depth. For this reason, the solutions for the stress intensity factor and crack-mouth opening displacement for a process zone at the planar surface of a finite thickness plate were used in the development of the process-zone model for a scrape flaw in this Appendix instead of the solutions for a process zone at the tip of a blunt flaw that were used in References [10,25,26]. A process-zone model based on a hydrided region at a planar surface is considered to be a reasonable representation for the geometry of a CWEST scrape flaw.

A-2 GENERAL THEORY AND FAILURE CRITERIA FOR PROCESS-ZONE MODEL FOR CWEST SCRAPE FLAWS

A hydrided region that emanates from a surface, together with the particular sub-region that is fracturing, can be viewed as a single entity. This single entity is represented by an infinitesimally thin, two-dimensional strip, or process zone, emanating from a flaw. A process zone emanating from a planar surface and subjected to an applied linear stress distribution is shown in Figure A-1. Within this process zone the tensile stress is idealized to have a uniform value p_H, while the relative displacement across the zone at the flaw-tip surface is equal to v_T, as illustrated in Figure A-1. As the amount of precipitated hydride increases, and because of the expansion associated with hydride precipitation, the stress p_H decreases while v_T increases. It is presumed that loss of cohesion at the trailing edge of the process zone at the flaw-tip surface,

Proprietary and Confidential

ASSESSMENT OF MARGINS AGAINST CRACK INITIATION AT CWEST SCRAPE FLAWS IN REGIONS OF INTEREST WITH HIGH LEVELS OF HYDROGEN EQUIVALENT CONCENTRATION IN OUTLET ROLLED JOINTS IN BRUCE UNITS 3 AND 7

Kinectrics Report No. B2083/RP/0001 R00

which corresponds to DHC initiation, occurs when v_T attains a critical value v_c. Furthermore, there exists a limiting threshold value of p_H below which the hydrided region is unable to fracture, and this threshold stress is denoted as p_c. In order for DHC initiation to occur, two conditions must be satisfied [10,25,26].

$$v_T \geq v_c \qquad \text{(A-2-1)}$$

and

$$p_H \geq p_c \qquad \text{(A-2-2)}$$

where

p_c	=	threshold stress for DHC initiation at a planar surface
p_H	=	process-zone restraining stress
v_c	=	critical process-zone displacement for DHC initiation
v_T	=	applied process-zone displacement

The parameter p_c is the threshold stress below which a hydrided region cannot fracture and this is the threshold stress for the conditions under which an effectively "infinitely" long hydrided region emanates from a planar surface. Regarding the critical process-zone displacement for DHC initiation, v_c, it is recognized that when the uniform stress process-zone representation, which is the Dugdale-Bilby-Cottrell-Swinden representation [28,29], is applied to a long crack at threshold conditions such that $p_H = p_c$, then [10,25,26]

$$v_c = \frac{K_{IH}^2}{E' p_c} \qquad \text{(A-2-3)}$$

where

$$E' = \frac{E}{1 - v^2} \qquad \text{(A-2-4)}$$

and

E	=	Young's modulus of the Zr-Nb pressure tube material
K_{IH}	=	isothermal threshold stress intensity factor for DHC initiation from a crack
v	=	Poisson's ratio of the Zr-Nb pressure tube material

A schematic illustration of whether DHC will initiate is shown in Figure A-2. This figure is for the situation of growth of the hydrided region with each thermal cycle under hydride ratcheting conditions. The hydrided region will grow in size with each Heatup/Cooldown cycle and p_H will

Proprietary and Confidential

ASSESSMENT OF MARGINS AGAINST CRACK INITIATION AT CWEST SCRAPE FLAWS IN REGIONS OF INTEREST WITH HIGH LEVELS OF HYDROGEN EQUIVALENT CONCENTRATION IN OUTLET ROLLED JOINTS IN BRUCE UNITS 3 AND 7

Kinectrics Report No.
B2083/RP/0001 R00

progressively decrease. In particular, the threshold peak stress for DHC initiation, σ_{th}, is defined as the lowest level of initial peak flaw-tip stress, p_H, prior to hydrided region formation, at which DHC initiation can occur, as indicated schematically by the middle curve in Figure A-2. Furthermore, if the hydrided region stress p_H falls below p_c prior to v_T having reached v_c, then DHC initiation will not occur despite further development of the hydrided region. This corresponds to the lower curve in Figure A-2. In this Appendix the criteria for DHC initiation are evaluated at threshold conditions to determine the threshold peak stress for DHC initiation, σ_{th}, as shown by the middle curve in Figure A-2. This is achieved by setting the process-zone restraining stress, p_H, equal to p_c, and requiring that at threshold conditions, v_T is equal to v_c.

A-3 STRESS DISTRIBUTION THROUGH THE WALL THICKNESS ADJACENT TO THE SCRAPE FLAW

With reference to the process zone that is emanating from a planar surface in Figure A-1, the stress distribution adjacent to the scrape flaw through the wall thickness is approximated as linear as given below

$$\sigma(x) = A_0 + A_1\left(\frac{x}{s}\right) \tag{A-3-1}$$

where

A_j = stress coefficient for the jth power term of the stress distribution
s = process-zone length
x = local coordinate with origin at the surface
$\sigma(x)$ = elastic stress distribution through the wall thickness

This equation can also be written in terms of the peak flaw-tip principal stress at the surface.

$$\sigma(x) = \sigma_{1p} + A_1\left(\frac{x}{s}\right) \tag{A-3-2}$$

where

σ_{1p} = peak flaw-tip principal stress

Equation (A-3-1) can be written in a normalized form.

$$\frac{\sigma(x)}{A_0} = 1 + \alpha_1(s)\left(\frac{x}{s}\right) \tag{A-3-3}$$

ASSESSMENT OF MARGINS AGAINST CRACK INITIATION AT CWEST SCRAPE FLAWS IN REGIONS OF INTEREST WITH HIGH LEVELS OF HYDROGEN EQUIVALENT CONCENTRATION IN OUTLET ROLLED JOINTS IN BRUCE UNITS 3 AND 7

Kinectrics Report No. B2083/RP/0001 R00

where

$$\alpha_1(s) \;=\; \frac{A_1}{A_0} \tag{A-3-4}$$

and

$\alpha_1(s)$ =   normalized linear stress coefficient that depends on the process-zone length, s

A fourth-order polynomial of the normalized stress distribution adjacent to the scrape flaw was fitted to the normalized distance through the wall thickness from the elastic finite element stress analysis with the form

$$\frac{\sigma_F(x)}{A_0} \;=\; 1 \;+\; \beta_1\!\left(\frac{x}{d}\right) \;+\; \beta_2\!\left(\frac{x}{d}\right)^2 \;+\; \beta_3\!\left(\frac{x}{d}\right)^3 \;+\; \beta_4\!\left(\frac{x}{d}\right)^4 \tag{A-3-5}$$

where

$$d \;=\; w \;-\; a \tag{A-3-6}$$

and

a =   depth of the scrape flaw
β_j =   normalized stress coefficient for the jth power term of the fitted fourth-order polynomial normalized stress distribution
d =   remaining wall thickness of the pressure tube at the scrape flaw
w =   wall thickness of the pressure tube
x =   local coordinate with origin at the surface
$\sigma_F(x)$ =   elastic stress distribution through the wall thickness from the fitted fourth-order polynomial stress distribution

The linear approximation of the normalized stress distribution through the wall thickness was conservatively treated as a secant to the fitted fourth-order polynomial normalized stress distribution where the linear approximation intersects the fourth-order normalized polynomial stress distribution at the distance x equal to s. The normalized stress coefficient $\alpha_1(s)$ therefore depends on the length, s, of the process zone. At x equal to s, one can write

$$1 \;+\; \alpha_1(s) \;=\; 1 \;+\; \beta_1\!\left(\frac{s}{d}\right) \;+\; \beta_2\!\left(\frac{s}{d}\right)^2 \;+\; \beta_3\!\left(\frac{s}{d}\right)^3 \;+\; \beta_4\!\left(\frac{s}{d}\right)^4 \tag{A-3-7}$$

Or,

ASSESSMENT OF MARGINS AGAINST CRACK INITIATION AT CWEST SCRAPE FLAWS IN REGIONS OF INTEREST WITH HIGH LEVELS OF HYDROGEN EQUIVALENT CONCENTRATION IN OUTLET ROLLED JOINTS IN BRUCE UNITS 3 AND 7

Kinectrics Report No. B2083/RP/0001 R00

$$\alpha_1(s) = \beta_1\left(\frac{s}{d}\right) + \beta_2\left(\frac{s}{d}\right)^2 + \beta_3\left(\frac{s}{d}\right)^3 + \beta_4\left(\frac{s}{d}\right)^4 \tag{A-3-8}$$

The conservative linear stress distribution approximation to the normalized fourth-order polynomial representation of the principal stress distribution at the scrape flaw is illustrated in Figure A-3.

A-4 STRESS INTENSITY FACTOR

The stress intensity factor for the linear stress distribution given by Eq. (A-3-1) is given by

$$K_I(s, \sigma(x)) = \left(A_0 G_0(s/d) + A_1 G_1(s/d)\right)(\pi s)^{1/2} \tag{A-4-1}$$

where

$G_j(s/d)$ = geometry correction factor for the stress intensity factor for the jth power term of the stress distribution

$K_I(s, \sigma(x))$ = stress intensity factor for the process-zone length, s, and the stress distribution, $\sigma(x)$

Equation (A-3-1) can be written in terms of membrane and bending stresses across the remaining wall thickness, d, of the pressure tube.

$$\sigma(x) = \sigma_m + \sigma_b\left(1 - 2\left(\frac{x}{d}\right)\right) \tag{A-4-2}$$

where

σ_m = membrane stress across the remaining wall thickness, d
σ_b = bending stress across the remaining wall thickness, d

Comparting Eq. (A-3-1) with Eq. (A-4-2) gives

$$A_0 = \sigma_m + \sigma_b \tag{A-4-3}$$

$$A_1\left(\frac{x}{s}\right) = -2\sigma_b\left(\frac{x}{d}\right) \tag{A-4-4}$$

Or,

Proprietary and Confidential

ASSESSMENT OF MARGINS AGAINST CRACK INITIATION AT CWEST SCRAPE FLAWS IN REGIONS OF INTEREST WITH HIGH LEVELS OF HYDROGEN EQUIVALENT CONCENTRATION IN OUTLET ROLLED JOINTS IN BRUCE UNITS 3 AND 7

Kinectrics Report No. B2083/RP/0001 R00

$$\sigma_b \;\; = \;\; -\frac{1}{2}A_1\frac{d}{s} \tag{A-4-5}$$

and

$$\sigma_m \;\; = \;\; A_0 \;-\; \sigma_b \tag{A-4-6}$$

$$\sigma_m \;\; = \;\; A_0 \;+\; \frac{1}{2}A_1\frac{d}{s} \tag{A-4-7}$$

From Reference [30], the stress intensity factor for an applied membrane stress, σ_m, is given by

$$K_{\mathrm{I}}(s,\sigma_m) \;\; = \;\; \sigma_m F_m(s/d)(\pi s)^{1/2} \tag{A-4-8}$$

where

$$F_m(s/d) \;\; = \;\; 1.122 \;-\; 0.231\left(\frac{s}{d}\right) \;+\; 10.550\left(\frac{s}{d}\right)^2 \;-\; 21.710\left(\frac{s}{d}\right)^3 \;+\; 30.382\left(\frac{s}{d}\right)^4 \tag{A-4-9}$$

and

$F_m(s/d)$ = geometry correction factor for the stress intensity factor for the membrane stress, σ_m

$K_I(s, \sigma_m)$ = stress intensity factor for the process-zone length, s, and the membrane stress, σ_m

From Reference [30], the stress intensity factor for an applied bending stress, σ_b, is given by

$$K_{\mathrm{I}}(s,\sigma_b) \;\; = \;\; \sigma_b F_b(s/d)(\pi s)^{1/2} \tag{A-4-10}$$

where

$$F_b(s/d) \;\; = \;\; 1.122 \;-\; 1.40\left(\frac{s}{d}\right) \;+\; 7.33\left(\frac{s}{d}\right)^2 \;-\; 13.08\left(\frac{s}{d}\right)^3 \;+\; 14.0\left(\frac{s}{d}\right)^4 \tag{A-4-11}$$

and

$F_b(s/d)$ = geometry correction factor for the stress intensity factor for the bending stress, σ_b

ASSESSMENT OF MARGINS AGAINST CRACK INITIATION AT CWEST SCRAPE FLAWS IN REGIONS OF INTEREST WITH HIGH LEVELS OF HYDROGEN EQUIVALENT CONCENTRATION IN OUTLET ROLLED JOINTS IN BRUCE UNITS 3 AND 7

Kinectrics Report No. B2083/RP/0001 R00

$K_I(s, \sigma_b)$ = stress intensity factor for the process-zone length, s, and the bending stress, σ_b

From Eqs. (A-4-8) and (A-4-10), the total stress intensity factor is given by

$$K_I(s, \sigma_m, \sigma_b) = \left[\sigma_m F_m(s/d) + \sigma_b F_b(s/d) \right](\pi s)^{1/2} \tag{A-4-12}$$

Substitution of Eqs. (A-4-5) and (A-4-7) into Eq. (A-4-12) gives

$$K_I(s, A_j) = \left[\left(A_0 + \frac{1}{2} A_1 \frac{d}{s} \right) F_m(s/d) - \frac{1}{2} A_1 \frac{d}{s} F_b(s/d) \right](\pi s)^{1/2} \tag{A-4-13}$$

Collecting terms in A_0 and A_1 gives

$$K_I(s, A_j) = \left[A_0 F_m(s/d) + A_1 \frac{d}{2s} \left(F_m(s/d) - F_b(s/d) \right) \right](\pi s)^{1/2} \tag{A-4-14}$$

Comparing Eq. (A-4-1) with Eq. (A-4-14) gives

$$G_0(s/d) = F_m(s/d) \tag{A-4-15}$$

$$G_1(s/d) = \frac{d}{2s} \left(F_m(s/d) - F_b(s/d) \right) \tag{A-4-16}$$

For very small s/d, one can write

$$G_1(s/d) = \frac{d}{2s} \left[1.122 - 0.231 \left(\frac{s}{d} \right) - 1.122 + 1.40 \left(\frac{s}{d} \right) \right] \tag{A-4-17}$$

$$G_1(s/d) = 0.5845 \tag{A-4-18}$$

The actual lower limit on $G_1(s/d)$ corresponds to crack at the surface of a semi-infinite solid. The value of $G_1(s/d)$ for a crack at the surface of a semi-infinite solid is given by [31]

$$G_1(s/d) = 0.6829 \tag{A-4-19}$$

In the calculations, when $G_1(s/d)$ is less than 0.6829, $G_1(s/d)$ is set equal to 0.6829.

ASSESSMENT OF MARGINS AGAINST CRACK INITIATION AT CWEST SCRAPE FLAWS IN REGIONS OF INTEREST WITH HIGH LEVELS OF HYDROGEN EQUIVALENT CONCENTRATION IN OUTLET ROLLED JOINTS IN BRUCE UNITS 3 AND 7

Kinectrics Report No.
B2083/RP/0001 R00

A-5 CRACK-MOUTH OPENING DISPLACEMENT

The crack-mouth opening displacement for the linear stress distribution given by Eq. (A-3-1) is given by

$$v_T\left(s,\sigma(x)\right) \;=\; \frac{5.1869\,s}{E'}\left(A_0 V_0\left(s/d\right) \,+\, A_1 V_1\left(s/d\right)\right) \tag{A-5-1}$$

where

$$E' \;=\; \frac{E}{1 \,-\, v^2} \tag{A-5-2}$$

and

E	$=$	Young's modulus of the Zr-Nb pressure tube material
$V_j(s/d)$	$=$	geometry factor for the crack-mouth opening displacement for the jth power term of the stress distribution
$v_T(s,\sigma(x))$	$=$	crack-mouth opening displacement for the process-zone length, s, and the stress distribution, $\sigma(x)$
v	$=$	Poisson's ratio of the Zr-Nb pressure tube material

From Reference [30], the crack-mouth opening displacement for an applied membrane stress, σ_m, is given by

$$v_T\left(s,\sigma_m\right) \;=\; \frac{4\sigma_m s}{E'} V_m\left(s/d\right) \tag{A-5-3}$$

where

$$V_m\left(s/d\right) \;=\; \frac{1.46 \,+\, 3.42\left[1 \,-\, \cos\!\left(\dfrac{\pi}{2}\dfrac{s}{d}\right)\right]}{\left(\cos\!\left(\dfrac{\pi}{2}\dfrac{s}{d}\right)\right)^2} \tag{A-5-4}$$

and

$V_m(s/d)$	$=$	geometry factor for the crack-mouth opening displacement for the membrane stress, σ_m
$v_T(s,\sigma_m)$	$=$	crack-mouth opening displacement for the process-zone length, s, and the membrane stress, σ_m

Proprietary and Confidential

ASSESSMENT OF MARGINS AGAINST CRACK INITIATION AT CWEST SCRAPE FLAWS IN REGIONS OF INTEREST WITH HIGH LEVELS OF HYDROGEN EQUIVALENT CONCENTRATION IN OUTLET ROLLED JOINTS IN BRUCE UNITS 3 AND 7

Kinectrics Report No. B2083/RP/0001 R00

From Reference [30], the crack-mouth opening displacement for an applied bending stress, σ_b, is given by

$$v_T\left(s,\sigma_b\right) \;=\; \frac{4\sigma_b s}{E'}V_b\left(s/d\right) \tag{A-5-5}$$

where

$$V_b\left(s/d\right) \;=\; 0.8 \;-\; 1.7\left(\frac{s}{d}\right) \;+\; 2.4\left(\frac{s}{d}\right)^2 \;+\; \frac{0.66}{\left(1 - \dfrac{s}{d}\right)^2} \tag{A-5-6}$$

and

$V_b(s/d)$ = geometry factor for the crack-mouth opening displacement for the bending stress, σ_b

$v_T(s,\sigma_b)$ = crack-mouth opening displacement for the process-zone length, s, and the bending stress, σ_b

From Eqs. (A-5-3) and (A-5-5), the total crack-mouth opening displacement is given by

$$v_T\left(s,\sigma_m,\sigma_b\right) \;=\; \frac{4s}{E'}\left[\sigma_m V_m\left(s/d\right) \;+\; \sigma_b V_b\left(s/d\right)\right] \tag{A-5-7}$$

From Eqs. (A-4-5) and (A-4-7), the membrane and bending stresses can be written in terms of A_0 and A_1 as

$$\sigma_m \;=\; A_0 \;+\; \frac{1}{2}A_1\frac{d}{s} \tag{A-5-8}$$

$$\sigma_b \;=\; -\frac{1}{2}A_1\frac{d}{s} \tag{A-5-9}$$

Substitution of Eqs. (A-5-8) and (A-5-9) into Eq. (A-5-7) gives

$$v_T\left(s,A_j\right) \;=\; \frac{4s}{E'}\left[\left(A_0 \;+\; A_1\frac{d}{2s}\right)V_m\left(s/d\right) \;-\; A_1\frac{d}{2s}V_b\left(s/d\right)\right] \tag{A-5-10}$$

Comparing terms in A_0 between Eqs. (A-5-1) and (A-5-10) gives

---

ASSESSMENT OF MARGINS AGAINST CRACK INITIATION AT CWEST SCRAPE FLAWS IN REGIONS OF INTEREST WITH HIGH LEVELS OF HYDROGEN EQUIVALENT CONCENTRATION IN OUTLET ROLLED JOINTS IN BRUCE UNITS 3 AND 7

Kinectrics Report No. B2083/RP/0001 R00

$$V_0\left(s/d\right) \;=\; \frac{4}{5.1869}V_m\left(s/d\right) \tag{A-5-11}$$

Comparing terms in A_1 between Eqs. (A-5-1) and (A-5-10) gives

$$\frac{5.1869s}{E'}A_1V_1\left(s/d\right) \;=\; \frac{4s}{E'}\left[A_1\frac{d}{2s}V_m\left(s/d\right) - A_1\frac{d}{2s}V_b\left(s/d\right)\right] \tag{A-5-12}$$

Or,

$$V_1\left(s/d\right) \;=\; \frac{2}{5.1869}\frac{d}{s}\left[V_m\left(s/d\right) - V_b\left(s/d\right)\right] \tag{A-5-13}$$

The lower limit on $V_1(s/d)$ corresponds to crack at the surface of a semi-infinite solid. The value of $V_1(s/d)$ for a crack at the surface of a semi-infinite solid is given by [31]

$$V_1\left(s/d\right) \;=\; 0.3415 \tag{A-5-14}$$

In the calculations, when $V_1(s/d)$ is less than 0.3415, $V_1(s/d)$ is set equal to 0.3415.

A-6   PROCESS-ZONE LENGTH

Following the Dugdale-Bilby-Cottrell-Swinden approach [28,29], the process-zone length is given by the solution of the equation given below.

$$K_I\left(s,\sigma(x)\right) + K_I\left(s,p_c\right) \;=\; 0 \tag{A-6-1}$$

where

$$K_I\left(s,\sigma(x)\right) \;=\; \left[A_0G_0\left(s/d\right) + A_1G_1\left(s/d\right)\right]\left(\pi s\right)^{1/2} \tag{A-6-2}$$

$$K_I\left(s,p_c\right) \;=\; -p_cG_0\left(s/d\right)\left(\pi s\right)^{1/2} \tag{A-6-3}$$

and

$K_I(s,\sigma(x)) =$ stress intensity factor for the process-zone length, s, and the stress distribution, $\sigma(x)$

$K_I(s,p_c) =$ stress intensity factor for the process-zone length, s, and the process-zone restraining stress, p_c

$p_c =$ process-zone restraining stress

ASSESSMENT OF MARGINS AGAINST CRACK INITIATION AT CWEST SCRAPE FLAWS IN REGIONS OF INTEREST WITH HIGH LEVELS OF HYDROGEN EQUIVALENT CONCENTRATION IN OUTLET ROLLED JOINTS IN BRUCE UNITS 3 AND 7

Kinectrics Report No. B2083/RP/0001 R00

Substitution of Eqs. (A-6-2) and (A-6-3) into Eq. (A-6-1) gives

$$(A_0 - p_c)G_0(s/d) + A_1G_1(s/d) = 0 \qquad \text{(A-6-4)}$$

The process-zone length is given by solving Eq. (A-6-4) by iteration.

A-7 PROCESS-ZONE DISPLACEMENT

Following the Dugdale-Bilby-Cottrell-Swinden approach [28,29], the process-zone displacement is given by

$$v_T\big(s,\sigma(x),p_c\big) = v_T\big(s,\sigma(x)\big) + v_T\big(s,p_c\big) \qquad \text{(A-7-1)}$$

where

$$v_T\big(s,\sigma(x)\big) = \frac{5.1869s}{E'}\big[A_0 V_0(s/d) + A_1 V_1(s/d)\big] \qquad \text{(A-7-2)}$$

$$v_T\big(s,p_c\big) = -\frac{5.1869s}{E'}p_c V_0(s/d) \qquad \text{(A-7-3)}$$

where

$v_T(s,\sigma(x))$ = crack-mouth opening displacement for the process-zone length, s, and the stress distribution, $\sigma(x)$

$v_T(s,p_c)$ = crack-mouth opening displacement for the process-zone length, s, and the process-zone restraining stress, p_c

Substitution of Eqs. (A-7-2) and (A-7-3) into Eq. (A-7-1) gives

$$v_T\big(s,\sigma(x),p_c\big) = \frac{5.1869s}{E'}\big[(A_0 - p_c)V_0(s/d) + A_1V_1(s/d)\big] \qquad \text{(A-7-4)}$$

Proprietary and Confidential

ASSESSMENT OF MARGINS AGAINST CRACK INITIATION AT CWEST SCRAPE FLAWS IN REGIONS OF INTEREST WITH HIGH LEVELS OF HYDROGEN EQUIVALENT CONCENTRATION IN OUTLET ROLLED JOINTS IN BRUCE UNITS 3 AND 7

Kinectrics Report No.
B2083/RP/0001 R00

A-8 THRESHOLD PEAK STRESS FOR DHC INITIATION

From Eq. (A-6-4),

$$A_0 - p_c = -\frac{A_1 G_1(s/d)}{G_0(s/d)} \tag{A-8-1}$$

Substitution of Eq. (A-8-1) into Eq. (A-7-4) gives

$$v_T(s, \sigma(x), p_c) = \frac{5.1869 s A_1}{E'}\left[V_1(s/d) - \frac{G_1(s/d)}{G_0(s/d)}V_0(s/d)\right] \tag{A-8-2}$$

From Eq. (A-3-4),

$$\alpha_1(s) = \frac{A_1}{A_0} \tag{A-8-3}$$

Substitution of Eq. (A-8-3) into Eq. (A-8-2) gives

$$v_T(s, \sigma(x), p_c) = \frac{5.1869 s \alpha_1(s) A_0}{E'}\left[V_1(s/d) - \frac{G_1(s/d)}{G_0(s/d)}V_0(s/d)\right] \tag{A-8-4}$$

Define A_0 to be the threshold peak stress for DHC initiation, σ_{th}.

$$A_0 = \sigma_{th} \tag{A-8-5}$$

where

σ_{th} = threshold peak stress for DHC initiation

Substitution of Eq. (A-8-5) into Eq. (A-8-4) gives

$$v_T(s, \sigma(x), p_c) = \frac{5.1869 s \alpha_1(s) \sigma_{th}}{E'}\left[V_1(s/d) - \frac{G_1(s/d)}{G_0(s/d)}V_0(s/d)\right] \tag{A-8-6}$$

Substitution of Eqs. (A-8-3) and (A-8-5) into Eq. (A-6-4) gives

$$(\sigma_{th} - p_c)G_0(s/d) + \sigma_{th}\alpha_1 G_1(s/d) = 0 \tag{A-8-7}$$

ASSESSMENT OF MARGINS AGAINST CRACK INITIATION AT
CWEST SCRAPE FLAWS IN REGIONS OF INTEREST WITH
HIGH   LEVELS   OF   HYDROGEN   EQUIVALENT
CONCENTRATION IN OUTLET ROLLED JOINTS IN BRUCE
UNITS 3 AND 7

Kinectrics Report No.
B2083/RP/0001 R00

Rearranging Eq. (A-8-7) gives

$$\sigma_{th}\big(G_0(s/d) + \alpha_1 G_1(s/d)\big) \;=\; p_c G_0(s/d) \tag{A-8-8}$$

Or,

$$\sigma_{th} \;=\; \frac{p_c G_0(s/d)}{G_0(s/d) + \alpha_1 G_1(s/d)} \tag{A-8-9}$$

Substitution of Eq. (A-8-9) into Eq. (A-8-6) gives

$$v_T\big(s,\sigma(x),p_c\big) \;=\; 5.1869 s\alpha_1(s)\frac{p_c}{E'}\frac{\big[G_0(s/d)V_1(s/d) - G_1(s/d)V_0(s/d)\big]}{G_0(s/d) + \alpha_1 G_1(s/d)} \tag{A-8-10}$$

Equation (A-2-1) that defines the process-zone displacement based criterion for DHC initiation is written below as an equality.

$$v_c \;=\; v_T \tag{A-8-11}$$

The critical process-zone displacement for DHC initiation, v_c, is given by Eq. (A-2-3) that is given below.

$$v_c \;=\; \frac{K_{IH}{}^2}{E' p_c} \tag{A-8-12}$$

where

K_{IH}	=	isothermal threshold stress intensity factor for DHC initiation from a crack
v_c	=	critical process-zone displacement for DHC initiation

Substitution of Eqs. (A-8-10) and (A-8-12) into Eq. (A-8-11) gives

$$\left(\frac{K_{IH}}{p_c}\right)^2 \;=\; 5.1869 s\alpha_1(s)\frac{\big[G_0(s/d)V_1(s/d) - G_1(s/d)V_0(s/d)\big]}{G_0(s/d) + \alpha_1 G_1(s/d)} \tag{A-8-13}$$

The only unknown in Eq. (A-8-13) is the process-zone length, s. Equation (A-8-13) is solved iteratively for s. The threshold peak stress for DHC initiation, σ_{th}, is then calculated using Eq. (A-8-9). From Eqs. (8-9) and (8-13), the process-zone length and threshold peak stress for DHC initiation are not dependent on Young's modulus, E.

ASSESSMENT OF MARGINS AGAINST CRACK INITIATION AT CWEST SCRAPE FLAWS IN REGIONS OF INTEREST WITH HIGH LEVELS OF HYDROGEN EQUIVALENT CONCENTRATION IN OUTLET ROLLED JOINTS IN BRUCE UNITS 3 AND 7

Kinectrics Report No.
B2083/RP/0001 R00

From Eq. (A-8-13), in the limiting case where K_{IH} approaches zero, the value of s approaches zero. From Eq. (A-3-8), in the limiting case where s approaches zero, the value of $\alpha_{1(s)}$ approaches zero. From Eq. (A-8-9), in the limiting case where $\alpha_{1(s)}$ approaches zero, σ_{th} approaches p_c. The result that σ_{th} approaches p_c in the limiting case where K_{IH} approaches zero is expected and consistent with other process-zone models for DHC initiation [25,26].

ASSESSMENT OF MARGINS AGAINST CRACK INITIATION AT CWEST SCRAPE FLAWS IN REGIONS OF INTEREST WITH HIGH LEVELS OF HYDROGEN EQUIVALENT CONCENTRATION IN OUTLET ROLLED JOINTS IN BRUCE UNITS 3 AND 7

Kinectrics Report No. B2083/RP/0001 R00
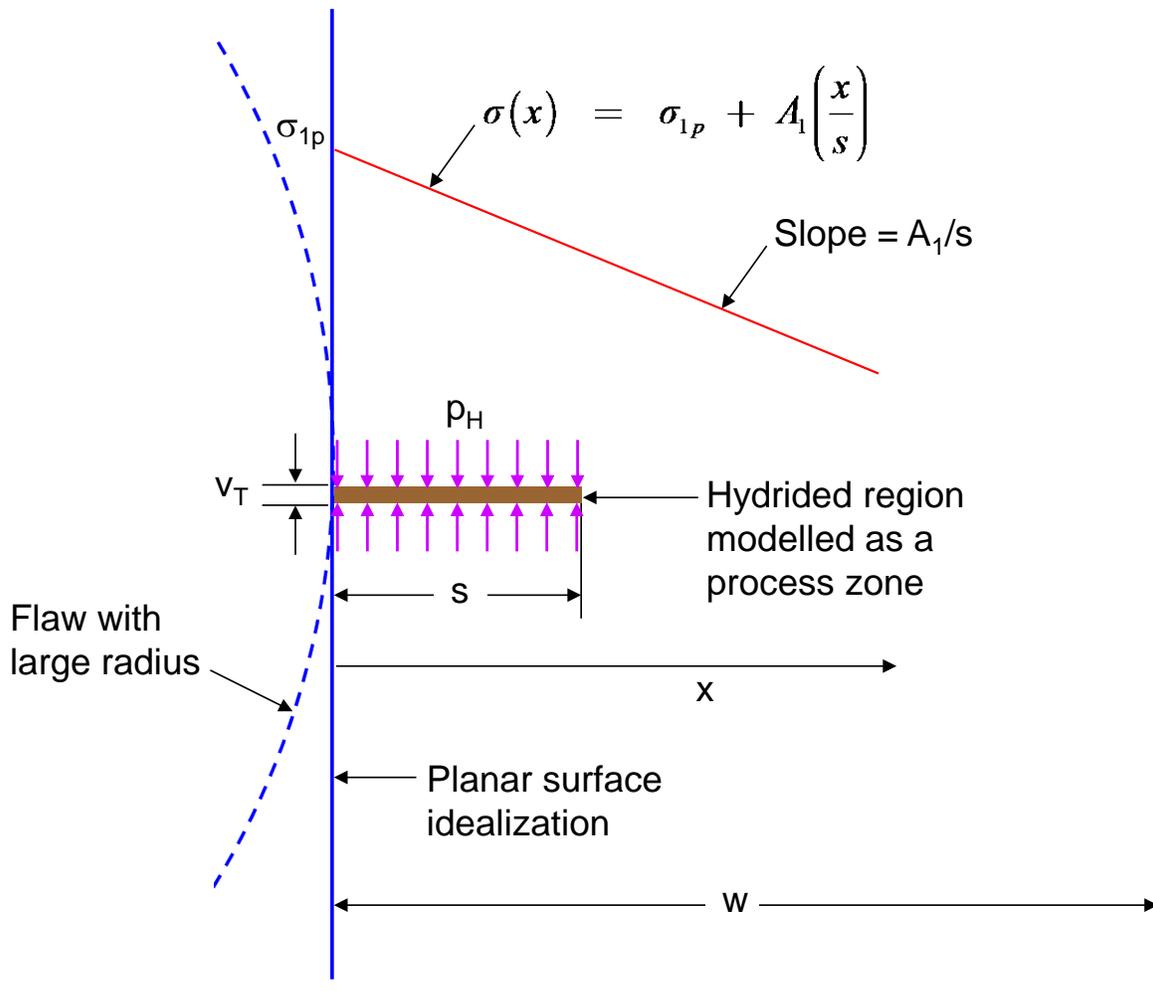
Figure A-1: Process Zone Emanating from a Planar Surface and Subjected to an Applied Linear Stress Distribution

ASSESSMENT OF MARGINS AGAINST CRACK INITIATION AT CWEST SCRAPE FLAWS IN REGIONS OF INTEREST WITH HIGH LEVELS OF HYDROGEN EQUIVALENT CONCENTRATION IN OUTLET ROLLED JOINTS IN BRUCE UNITS 3 AND 7

Kinectrics Report No. B2083/RP/0001 R00
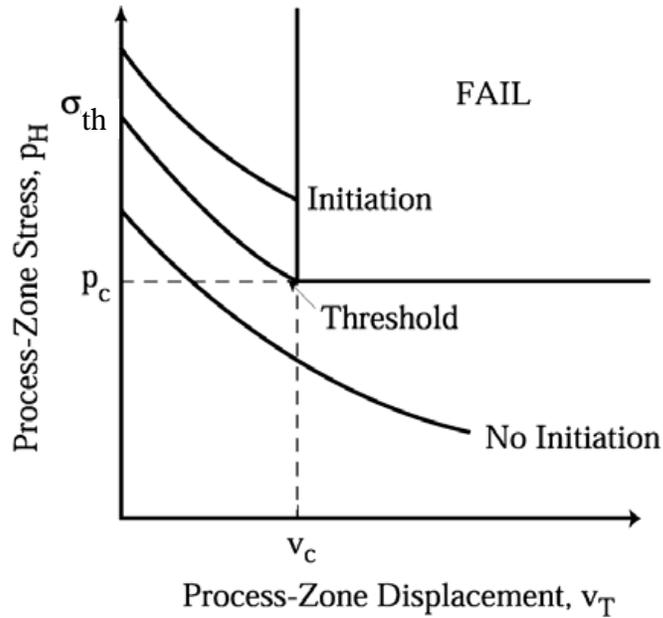
Figure A-2: Various p_H Versus v_T Behaviour as a Hydrided Region Develops at a Flaw Tip Illustrating the Threshold Peak Stress for DHC Initiation, σ_{th}

ASSESSMENT OF MARGINS AGAINST CRACK INITIATION AT
CWEST SCRAPE FLAWS IN REGIONS OF INTEREST WITH
HIGH   LEVELS   OF   HYDROGEN   EQUIVALENT
CONCENTRATION IN OUTLET ROLLED JOINTS IN BRUCE
UNITS 3 AND 7

Kinectrics Report No.
B2083/RP/0001 R00
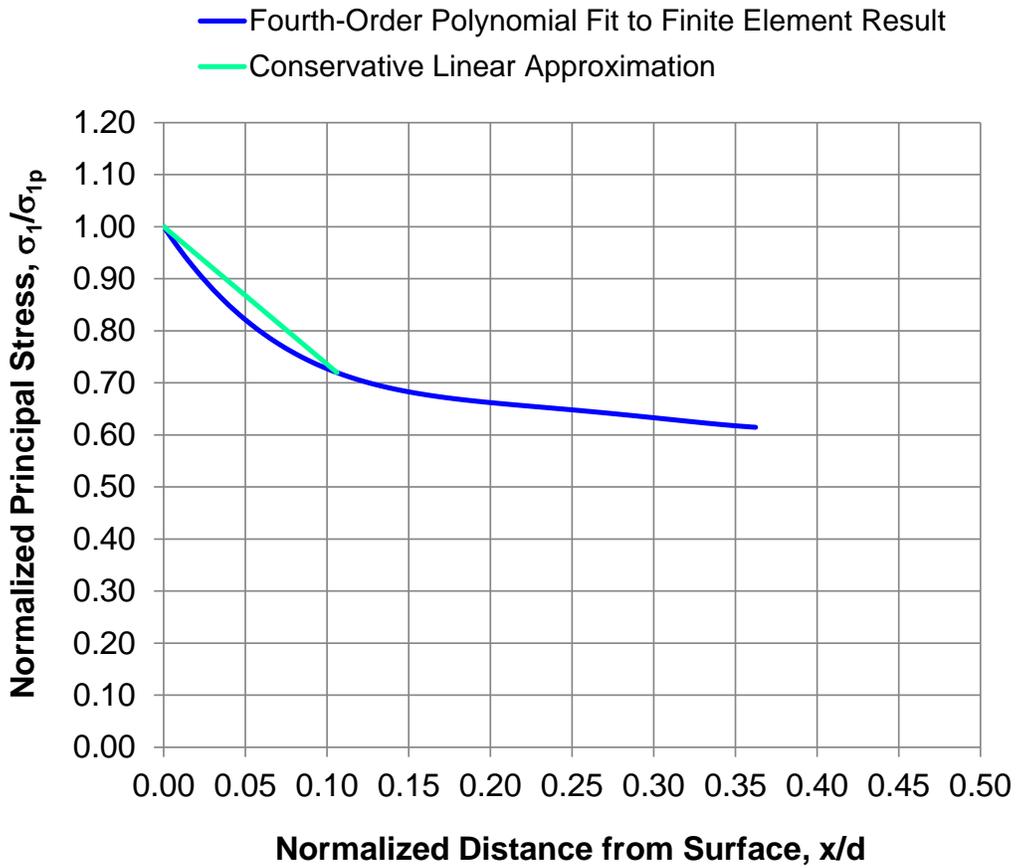
**Figure A-3: Illustration of the Conservative Linear Stress Distribution
Approximation to the Normalized Fourth-Order Polynomial Representation
of the Principal Stress Distribution at the Scrape Flaw**